Progress in Polymer Science 36 (2011) 671–712

Contents lists available at ScienceDirect

Progress in Polymer Science

journal homepage: www.elsevier.com/locate/ppolysci

One-dimensional conducting polymer nanocomposites: Synthesis, properties and applications

Xiaofeng Lu [a], Wanjin Zhang [a], Ce Wang [a,*], Ten-Chin Wen [b], Yen Wei [c,*]

[a] Alan G. MacDiarmid Institute, Jilin University, Changchun 130012, PR China
[b] Department of Chemical Engineering, National Cheng Kung University, Tainan 70101, Taiwan
[c] Department of Chemistry, Drexel University, Philadelphia, PA 19104, USA

ARTICLE INFO

Article history:
Received 6 November 2009
Received in revised form 26 March 2010
Accepted 21 July 2010
Available online 11 August 2010

Keywords:
One-dimensional
Conducting polymers
Composite
Synthesis
Property
Application

ABSTRACT

Intrinsically conducting polymers have been studied extensively due to their intriguing electronic and redox properties and numerous potential applications in many fields since their discovery in 1970s. To improve and extend their functions, the fabrication of multi-functionalized conducting polymer nanocomposites has attracted a great deal of attention because of the emergence of nanotechnology. This article presents an overview of the synthesis of one-dimensional (1D) conducting polymer nanocomposites and their properties and applications. Nanocomposites consist of conducting polymers and one or more components, which can be carbon nanotubes, metals, oxide nanomaterials, chalcogenides, insulating or conducting polymers, biological materials, metal phthalocyanines and porphyrins, etc. The properties of 1D conducting polymer nanocomposites will be widely discussed. Special attention is paid to the difference in the properties between 1D conducting polymer nanocomposites and bulk conducting polymers. Applications of 1D conducting polymer nanocomposites described include electronic nanodevices, chemical and biological sensors, catalysis and electrocatalysis, energy, microwave absorption and electromagnetic interference (EMI) shielding, electrorheological (ER) fluids, and biomedicine. The advantages of 1D conducting polymer nanocomposites over the parent conducting polymers are highlighted. Combined with the intrinsic properties and synergistic effect of each component, it is anticipated that 1D conducting polymer nanocomposites will play an important role in various fields of nanotechnology.

Contents

* Corresponding authors.
E-mail addresses: cwang@jlu.edu.cn (C. Wang), weiyen@drexel.edu (Y. Wei).

0079-6700/$ – see front matter © 2010 Elsevier Ltd. All rights reserved.
doi:10.1016/j.progpolymsci.2010.07.010

1. Introduction

During the past decade, nanotechnology has become an active field of research because of its tremendous potential for a variety of applications [1]. When the size of many established, well-studied materials is reduced to the nanoscale, radically improved or new surprising properties often emerge. There are mainly four types of nanostructures: zero, one, two and three dimension structures. Among them, one-dimensional (1D) nanostructures have been the focus of quite extensive studies worldwide, partially because of their unique physical and chemical properties. Compared to the other three dimensions, the first characteristic of 1D nanostructure is its smaller dimension structure and high aspect ratio, which could efficiently transport electrical carriers along one controllable direction, thus are highly suitable for moving charges in intergrated nanoscale systems. The second charateristic of 1D nanostructure is its device function, which can be exploited as device elements in many kinds of nanodevices [2–4]. Many synthetic strategies, such as solution or vapor-phase approaches, template-directed methods, electrospinning techniques, solvothermal syntheses, self-assembly methods, etc., have been developed to fabricate several classes of 1D nanostructured materials, including metals, semiconductors, functional oxides, structural ceramics, polymers and composites [2–24]. Previous researcher emphasized the fabrication of 1D nanostructures of metal and inorganic semiconductors due to their novel electronic and optical properties. Recently, small molecular and polymeric (semi)conductors have attracted increasing interest for their advantages of readily tunable bandgaps, rich redox chemistry (or electroactivity), excellent flexibility and/or good processibility over conventional inorganic nanomaterials [25–27]. To improve and extend the functions of these organic nanomaterials, one or more components are often incorporated to form multi-functionalized nanocomposites for various applications in the fields of electronics, sensors, catalysis, energy, electromagnetic interference (EMI) shielding, electrorheological (ER) fluids and biomedicine. In this review, we focus on the preparation of 1D conducting polymer nanocomposites and their novel properties and applications.

Intrinsically conducting polymers, also known as "synthetic metals", are polymers with a highly π-conjugated polymeric chain [28–30]. For the discovery of conducting polymers, Alan J. Heeger, Alan G. MacDiarmid and Hideki Shirakawa were awarded the Nobel Prize in Chemistry in 2000. Typical conducting polymers include polyacetylene (PA), polyaniline (PANI), polypyrrole (PPy), polythiophene (PTh), poly(*para*-phenylene) (PPP), poly(phenylenevinylene) (PPV), polyfuran (PF), etc. The chemical structures of these polymers are illustrated in Fig. 1. These conjugated polymers can be electrical insulators, semiconductors or conductors, depending on the level of doping and nature of the dopants. Upon treating with dopants and/or subjecting to chemical or electrochemical redox reactions, the electrical conductivity of these

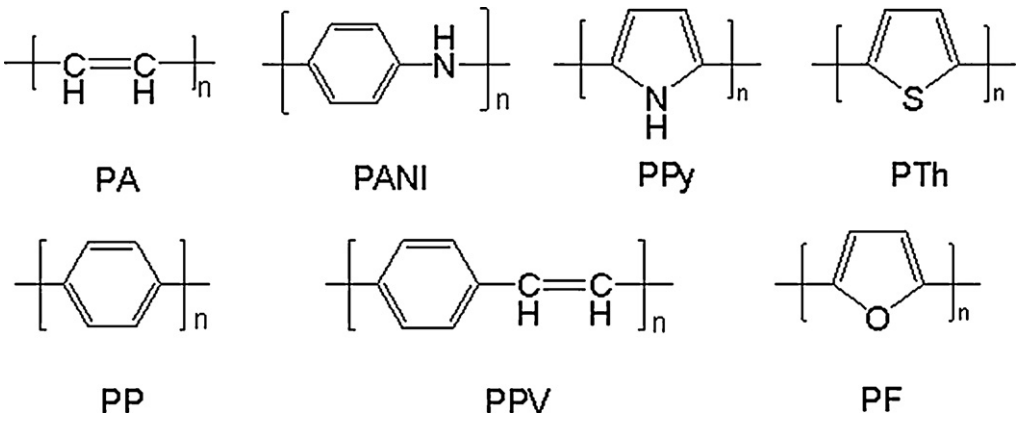

Fig. 1. The chemical structures and their abbreviations of several kinds of conducting polymers.

conjugated polymers can increase by several orders of magnitude. For example, the emeraldine base PANI (undoped form) is an insulator, with a conductivity, of only 10^{-10} to 10^{-8} S/cm. Upon doping the conductivity of the emeraldine salt PANI (doping form) can increase to 10^2 to 10^3 S/cm or higher. The high conductivity upon doping makes these polymers promising materials for applications ranging from electro-optic, molecular and nanoelectronic devices to microwave absorbing and corrosion protection coatings. In addition, the ability of the reversible doping–dedoping properties provides them for the applications in sensors, actuators and separation membranes [31–36].

Recently, nanostructured conducting polymers have been subjected to intensive investigation owing to the unique combination of electronic properties of conductive polymers and large surface area of nanomaterials. In particular, 1D conducting polymeric nanomaterials are exploited as nanowires in electronic devices [37–43]. For example, Chen and co-workers showed that the electrical conductivity of an individual PANI nanotube doped with camphor-10-sulfonicacid (CSA) reached about 30.5 S/cm. Moreover, the contact resistance of the individual nanotube was much smaller than that of crossed PANI nanotube [44]. Over the last few years, many synthetic strategies have been derived for the fabrication of 1D conducting polymer nanomaterials, including template-directed approach, self-assembly, interfacial polymerization, seeded polymerization, rapid-mixing polymerization, radialysis or ultrasonic assisted method, etc. [15,39,40,45–50].

In addition to the formation of 1D nanostructures, incorporation of at least one secondary component into conducting polymers to form nanocomposite is another useful approach to improve or extend the functionality of conducting polymers [51]. It is anticipated that distinct properties from the synergistic effect of each component will be observed in the conducting polymer nanocomposites. This may include improved chemical properties or combined multi-functionalized chemical/physical/biological properties. For example, the addition of carbon nanotubes (CNTs) into conducting polymers was demonstrated by Zhang and co-workers to enhance the electrical properties. The conductivity of CNT/PPy composite nanocables synthesized by cetyltrimethylammonium bromide (CTAB) directed polymerization approach was one order of magnitude higher than that of PPy synthesized under the same conditions, but without the addition of CNTs [52]. Multi-functionalized nanomaterials with both conductivity and magnetism were also prepared by incorporating magnetic Fe_3O_4 nanoparticles into conducting polymers [53]. Here, we concentrate on the various strategies for the preparation of 1D conducting polymer nanocomposites, with special attention to some exciting properties of such nanocomposites, as well as their potential uses in selected applications including electronic nanodevices, sensors, catalysis, energy, EMI shielding, ER fluids and biomedicine. We conclude with a discussion of fabrication methods, and possible future research directions on 1D conducting polymer nanocomposite.

2. Synthesis of 1D conducting polymer nanocomposites

For the fabrication of 1D conducting polymer nanocomposites, there are two important questions: how 1D conducting polymer nanostructures can be obtained, and how other components can be incorporated into conducting polymers. The structure of 1D conducting polymer nanocomposites, the interfacial adhesion between conducting polymers and the secondary component, and the aspect ratio will all affect the properties of the nanocomposites. Therefore, the synthetic strategies for the fabrication of 1D conducting polymer nanocomposites are of great importance. The synthesis of several types of 1D conducting polymer nanocomposites using different kinds of methods is discussed in the following.

2.1. 1D conducting polymer nanocomposites with CNTs or carbon fibers

In 1991, Iijima reported the structure of CNTs [54]. Since then, there has been tremendous progress made in the preparation and applications of this class of nanomaterials [55–62]. CNTs not only have high mechanical strength and modulus, good electrical conductivity and excellent chemical stability, but also have characteristics

of low-dimensional nanomaterials and promising applications in nanodevices. However, poor processability has limited their applications. Therefore, many researchers have focused on the chemical modification of CNTs with organic molecules or polymers to enhance their solubility. Generally, organic molecules or polymers can be functionalized on the surface of CNTs through "grafting to" and "grafting from" techniques using a range of methodologies, such as esterification reaction, amidation reaction, atom transfer radical polymerization (ATRP), radical addition-fragmentation chain transfer polymerization (RAFT), ring-opening metathesis polymerization (ROMP), etc. [59,63–68]. On the other hand, the lack of chemical properties in some aspects is also a great obstacle for the applications of CNTs. For example, the selectivity was minimal when the CNTs were used in sensors [51]. Therefore, the formation of CNTs/functional polymer composites would be a meaningful way to improve or extend the properties of polymers or CNTs. In particular, CNTs/conducting polymer composites with strong interactions between the CNTs and conducting polymers were demonstrated to facilitate electron/hole transport [69]. Since CNTs are 1D nanostructures, coating a layer of conducting polymers on CNTs represents one of the simplest method to fabricate 1D conducting polymer nanocomposite with CNTs. Therefore, it is important to investigate effective methods to make conducting polymers grow on the surface of CNTs.

Electrochemical polymerization provides a convenient approach to fabricate 1D CNTs/conducting polymer nanocomposites [70–77]. Using such a strategy, the morphology and properties of the nanocomposites can be controlled by the electropolymerization conditions, such as the applied potential or current density. Ajayan and co-workers have reported the electrochemical oxidation of aniline in H_2SO_4 on the CNTs electrode to fabricate CNT/PANI composites [70]. Scanning electron microscopy (SEM) images showed both complete and partial coating of PANI on the surface of CNTs. Chen et al. fabricated 1D CNT/PPy nanocomposites, the first example of anionic CNTs acting as the dopant of a conducting polymer [71]. Their results showed that PPy was uniformly coated on the surface of individual CNTs by electrolysis at a low applied potential for a short time, rendering them potential applications in nanoelectronic devices. Compared to unaligned CNTs, aligned array of CNTs have proved to be an excellent substrate for the electrodeposition of conducting polymers because conducting polymers can grow well on the surface of each individual CNT, facilitating the fabrication of uniform coaxial CNTs/conducting polymer nanocomposites [72]. Furthermore, the thickness of the conducting polymers on each CNT can be well controlled. In addition to coaxial nanostructures, another kind of CNTs/conducting polymer composite nanostructures, e.g., CNTs as inorganic fillers in conducting polymer matrices, can be prepared by a template-directed electropolymerization method [73]. The CNTs were incorporated into the conducting polymer nanowires and served as the sole charge-balancing "counterions"; the CNT/PPy composite nanowires was straight and with a surface.

Besides electrochemical polymerization, chemical polymerization has also been widely studied to for the preparation of 1D conducting polymer nanocomposites [78–88]. The first example of a 1D CNT/PA nanocomposite was the *in situ* chemical polymerization of phenylacetylene in the presence of CNTs [84]. Transmission electron microscopic (TEM) images showed that a certain amount of CNTs was wrapped by the PA coils along the latitudes of tubular surface. The helical wrapping of the PA chains along the CNTs enhanced the solubility of the nanocomposites in common organic solvents, such as tetrahydrofuran, toluene, chloroform, and 1,4-dioxane. Compared to the "ex-situ" polymerization method (i.e., mixing the conducting polymers with CNTs directly), CNTs/conducting polymer nanocomposites synthesized by *in situ* chemical polymerization can have better site-selective interactions between the quinoid rings of PANI and CNTs, improving the charge-transfer processes between the two components [78]. However, the morphology of the as-synthesized CNTs/conducting polymer nanocomposites is not very uniform. In order to enhance the interactions between conducting polymers and CNTs, introduction of covalent bonding between conducting polymers and CNTs has been explored. Philip et al. functionalized multiwalled CNTs (MWNTs) with *p*-phenylenediamine, giving phenylamine functional groups on the surface of MWNTs [85]. PANI was formed on the surface of MWNTs via covalent bonds after *in situ* chemical oxidative polymerization. The microscopic studies indicated that the as-synthesized MWNT/PANI nanocomposites had a uniform core-sheath structure and that PANI formed a thick homogeneous coating on the surface of MWNTs. Yao and co-workers further treated such 1D MWNT/PANI nanocomposites with chlorosulfonic acid, followed by hydrolysis to obtain a 1D sulfonated MWNT/PANI nanocomposite, which was easily soluble in water [86]. MWNTs/sulfonated PANI nanocomposite could also be prepared by covalently bonding of poly(*m*-aminobenzene sulfonic acid) with –COCl functionalized MWNTs, as demonstrated by Haddon and co-workers [87]. Similarly, 1D CNT/PTh nanocomposites were fabricated by covalently bonding of poly[3-(2-hydroxyethyl)-2,5-thienylene] with –COCl functionalized CNTs [88].

Surfactants have been employed to enhance the uniformity of the conducting polymer coatings on CNTs. The surfactants can adsorb and arrange regularly on the surface of CNTs at relatively high concentrations, forming a columnar microregion, where monomers of conducting polymers can be polymerized, thus to obtain core-sheath structures of 1D CNTs/conducting polymer nanocomposites. Zhang et al. have prepared a series of CNTs/conducting polymer nanocables by such an *in situ* chemical polymerization directed by the cationic surfactant CTAB [52,89–91]. The uniform cable-like nanostructures of CNT/PANI and CNT/PPy thus formed via such a CTAB-directed chemical polymerization are shown in Fig. 2. Through *in situ* chemical polymerization in the presence of sodium dodecyl sulphate (SDS) surfactant molecules, cable-like structures of carbon nanofibers/PPy can also be prepared [92]. However, attainment of highly regulated nanocoatings of PPy on the surface of carbon nanofibers could only be achieved using ultrasonic irradiation. This was attributed to that H_2O_2 formed by the sonolysis of water under ultrasonic irradiation accelerated the polymerization of pyrrole,

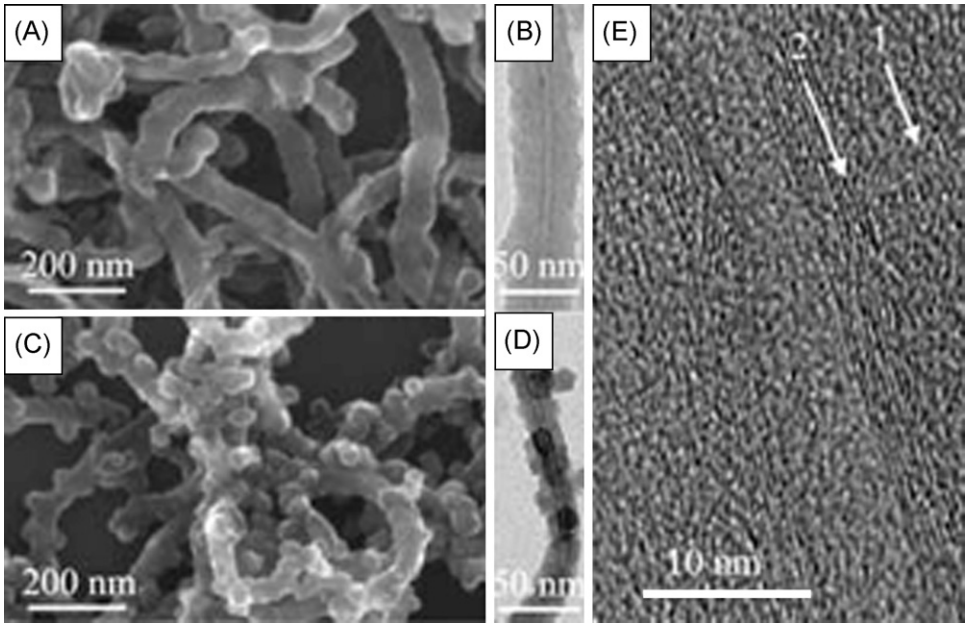

Fig. 2. SEM and TEM images of CNTs/PPy nanocables synthesized by surfactant-directed polymerization approach, showing that smooth and uniform cable-like structures of CNTs/PPy have been prepared using CTAB as surfactant. (A, B) SEM and TEM images of CNTs/PPy nanocables synthesized by CTAB-directed polymerization. (C, D) SEM and TEM images of CNTs/PPy nanocables synthesized by Oπ-10 directed polymerization. (E) HRTEM image of an individual CNTs/PPy nanocables synthesized by CTAB-directed polymerization [52]. Copyright 2004, Wiley-VCH Verlag GmbH&Co. KGaA, Weinheim.

resulting in the deposition of polymer chains on the surface of carbon nanofibers. Polymerizaion by γ-radiolysis is another method to fabricate regulated cable-like structures of CNTs/conducting polymer nanocomposites. Lim and co-workers have prepared the nanocomposites of PTh with MWNTs by the *in situ* γ-irradiation-induced chemical polymerization of thiophene at room temperature [93]. Microscopic studies showed that PTh films with thicknesses of 20–50 nm were smoothly coated on the surface of MWNTs. Wan and co-workers demonstrated a self-assembly process for the fabrication sulfonated MWNT/PANI nanocomposites [94]. The morphology of the resulting nanocomposite was shown to be dependent on the ratio of aniline/sulfonated MWNTs. At the ratios $\leq$1, PANI was found to coat on the surface of sulfonated MWNTs. While supramolecular-type sulfonated MWNTs doped PANI nanotubes were obtained at the aniline/sulfonated MWNTs ratios $\geq$2, which might have been derived from a self-assembly process.

In addition to the solution polymerization, emulsion polymerization has also been used to prepare 1D CNTs/conducting polymer nanocomposites with uniform core-sheath structures [95–97]. Xue and co-workers reported an *in situ* inverse microemulsion approach for the fabrication of 1D MWNT/PPy nanocomposites [95]. The microemulsion system included sodium dodecylbenzenesulfonate (SDBS) surfactant, butanol, hexane and hydrochloric acid. Pyrrole monomers were polymerized in the adsorbed micelles on the surface of MWNTs, leading to the adhesion of PPy particles on the surface of MWNTs. Their results also showed the formation of core-sheath-shaped nanostructured agglomerates. The thickness of PPy layer on the surface of MWNTs can be controlled between several and several tens of nanometers, which depended on the MWNT content. Vapor deposition polymerization is another versatile approach for the preparation of core-shell or core-sheath nanostructures. Jang and Bae have fabricated carbon nanofibers/PPy nanocables using such a strategy [98]. Microscopic studies revealed the formation of uniform PPy layer on the surface of carbon nanofibers. The thickness of PPy layer can be well controlled by varying the amount of the monomer in the feed.

It is noted that not all of the core-sheath-shaped CNTs/conducting polymer nanocomposites are nessassary to have structures with CNTs component as core and conducting polymers components as shell layer. Monomers of conducting polymers can also be filled into and polymerized inside CNTs to form 1D nanocomposites. Park and co-workers impregnated CNTs with pyrrole monomer assisted with supercritical carbon dioxide, followed by polymerization using $FeCl_3$ as an oxidant in water, to afford PPy filled CNTs. However, the characterization of this kind of material was quite difficult [99].

2.2. 1D conducting polymer nanocomposites with metal nanomaterials

Metal nanoparticles or 1D structured nanomaterials are of great importance for their numerous electrical, optical and catalytical properties and a wide range of applications including nanoelectronics and sensing devices [100]. In the past decade or so, the composition and shape control of metal nanoparticles have been extensively studied. Combining the metal nanomaterials with

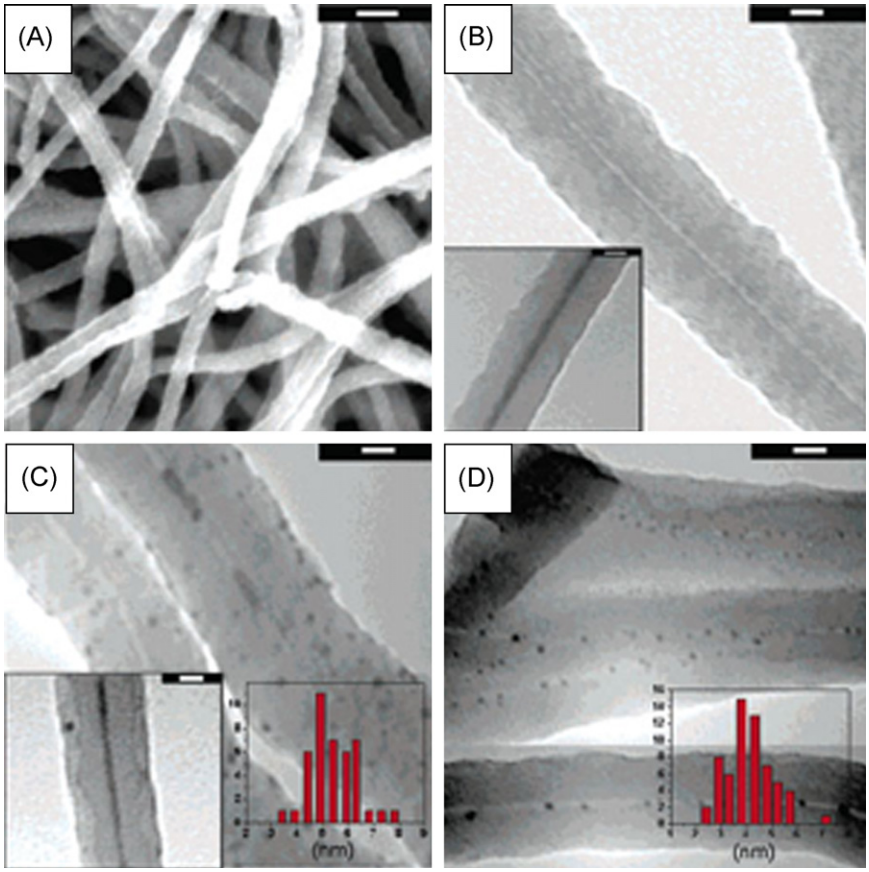

Fig. 3. (A) SEM image of the as-synthesized PPy·Cl nanotubes using V_2O_5 nanofibers as polymerization template. (B) TEM image of the PPy·Cl nanotubes, showing the hollow tubes structures. Inset: TEM image shows the pore of the nanotubes is filled with V_2O_5. (C) Ag/PPy composite nanotubes. Insets: coaxial cable of Ag and particle size distribution. (D) Au/PPy composite nanotubes. Inset: particle size distribution. Scale: (A) 100 nm; (B, C, D) 20 nm [104]. Copyright 2005, American Chemical Society.

1D conducting polymers, in addition to the anisotropic electrical properties of 1D conducting polymers and optical properties of metal nanostructures, new and yet-to-be imagined properties can be attained because of the electron transfer between the two components. One of the most important properties for conducting polymers is their reversible oxidation/reduction (i.e., redox) chemistry. It means that conducting polymers can be oxidized by strong oxidants such as $HAuCl_4$, H_2PdCl_4, H_2PtCl_6, $AgNO_3$, etc., to an over-oxidized state. This property can be applied for the fabrication of 1D conducting polymer nanocomposites with metal component. Kaner and co-workers have demonstrated that PANI/Ag composite nanofibers can be prepared by the redox process between PANI nanofibers and the corresponding $AgNO_3$ [101]. Similarly, gold and Pd nanoparticles were also easily produced inside or on the surface of the PANI nanofibers via such an *in situ* redox reaction [102,103]. In addition to PANI nanofibers, PPy nanostructures were also proven a good matrix for loading metal nanoparticles to form 1D PPy/metal nanocomposite. Fig. 3 shows that Ag and Au nanoparticles 3–5 nm in size can be deposited into PPy nanotubes with an inner diameter of less than 10 nm [104]. The results demonstrated Ag nanoparticles synthesized via a rapid reduction by PPy were on the surface and in the interior of the PPy sheath. Cable-like Ag/PPy nanocomposites could also be obtained by the agglomeration of Ag nanoparticles in the pore of PPy nanotubes. In contrast, Au nanoparticles were mainly formed in the pore region of PPy nanotubes. Wei and co-workers have reported the fabrication of PPy nanotubes with the inner diameter of about 20 nm or more by a self-degraded template method. These were used matrices for loading Au nanoparticles to form 1D PPy/Au nanocomposites [105]. The results represented a somewhat different loading pathway compared to the above mentioned PPy nanotubes with an inner diameter of less than 10 nm, in which the as-synthesized Au nanoparticles were formed on every region of PPy nanotubes (i.e., in the pore and sheath, and on the surface). Furthermore, the size of the as-synthesized Au nanoparticles was not uniform, the average diameter for small Au nanoparticles was about 13 nm, while that for the large nanoparticles could reach about 80 nm. However, adding surfactant molecules such as Tween-80 into the reaction system could make monodispersed Au nanoparticles with a diameter of about 13 nm on PPy nanotubes.

In addition to *in situ* reduction by the conducting polymers, metal nanoparticles can also be synthesized on the

surface of the 1D conducting polymers via a reduction process in the presence of other reducing agents. Yan and co-workers prepared PANI/Pt composite nanofibers by reducing a Pt salt with ethylene glycol on the surface of PANI nanofibers [106]. The diameter of PANI nanofibers was about 60 nm, and that of as-synthesized Pt nanoparticles was only about 1.8 nm as calculated from XRD data. The small size of Pt nanoparticles on the 1D conducting polymer matrix enhanced the electrocatalytic activity for the methanol oxidation reaction. Through the polyol reduction approach with assistance by microwave technique, Hu and co-workers have also fabricated PPy/Pt composite nanofibers [107]. They found that the average size of the Pt nanoparticles was about 2.5 nm. Besides ethylene glycol, Wang and co-workers reported a HCOOH reduction method for the fabrication of PANI nanofibers supported Pt nanoparticles with a diameter of about 3 nm [108]. Importantly, the amount of Pt nanoparticles on the surface of PANI nanofibers can be well controlled by adjusting the molar ratio of PANI to Pt precursors. Furthermore, Pt/Pd hybrid nanoparticles could also be readily loaded on the surface of PANI nanofibers to form 1D nanocomposites via simultaneously reducing Pt and Pd precursors by HCOOH reducing agent. The ease in the control of density and composition rendered such 1D conducting polymers/metal nanocomposites of interest for potential applications in sensors, nanoelectronics and other electrochemical devices.

Template techniques are among the most versatile and simple approaches for the fabrication of 1D nanostructures from many kinds of materials, including conducting polymers. The processes based on these techniques include deposition of the desired materials within the pores of the self-assembled template molecules, followed by the dissolution of the template. Metal/conducting polymers with core-sheath structure have been fabricated by template techniques. For example, Xu and co-workers prepared metal/PANI nanotubules using the template approach via a synthetic strategy consisting of three steps: (1) polymerization of aniline using ammonium persulphate (APS) as an oxidant in the pores of anodic aluminum oxide (AAO) template to form PANI nanotubules; (2) preparation of metal nanowires within PANI nanotubules by electrodeposition; (3) dissolution of AAO template with an alkali solution [109–111]. The PANI might also protect the metal nanowires from oxidation and corrosion, a deirable property for a candidate for use in electronic devices. The Au/PTh composite nanowires with core-sheath structures can also be fabricated by electrochemical preparation of PTh, followed by electrochemical depositon of Au into the pores of AAO [112]. To avoid a multi-step synthesis, metal/conducting polymers composite nanowires can be prepared by simultaneous polymerization of the monomers of conducting polymers such as PANI and the reduction of metal within the pores of the AAO template. High-resolution transmission electron microscopy (HRTEM) images showed that cable-like nanocomposites were formed with a metal core surrounded by PANI coating [113]. Besides the core-sheath structures, segmented architectures of metal/conducting polymers can be fabricated electrochemically within AAO template [114–117].

In addition to porous templates such as AAO, polymer or organic fibers can also be employed as templates to fabricate 1D PANI/metal composites [118,119]. To prevent leaching of metal nanoparticles from conducting polymers matrices, Zhang and co-workers have developed a template method to synthesize PANI/Pd nanotubes with Pd nanoparticles attached to the inner walls of PANI nanotubes [118]. The first step was to coat Pd nanoparticles on the surface of sulfonated polystyrene (PS) nanofibers. Then the PANI layer was coated on the surface of PS/Pd composite nanofibers by a self-assembling polymerization method. Finally, the PS nanofibers as the templates were removed by dissolution in tetrahydrofuran. TEM images revealed that Pd nanoparticles with average size of about 3.4 nm were attached onto the inner walls of PANI nanotubes. This approach can be extended to the fabrication of other 1D conducting polymers/metal nanocomposites with metal nanoparticles on the inner walls of conducting polymer nanotubes.

As mentioned above, metal/conducting polymers with core-sheath structure can be prepared by the template method. However, the approach based on the template technique is complicated and non-economical because of the need to remove the templates. In fact, metal/conducting polymers with core-sheath structure can be fabricated via a one-step chemical polymerization [120–124]. It is well known that the standard reduction potential of most common noble metal salts, such as $HAuCl_4$, H_2PtCl_6, H_2PdCl_4, and $AgNO_3$, is higher than that of the monomers of conducting polymers, including aniline, pyrrole and ethylenedioxythiophene (EDOT), so that the noble metal salts have the ability to oxidatively polymerize such monomers. Cable-like structures of metal/conducting polymers can be synthesized by controlling the reaction conditions. Li and co-workers were the first to report that Ag/PPy nanocables can be prepared through the redox reaction between pyrrole and silver nitrite in aqueous solution in the presence of poly(vinyl pyrrolidone) (PVP) [120]. During the reaction process, the formation of Ag nanowires and the polymerization of a pyrrole sheath proceeded simultaneously. Fig. 4 shows the TEM images of the as-synthesized Ag/PPy nanocables, displaying the coaxial nanostructures with a dark core and a lighter sheath. The diameter of the Ag nanowires core was about 20 nm, while the outer diameter of PPy sheath reached about 50 nm. In such a system for the preparation of Ag/PPy nanocables, PVP played an important role in kinetic control of the growth rates of various faces of silver. In the absence of PVP, the growth rate of the redox reaction can be controlled by lowering reduction potential of the oxidants. Replacing $AgNO_3$ with Ag_2O as the oxidant, snake-like Ag/PPy core-sheath structures have been prepared by one-pot procedure involving hydrothermal reactions in the absence of any surfactant [121]. The mechanism of the formation of Ag/PPy core-sheath nanostructures might be related to the self-assembly of the silver nanoparticles reduced from Ag_2O particles inside the PPy matrix oxidatively polymerized from pyrrole monomer. Niu and co-workers demonstrated that Au/PANI coaxial nanocables could also be fabricated by the redox reaction between chlorauric acid and aniline in the presence of D-CSA [122]. In that case, CSA acted not only as a dopant, but also as a surfactants

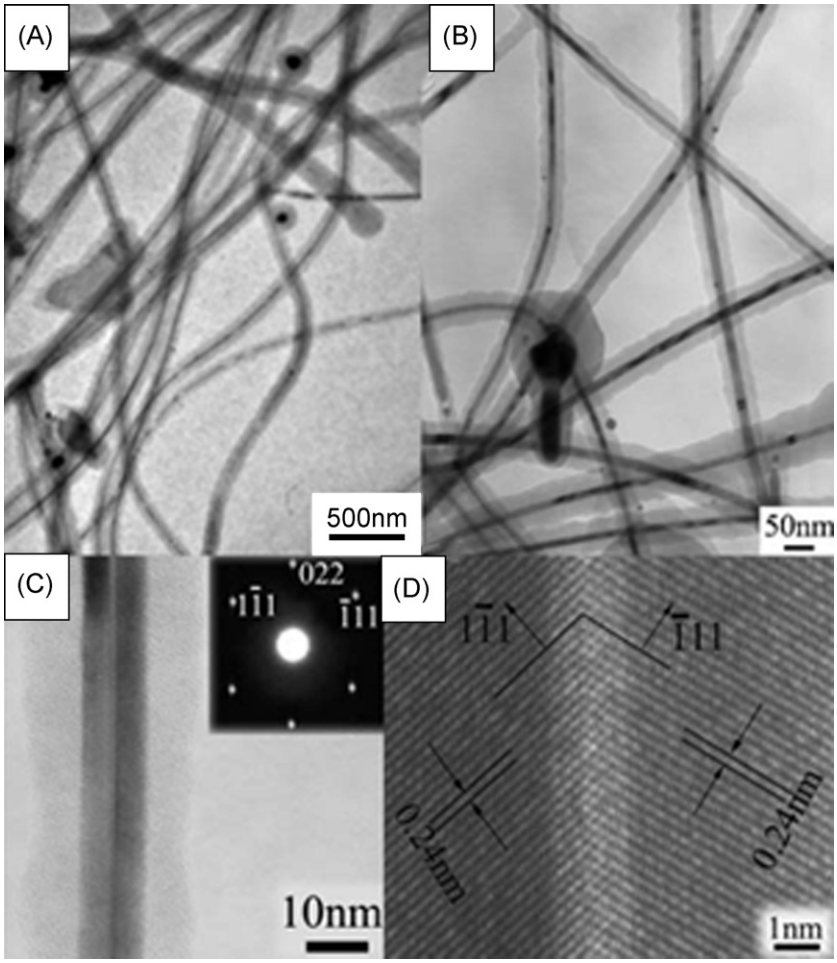

Fig. 4. (A, B) TEM images of Ag/PPy nanocables with low-magnification. (C) High-magnification TEM image of a single Ag/PPy nanocable; inset: ED patten of silver core, showing the diffracton dot of silver. (D) HRTEM image of Ag core, showing the silver grows as a crystal twinned at the (111) planes [120]. Copyright 2005, the Royal Society of Chemistry.

or a soft template, just as the role of PVP in the system to the fabrication of Ag/PPy nanocables. TEM images exhibited coaxial nanocables structures with an outer (PANI–CSA sheath) diameter of 50–60 nm and an inner (Au core) diameter of about 20 nm. The as-synthesized Au/PANI coaxial nanocables can be converted to hollow PANI nanotubes by dissolution of Au nanowire core by a saturated I_2 solution. In addition to Ag/PPy and Au/PANI nanocables, cable-like Au/poly(3,4-ethylenedioxythiophene) (PEDOT) nanostructures have been synthesized in the absence of any surfactant or stabilizer through one-step interfacial polymerization of EDOT dissolved in dichloromethane solvent and $HAuCl_4$ dissolved in water [123]. Microscopy studies showed that the outer and inner diameters of Au/PEDOT nanocables were around 50 and 30 nm, respectively. Similar to the Au/PANI nanocables, PEDOT nanotubes can be obtained by dissolution of the Au component in saturated I_2 solution. Furthermore, pure gold nanowires could also be produced by removing PEDOT sheath via oxygen plasma decomposition.

While the greatest advantage of the one-step approach for fabricating metal/conducting polymer nanocables is its simplicity, the thickness of the conducting polymer sheaths is not easily controlled. Li and co-workers developed an interesting post-polymerization method to coat conducting polymers on the surface of metal nanowires [125]. To ensure the polymerization occurs on the surface of silver nanowires, Ag ions were firstly adsorbed onto the closest surface of silver nanowires through the common ions adsorption effect. Pyrrole monomer was then added into the system of Ag^+/Ag nanowires and the polymerization would begin between the pyrrole monomer and Ag^+ to produce Ag/PPy nanocables. TEM images proved the core-sheath structures of the as-prepared Ag/PPy nanocables. More importantly, the thickness of PPy sheath layer can be well controlled by changing the concentration of the $AgNO_3$ aqueous solution used to adsorb Ag^+ onto the surface of the Ag nanowires. The thickness of the PPy layer increased from 3 nm to more than 20 nm as the concentration of $AgNO_3$ solution was increased from 1 to 10%. In addition to the core-sheath structures, 1D conducting PANI decorated with metal nanoparticles can be obtained by γ radiolysis. The size of metal nanoparticles can be varied by adjusting the ratio of aniline to the metal precursors [126].

2.3. 1D conducting polymer nanocomposites with metal oxides

The fabrication of 1D conducting polymer nanocomposites with metal oxides has become an alluring aspect for their potential applications in sensors and energy devices. The synergy between 1D conducting polymers and metal oxides provides the resultant nanocomposites with added functionalities compared to their individual parent materials. The self-assembly method, also called "template-free" method, is a facile and versatile technique for the preparation of 1D conducting polymers and their nanocomposites. Wan and co-workers demonstrated that 1D PANI/TiO_2, PANI/Fe_3O_4 and PANI/γ-Fe_2O_3 nanocomposites can be readily fabricated by a self-assembling process [53,127,128]. The mechanism of the self-assembly can be related to the formation of micelles by β-naphthalene sulfonic acid (β-NSA) anions and anilinium cations as soft templates. As an example for the preparation of 1D PANI/TiO_2 nanocomposites, TiO_2 nanoparticles can be well dispersed in a β-NSA solution prior to the polymerization of aniline monomer. The micelles contained TiO_2 nanoparticles act as the "core", with the aniline/β-NSA salt the "shell", to function as a soft template in the formation of PANI/TiO_2 composite nanofibers or nanotubes. After adding APS to the system to induce the polymerization, the micelles containing TiO_2 become larger spheres or tubes/fibers by elongation, resulting in the formation of a 1D PANI/TiO_2 nanocomposite. Microscopic studies indicated that PANI/TiO_2 nanotubes or nanofibers were formed at low concentrations of TiO_2. However, granular PANI/TiO_2 composites would form when the concentration of TiO_2 was increased to 0.12 M. Introducing ultrasonic irradiation into the self-assembly process for the fabrication of 1D conducting polymers/metal oxide nanocomposites dispersed the inorganic nanocomponents in the conducting polymer matrix. Our group reported the synthesis of PANI/Fe_3O_4 composite nanotubes by chemical polymerization assisted with ultrasonic irradiation [129]. To enhance the compatibility between PANI and Fe_3O_4, Fe_3O_4 nanoparticles were capped with an aniline dimmer, which can be covalently bonded with PANI. TEM images showed a morphology with the nanotubes and Fe_3O_4 nanoparticles well dispersed in the PANI matrix. During the preparation of conducting polymers, an inorganic or organic acid is often added to the reaction system as the doping agent to increase the conductivity of the conducting polymers. Recently, scientists have found that novel conducting polymer nanostructures can be synthesized in the absence of inorganic or organic acid, or even in a basic solution [130–132]. 1D conducting polymers/metal oxide nanocomposites have also been fabricated in the absence of acids [133–136]. Guo and co-workers demonstrated that rectangular tubes of PANI/NiO composites can be prepared in the presence of SDBS without adding any acid through a self-assembly process [134]. TEM images showed that the wall thickness of rectangular PANI/NiO composite tubes was approximately 150 nm, with a length of several micrometers. By changing the molar ratio of aniline to NiO, nanobelts of PANI/NiO composite could also be obtained [135]. Ćirić-Marjanović et al. reported the similar self-assembly technique for the fabrication PANI/silica composite nanotubes without any added acid, also in the absence of any surfactants [136]. The weight ratio of silica to aniline was found to influence the morphology of the as-prepared PANI/silica nanocomposites. With an initial weight ratio of silica to aniline lower than 0.2, nanotubes of PANI/silica with an outer diameter of 100–250 nm and an inner diameter of 10–80 nm can be observed, while only nanogranules have been obtained as the weight ratio of silica to aniline reaches about 2.

Similar to the fabrication of conducting polymer/metal nanocomposites, 1D conducting polymer/metal oxide nanocomposites could also be prepared via a one-step approach. Zhang et al. demonstrated that PEDOT/β-$Fe^{3+}O$(OH,Cl) nanospindles can be synthesized through chemical oxidation polymerization using $FeCl_3{\cdot}6H_2O$ as an oxidant in the presence of CTAB and poly(acrylic acid) (PAA) [137]. At the same time of the polymerization of EDOT, $FeCl_3$ would hydrolyze to form β-$Fe^{3+}O$(OH,Cl), resulting in the formation of PEDOT/β-$Fe^{3+}O$(OH,Cl) nanospindles. Microscopy revealed that the nanospindles had a length in the range of 350–370 nm and a width of about 80–90 nm. Single crystals of β-$Fe^{3+}O$(OH,Cl) were dispersed in the PEDOT matrix (Fig. 5). The reaction conditions, such as the concentration of EDOT, the molar ratio of EDOT to $FeCl_3{\cdot}6H_2O$, the temperature, the type of oxidant, surfactants and even solvents all influenced the morphology of the as-synthesized products. The core-sheath structure of conducting polymers/metal oxides is one of the most interesting features of nanocomposites for the potential synergic behavior between the good electrical conducting polymers and a functional metal oxide. In a one-step process, Li et al. presented an *in situ* polymerization method for the fabrication of V_2O_5/PANI nanobelts with core-sheath structure, without adding any other oxidant or initiator [138]. In a typical polymerization, V_2O_5 acted not only as a template, but also the oxidant for the preparation of PANI. In an appropriate acidic solution, V_2O_5 can be partly dissolved to form vanadic acid, which could function as an oxidant for the polymerization of aniline. The results showed that V_2O_5/PANI core-sheath nanobelts with a width and thickness of 400 and 50 nm had been formed. Furthermore, the morphologies of the V_2O_5/PANI core-sheath nanobelts are influenced by the pH of the solution and the additional initiator.

Vapor-phase polymerization gives another versatile approach for the fabrication of metal oxide/conducting polymers core-sheath structures. Our group demonstrated that core-sheath nanocables of TiO_2/PPy can be obtained by the polymerization of pyrrole on the surface of electrospun TiO_2 nanofibers, with $FeCl_3$ as the oxidant [139]. The electrospun TiO_2 nanofibers have a rough surface and some voids, which favor the existence of $FeCl_3$ oxidant on their surface; thus pyrrole can be polymerized on the surface of TiO_2 nanofibers to form core-sheath structures. TEM images showed a typical coaxial nanocable structure of the TiO_2/PPy nanocomposites obtained. The thickness of the sheath of as-synthesized TiO_2/PPy composite nanocables is about 20 nm under such an experimental procedure. However, the thickness of the conducting polymer layers is not well controlled in the vapor-phase

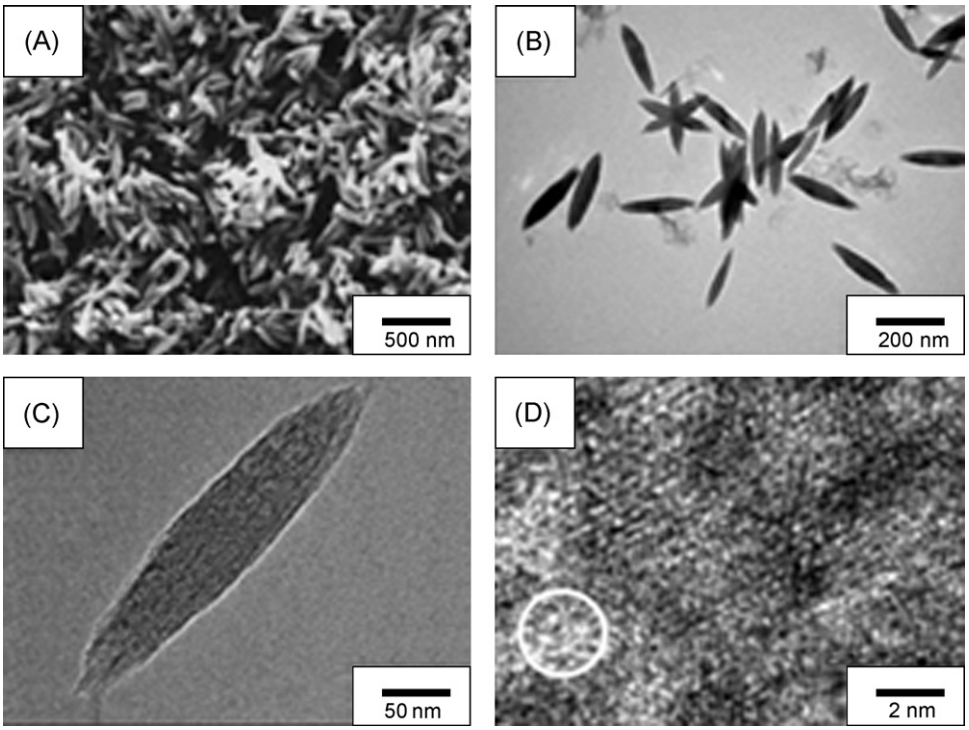

Fig. 5. (A, B) SEM and TEM images of PEDOT/β-Fe^{3+}O(OH,Cl) nanospindles. (C) High-magnification TEM image of a single PEDOT/β-Fe^{3+}O(OH,Cl) nanospindles. (D) HRTEM image of PEDOT/β-Fe^{3+}O(OH,Cl) nanospindles [137]. Copyright 2008, American Chemical Society.

polymerization. Surfactant-directed *in situ* polymerization approach can be used to prepare TiO_2/PPy coaxial nanocables with controlled thickness of the PPy layer [140]. Very uniform and smooth PPy layer was coated on the surface of electrospun TiO_2 nanofibers via the surfactant-directed polymerization with the assistance of the ultrasonic irradiation. In addition to the surfactants, block copolymers have also been used to direct the formation of metal oxide/conducting polymers nanocomposites with core-sheath structure [141]. A poly(ethylene oxide)–poly(propylene oxide)–poly(ethylene oxide) (PEO–PPO–PEO) triblock copolymer, adsorbed on the surface of titanate nanotubes during the process of the polymerization of aniline, acting as a soft template for the fabrication of titanate/PANI core-sheath nanotubes. TEM images indicated that the outer layer was amorphous PANI, while the inner layer was crystalline of titanate. Furthermore, PANI was almost uniformly grown on the surface of titanate nanotubes to form titanate/PANI core-sheath nanotubes with a smooth surface.

Hydrothermal reaction offers another simple approach for the preparation of metal oxide/conducting polymer core-sheath nanostructures. Li and co-workers synthesized a series of metal oxide/conducting polymers, including MoO_3/PPy, MoO_3/PANI, VO_2/PPy, SnO_2/PPy and so on, via the hydrothermal reaction [142]. For example, TEM images of MoO_3/PPy proved that the core-sheath structure had formed. ED patterns and EELS spectra showed that the core phase was the single crystalline MoO_3 and the amorphous PPy shell with average thickness of around 70 nm was coated on the surface of MoO_3 nanobelts. The morphology and chemical structures of the core-sheath MoO_3/PPy nanostructures were dependent on the pH and the reaction temperature. This approach provides a general methodology for preparing many different kinds of metal oxide/conducting polymer nanocomposites with core-sheath structure.

2.4. 1D conducting polymer nanocomposites with chalcogenides

The chalcogenides are compounds of the heavier chalcogens, including the sulfides, selenides, and tellurides. In this section, we describe the synthetic methods of 1D conducting polymer nanocomposites with chalcogenides, which are potentially applicable in nanoelectronics, solar cells, batteries, and sensors. Alivisatos and co-workers reported that poly-3(hexylthiophene) (P3HT)/CdSe nanorod composites can be fabricated into efficient hybrid solar cells with an amazing external quantum efficiency of over 54% [143,144]. Similar to the preparation of 1D metal oxide/conducting polymer nanocomposites, chalcogenides can be incorporated into 1D conducting polymers through a self-assembly process. Surface modification chalcogenide nanoparticles is necessary to disperse them in the conducting polymer matrix. For example, mercaptocarboxylic acid capped CdS nanoparticles can be well dispersed in PANI wires through a self-assembly polymerization process because the hydrogen bonding and/or electrostatic interaction between carboxy group on the surface of CdS nanoparticles and aniline during the process of the polymerization [145]. In a typical experiment, the molar ratio

of CdS nanoparticles to the monomer of conducting polymers has significant influence on the morphology of the 1D nanocomposites. Template-directed techniques, which are a versatile approach to synthesize 1D nanomaterials, have been demonstrated to be suitable for the preparation of chalcogenides/conducting polymers core-sheath structures. Lin and co-workers reported the fabrication of CdS/PANI coaxial nanocables by electrochemical synthesis in the AAO membrane employed as the hard template [146]. The diameter of the CdS core was about 50 nm, while that of PANI tube was around 90 nm.

In addition to the template technique, an *in situ* polymerization at the organic solvent/water interfacial layer has been developed for the preparation of 1D sulfide/conducting polymer nanocomposites with a core-sheath structure [147]. Smooth and uniform coaxial nanocables of Cu_2S/PPy nanocomposites have been fabricated by controlling the reaction conditions (e.g., a molar ratio of pyrrole to oxidant is 1:1 with 0.036 M pyrrole in chloroform). Furthermore, the thickness of the PPy layer on the surface of Cu_2S nanorods can be controlled by adjusting the polymerization time. The hydrothermal reaction was also applied to prepare 1D Bi_2S_3/PPy nanocomposites [148]. TEM images showed the 1D core-sheath structure of the Bi_2S_3/PPy nanocomposites. The PPy coating on the surface of Bi_2S_3 nanorods was smooth and uniform in thickness. Likely, the thickness of the PPy layer can be controlled by changing reaction conditions. The results showed that the thickness of PPy increased almost linearly with pyrrole monomer concentration.

P–N junctions are very important in modern electronic applications. Conducting polymers, such as PANI and PPy, are p-type semiconductors, while sulfide nanoparticles are n-type semiconductors. Heterojunction nanowires containing conducting polymers and sulfides could be good candidates for fabrication of light controlled diode. Based on this idea, Li and co-workers synthesized CdS/PPy hetero P–N junction nanowires by a template technique [149]. Element mapping and TEM images both proved the formation of the heterojunction structures. The nanowires had a smooth surface with diameters in the range of 200–400 nm (Fig. 6). The heterojunction nanowires of CdS/PPy exhibited interesting photoelectrical properties.

2.5. 1D conducting polymer nanocomposites with other polymers

To enhance processability, mechanical and thermochemical stability, conducting polymers are often combined with other insulating flexible polymers, such as poly(vinylalcohol) (PVA), poly(methyl methacrylate) (PMMA), poly(vinylacetate) (PVAc), etc [36]. The electrospinning technique affords the most versatile and simple approach for the combination of 1D conducting polymers with insulating polymers. When the conducting and insulating polymers are dissolved in a common solvent with acertain appropriate viscosity, they can be electrospun into composite nanofibers [150]. MacDiarmid and co-workers demonstrated the fabrication of PANI/PEO composite fibers via co-electrospinning technique [151]. In order to increase the solubility of PANI, camphorsulfonic

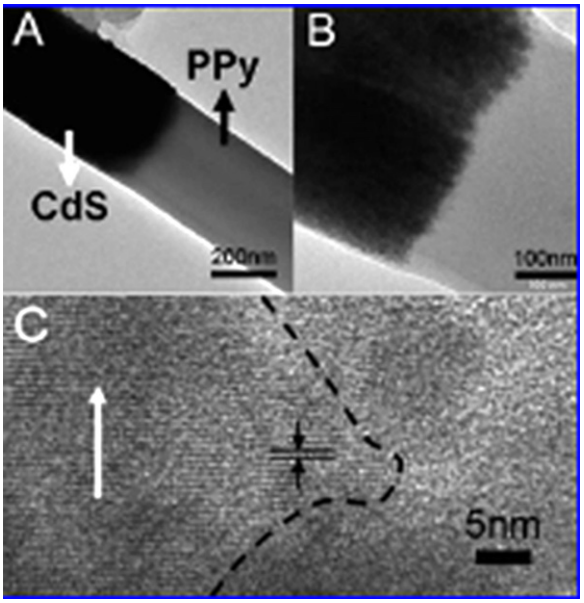

Fig. 6. (A, B) TEM images of CdS/PPy heterojunction nanowire. Figure B showing the interface of CdS/PPy heterojunction nanowire with higher magnification. (C) HRTEM image of the interface of CdS/PPy heterojunction nanowire [149]. Copyright 2008, American Chemical Society.

acid was used as a dopant. Microscopic studies revealed that the as-prepared PANI/PEO composite fibers have a diameter ranging between 950 nm and 2.1 μm. Although the diameter of the PANI/PEO composite fibers was quite large, they had potential applications in electronic devices and sensors. The composition of PANI and PEO in the composite fibers can be controlled in a wide range by varying the ratio of PANI to PEO. Another type of conducting polymers, poly-3-alkylthiophene (P3DDT), has also been combined with PEO to form composite fibers by electrospinning their blends from chloroform solution [152]. The results showed that the fiber diameter was approximately 1 μm, a similar order of magnitude with that of PANI/PEO composite fibers. Furthermore, the PEO component can be rapidly and completely removed by washing the composite fibers with acetonitrile, resulting in the formation of long and homogenous P3DDT fibers. Other conducting polymer/insulating polymer composite fibers, such as PANI/PS and PANI/nylon-6 have also been synthesized by co-evaporation electrospinning techniques [153–155]. In particular, composites based on the conducting polymers and biodegradable and biocompatible polymers have attracted attention for their potential applications in drug delivery and tissue engineering. Mattoso and co-workers synthesized *p*-toluene sulfonic acid doped PANI/poly(L-lactic acid) (PLA) composite nanofibers by electrospinning technique [156]. The composite nanofibers had diameters in the range of 100–200 nm, much smaller than that of PANI/PEO and PEDOT/PEO composite fibers. The composite nanofibers have a lower degree of crystallinity because of the strong interactions between PANI and PLA and the rapid solvent evaporation during the electrospinning process.

Composite nanofibers may be formed from monomers of conducting polymers polymerized *in situ* in an insu-

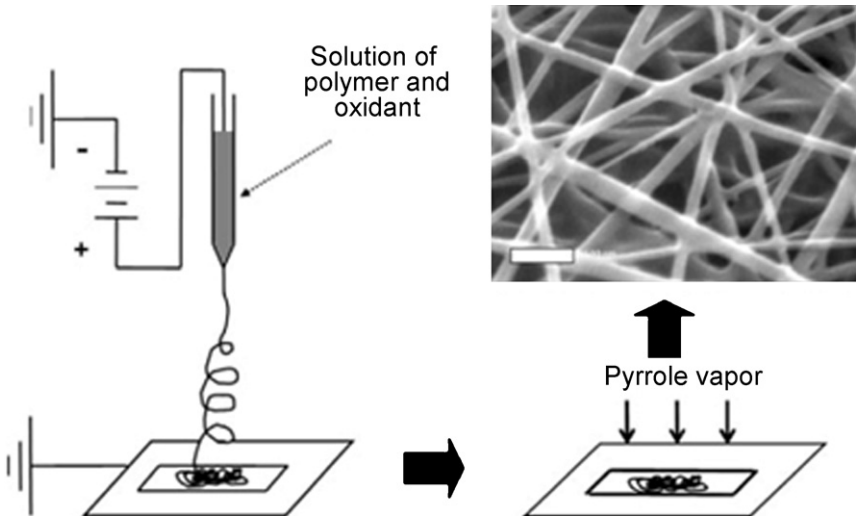

Fig. 7. Schematic illustration of the fabrication of PEO/PPy composite fibers through vapor-phase polymerization of pyrrole on the surface of electrospun PEO nanofibers containing the oxidant of $FeCl_3$. The figure also shows the typical SEM image of the as-prepared PEO/PPy composite fibers. The scale bar in the image is 500 nm [157]. Copyright 2005, Wiley-VCH Verlag GmbH&Co. KGaA, Weinheim.

lating polymer fiber matrix previously prepared by the electrospinning technique. Oxidant should be incorporated into the electrospun insulating nanofibers to promote polymerization of monomer taken up by exposure to the vapor of the monomers, resulting in the formation of conducting polymers in the insulating nanofibers. Kim and co-workers demonstrated the fabrication the PPy/PEO composite nanofibers using such a strategy [157]. The as-synthesized PPy/PEO composite nanofibers had a diameter of around 96 ± 30 nm (Fig. 7). Similarly, PPy/polyamide (PA-6), PPy (PANI, PEDOT)/PMMA, and PPy (PANI, PEDOT)/PS composite nanofibers have also been prepared using the electrospinning technique and vapor deposition polymerization [158–160]. To synthesize conducting polymers/hydrophobic insulating polymer (CP/HIP) composite nanofibers, such as conducting polymers/PMMA and conducting polymers/PS, an organic oxidant is usually needed. Shi and co-workers described the fabrication of PPy (PANI, PEDOT)/PMMA, and PPy (PANI, PEDOT)/PS composite nanofibers by incorporating benzoyl peroxide (BPO) into PMMA and PS nanofibers by electrospinning, followed by exposure to vapor momomers of conducting polymers to initiate polymerization [159]. The content of conducting polymers can be controlled by reaction conditions. Kim and co-workers also prepared PEDOT/PS composite nanofibers with the combined electrospinning and vapor deposition polymerization techniques [160]. Instead of $FeCl_3$ and BPO, they used ferric *p*-toluenesulfonate as the oxidant to initial the polymerization. The as-synthesized PS/PEDOT composite fibers would completely melt to form a continuous film if exposed for too long to EDOT monomer.

Core-sheath nanostructures of insulating/conducting polymer composites could also be fabricated through co-evaporation electrospinning. Mead and co-workers demonstrated PS/PANI and polycarbonate (PC)/PANI nanocomposites with a core-sheath structure prepared by electrospinning their blends [161,162]. TEM images proved that the dark regions in the core were a PANI phases a continuous fibrillar structure. By contrast, the light regions presented PS or PC phases. A possible explanation for the formation of core-sheath structure of PS/PANI and PC/PANI nanocomposites can be ascribed to the high-surface tension of PANI. A lower surface tension of the electrospun solutions is known to prevent the formation of beads [163]. After mixing PANI with PS or PC, the surface tension of the electrospinning solutions decreased, reducing the tendency to form beads and generating the core-sheath structures. In addition, the incompatibility of PANI and PS or PC and the low molecular of PANI may also be important factors for the formation of core-sheath structured nanocomposites. The viscosity of the system would increase during on solvent evaporation in electrospinning. The low molecular weight endowed PANI with enough mobility to complete the coalescence process prior to solidification of the nanofiber. Moreover, PANI is poorly soluble in chloroform, while PS or PC have a much better solubility. Thus, PANI would begin to solidify first during solvent evaporation, with PANI forming a core in a sheath of PS or PC. Co-axial electrospinning techniques offer another facile approach for the fabrication of insulating/conducting polymer nanocomposites with core-sheath structures. The coaxial electrospinning setup utilizes two capillary tubes as the spinnerets. Chen and co-workers demonstrated the fabrication of core-sheath PMMA/P3HT composite nanofibers via a two-fluid coaxial electrospinning process [164]. Microscopic studies showed that the diameter of the as-synthesized PMMA/P3HT composite nanofibers was in the range of 500–700 nm. The sheath composed of worm-like P3HT phase was clearly observed on the surface of fibers.

Core-sheath nanostructures of insulating/conducting polymer composites could also been prepared by *in situ* polymerization of conducting polymers on the surface of insulating polymer fibers. Jones and co-workers prepared PMMA/PANI coaxial fibers by deposition PANI on

electrospun PMMA fibers via *in situ* chemical oxidative polymerization [165]. The resulting PMMA/PANI coaxial fibers have a diameter of approximately 290 nm with a PANI layer of around 30 nm thick. The organic solution properties have a significant influence on the morphology and diameter of the electrospun fibers. The same group also prepared PMMA/PPy coaxial nanocables using electrospun PMMA nanofibers as templates [166]. The thickness of the PPy layer on the surface of PMMA fibers can be controlled by the reaction time; a typical 8 min deposition resulted in a 35 nm PPy wall. Furthermore, the PMMA/PPy coaxial nanofibers can be converted to hollow PPy or carbon tubes by chloroform extraction and thermolysis, respectively. Nylon-6/PANI composite fibers have been synthesized via the chemical polymerization using electrospun nylon-6 fibers as templates [167]. In addition to the chemical oxidative polymerization, conducting polymers can be polymerized on the surface of electrospun polymer nanofibers by electrochemical polymerization. Martin and co-workers demonstrated the deposition of PEDOT on the surface of drug-loaded electrospun poly(lactide-*co*-glycolide) (PLGA) nanofibers on the electrode sites [168]. The thickness of the as-synthesized core-sheath PLGA/PEDOT composite fibers was in the range of 50–100 nm. Such nanomaterials can be used for controlled drug delivery and had potential applications in biomedical engineering and pharmacology.

As demonstrated by the preceding examples, the template-directed method provides a powerful means to fabricate various 1D nanomaterials. Jang et al. demonstrated the preparation of PPy/PMMA coaxial nanocables using mesoporous SBA-15 silica as a template [169]. Methyl methacrylate and pyrrole monomers were sequentially polymerized inside the channels of SBA-15 silica using BPO initiator and iron chloride oxidant, respectively, resulting in PPy/PMMA composites in the SBA-15 silica. PPy/PMMA coaxial nanocables can be obtained on removal of the silica template. Atomic force microscope (AFM) studies revealed that almost all the samples have an oriented and unidirectional structure, indicating that the polymerization mainly occurs inside the channels of SBA-15 silica.

One of the important properties of conducting polymers is their reversible doping–dedoping process. For example, inorganic acids, organic acids and even polymeric acids are common dopants for PANI or PPy. Therefore, insulating polymers with an acid group can be easily combined with conducting polymers by the doping process. To obtain 1D conducting polymer nanocomposites, acidic insulating polymers can be directly combined with the dedoped conducting polymer nanofibers or nanotubes. On the other hand, polymeric acids can also be covalently bonded with conducting polymers during polymerization. Hopkins et al. prepared PANI/PS composite nanofibers through an interfacial polymerization technique in the presence of sulfonated PS [170]. The results confirmed the formation of PANI/PS composite nanofibers with a diameter about 40–50 nm. In addition to insulating polymers, sulfonated conducting polymer can dope other conducting polymers, affording conducting nanocomposites. Wallace and co-workers prepared nanocomposites of poly(2-methoxyaniline-5-sulfonic acid) (PMAS) (a derivative of PANI) with PANI using PMAS as the dopant [171]. The morphologies of the nanocomposites include both well-fined nanofibers and nanoparticles with diameters between 20 and 100 nm. Furthermore, the PMAS/PANI composites exhibited very stable dispersion compared to that of hydrochloric acids doped PANI nanofibers.

2.6. 1D conducting polymer nanocomposites with biological materials

The composite materials generated from conducting polymers and biological materials exhibited enhanced physical and/or chemical properties compared to the neat conducting polymers. For example, incorporating or immobilizing enzymes into conducting polymer matrix provided the nanocomposites with enhanced speed, stability, and sensitivity properties as biosensors [172,173]. Many biological materials, including enzymes, DNA, RNA, proteins (amino acids), antibodies, antigens, etc., have been incorporated into conducting polymers to form biologically active composites for a variety of applications. Most previous studies focused on the fabrication of conducting composites comprising polymers and biological materials composites in the form of films on electrodes instead of 1D nanostructures. However, diffusion limited processes and the transport of large ions and molecules will be restricted for thick composite films with certain capacities. To improve the capacity of the electrode, fabrication of thick films composed of fibers with porous structures is an alternative approach. For high-surface area and the presence of conducting polymer layers, films of composite fibers have applications in electrochemically controlled ion exchange or separation devices, and potential use in sensors.

1D conducting polymer nanocomposites with DNA have been fabricated via several approaches [174–180]. He and co-workers demonstrated the fabrication of PANI nanowires using DNA as templates on thermally oxidized Si surfaces using a horseradish peroxidase (HRP) enzymatic polymerization approach [174]. Typical synthetic procedures involve three steps. First, the molecular combining method is used to fabricate double-stranded DNA immobilized on Si chip. Then protonated aniline monomers are added and organized along the DNA chains. Finally, aniline momomers are polymerized along the DNA chains to form a PANI/DNA composite nanowires. Compared to previous reports on the fabrication of PANI/DNA complexes, this method prevents agglomeration of the DNA/PANI strands during the polymerization process, leading to the formation of 1D nanocomposites of PANI/DNA. The 1D morphology of the PANI/DNA complexes have been proved by AFM images, demonstrating that a thin layer less than 1 nm of PANI were fomed along the DNA templates. To obtain continuous and conductive DNA/PANI composite nanowires, a controlled acid solution with pH value around 4.0 was necessary to ensure the alignment of aniline monomer along the DNA templates. In addition to the HRP enzymatic polymerization approach, chemical polymerization oxidized by APS at moderate pH values and photo-oxidation using a ruthenium complex as a photooxidant has also been used to prepare DNA/PANI composite

nanowires [175]. AFM images showed that chemical polymerization using APS as an oxidant seems to provide the best 1D morphology of DNA/PANI nanocomposites either in solution or on a chip; while less uniform DNA/PANI composite nanostructures have been formed through the photo-oxidation method. Double-stranded DNA could also be immobilized on the conducting polymer nanofibers by post-treatment. Malhotra and co-workers demonstrated that DNA can be immobilized on the surface of PANI nanofibers using avidin-biotin as cross-linking agent [176]. SEM images exhibited increased bright streaks on the surface of PANI nanofibers, indicating the immobilization of fibrous DNA molecules. Mousavi and co-workers prepared PPy nanofibers with diameters in the range 30–90 nm by electropolymerization using a normal pulse voltammetry method [177]. After adsorption of DNA, new peaks attributed to the NH stretching vibration of nucleic acid bases, NH–N hydrogen bonds, guanine, cytosine, adenine and thymine were all observed, proving the formation of DNA/PPy nanocomposites. PPy nanotubes functionalized by carboxylic acid have also been used for the immobilization DNA [178]. The carboxylates on the surface of PPy nanotubes could act as binding sites for amino-terminal DNA. Confocal laser scanning microscopy (CLSM) images proved the successful DNA immobilization on PPy nanotubes.

Another nucleic acid, RNA, can also be used as a template for the formation of RNA/PANI composite nanowires [181]. First, the target microRNA (miRNA) is hybridized with peptide nucleic acid capture probes, resulting in a negatively charged surface. Then protonated aniline molecules are added and aligned around miRNA strands through electrostatic interaction. Similar with the formation of DNA/PANI complexes, PANI wraps around the miRNA template during the final polymerization process. A sizable increase in the conductivity of miRNA/PANI nanocomposites was observed after doping with HCl vapor. Compared to DNA/PANI composite nanowires, the morphology of miRNA/PANI nanocomposites comprises overlapped nanowires, dots and even short rods. This may be due to the short chain of the target miRNA used in this study and agglomeration of PANI nanowires owing to shielding of the negative charges on the miRNA template during the polymerization process.

In addition to nucleic acids, enzymes have also been incorporated into conducting a polymer matrix for biosensor applications. As a transducer, a conducting polymer can convert the chemical response into an electric current. To enhance the sensitivity and the response time, fabrication of 1D conducting polymers/enzyme nanocomposites with large surface area is a meaningful objective. Syu and Chang demonstrated the immobilization of urease onto PPy nanotubes over carbon paper substrate by a physical entrapment approach [182]. The composite electrodes exhibited a detection sensitivity for the determination of urea of 53.74 mV decade^{-1} and a detection limit on the urea concentration of 1.0 μM. Such values are superior to most biosensors of the same types reported in the literature. Furthermore, the composite electrode shows rapid response, storage stability and reusability. Lipase can also be covalently immobilized onto PANI nanotubes with diameters varying in the range of 120–275 nm via gultaraldehyde reactions [183]. High enzyme loading onto PANI nanotubes have been obtained for their fibrous network providing the increased surface area. The PANI/lipase composite nanotubes can be used as biosensors for triglyceride detection.

Disaccharide and polysaccharide have been employed as the templates for the preparation of 1D conducting polymer nanostructures. At the same time, disaccharide and polysaccharide have been incorporated into the conducting polymer matrix to form 1D conducting polymers nanocomposites [184–186]. Shinkai and co-workers demonstrated a polymer wrapping technique to fabricate PANI/schizophyllan (SPG) composite nanofibers [184]. SPG, a natural polysaccharide, can act as a host to assemble PANI into 1D nanostructures. TEM images showed that the diameter of the composite fibers was about 10–15 nm, indicating that several pieces of PANI were included in the SPG tubular cavity. Ge and co-workers prepared PPy/heparin composite nanowires using heparin as the morphology directing agent and an anion dopant [185]. The diameter of the composite nanowires was approximately 90–100 nm. The results suggested that the ratio of pyrrole to heparin had much effect on the formation and the size of composite nanowires.

Electrospinning provides a simple method for the fabrication of 1D conducting polymer/biological material nanocomposites. Before electrospinning, biological materials are co-dissolved in one solvent with polymers. During the evaporation of solvent in the electrospinning process, solid fibers composed of polymer and biological materials will form. Using such a technique, a natural protein, gelatin/PANI composite nanofibers have been fabricated for tissue engineering purposes [187]. The studies indicated that the average diameter of the composite fibers changed from 803 ± 121 to 61 ± 13 nm as the PANI fraction increased from 0 to 5% w/w (Fig. 8).

2.7. 1D conducting polymer nanocomposites with metal phthalocyanines and porphyrins

Generally, incorporating metal-phthalocyanines and porphyrins into conducting polymer matrix will decrease the conductivities of conducting polymers [188]. However, such composites will show some enhanced chemical or physical properties such as sensing for vapors in comparison with the conducting polymers alone [189,190]. It is well known that porphyrin tends to aggregate into J-aggregate mode and one-dimensional rod-like structure, which can be used as template for polymerization of momomers of conducting polymers to form 1D conducting polymers/porphyrin nanocomposites [191–193]. Shinkai and co-workers demonstrated the fabrication of PEDOT (PPy)/5,10,15,20-tetrakis(4-sulfonatophenyl) porphyrin (TPPS) composite nanorods using anionic TPPS aggregates as a template through electrochemical polymerization [194] (Fig. 9). Ultraviolet-visible (UV–vis) spectroscopy was used to characterize the aggregates of TPPS in the film made of PEDOT fibers. The results showed an exciton-coupling band (489 nm) and a Soret band (429 nm). The red-shift of the Soret band in relation to that in dilute aqueous solutions suggests that

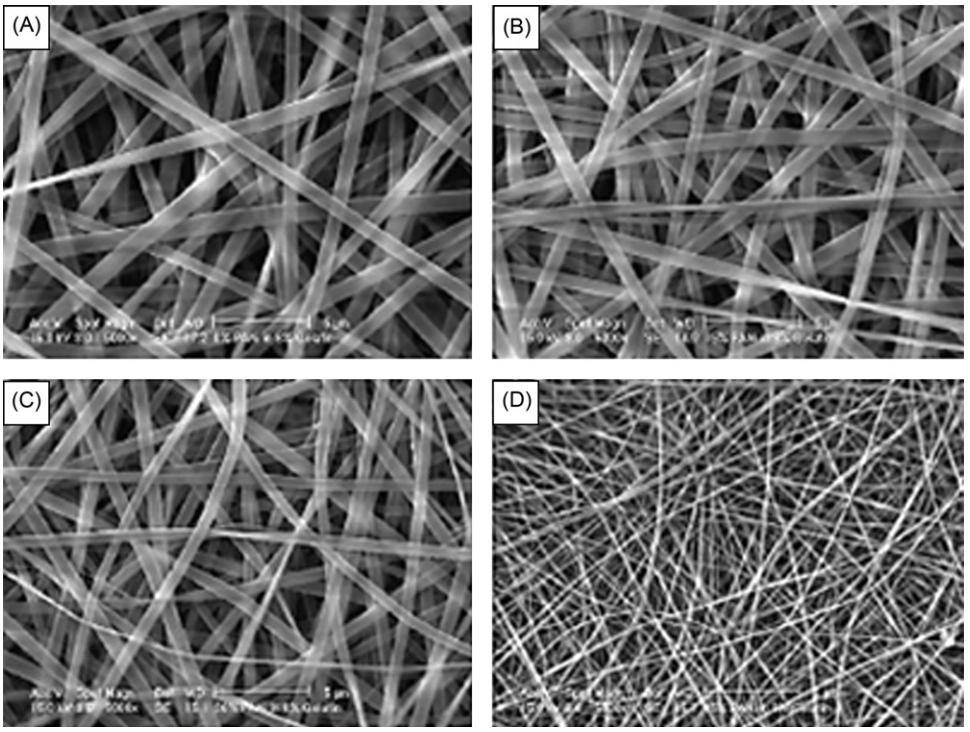

Fig. 8. SEM images of (A) gelatin fibers and PANI/gelatin composite fibers with ratios of (B) 15:85; (C) 30:70; (D) 60:40. Figure shows the fiber size decreases with increasing the concentration of PANI [187]. Copyright 2006, Elsevier Ltd.

TPPS was presented as the J-aggregates in the films of PEDOT fibers. Similar results were obtained for PPy/TPPS composite nanorods. SEM images gave a 30–50 nm diameter and 300–500 nm length of PEDOT/TPPS composite nanorods; while PPy/TPPS composite nanofibers had a 50–80 nm diameter and 300–500 nm length. The template approach for the fabrication of 1D PEDOT/porphyrin nanocomposites affords a good chance to combine the electronic and steric properties of porphyrin and conductive properties of conducting polymers. The PANI/porphyrin nanocomposites have been fabricated using the similar approach [195,196]. To extend the functionalities of the 1D nanocomposites, metalloporphyrin has also been used as template to synthesize 1D conducting polymer/cobalt porphyrin nanocomposites through electrochemical polymerization. Similar to porphyrin, cobalt porphyrin can also form J-aggregates, and many rod-like structures have been observed after dispersing their aqueous solution onto freshly cleaved mica. An electrochemically polymerization forming PPy was templated by J-aggregates of cobalt porphyrin to form 1D PPy/cobalt porphyrin nanocomposites in the presence of cobalt porphyrin in the pyrrole solution [197]. The diameter of the as-synthesized PPy/cobalt porphyrin composite nanorods was around 50 nm when the cobalt porphyrin solution was ultrosonicated for at least 3 h before the electropolymerization of pyrrole on the electrode surface. In the presence of cobalt porphyrin, the composite nanorods exhibited excellent electrocatalytic activity. Such composite nanorods of PPy/cobalt porphyrin may also be applicable in energy storage systems, biofuel cells, electrochemical and biosensors. The same group also prepared 1D PANI/cobalt porphyrin nanocomposite, using the same strategy [198]. The as-synthesized PANI/cobalt porphyrin composite nanorods had a diameter of 30–50 nm and a length of about 500 nm. The results of the fabrication of 1D conducting polymer/porphyrin (metal porphyrin) nanocomposites have several important

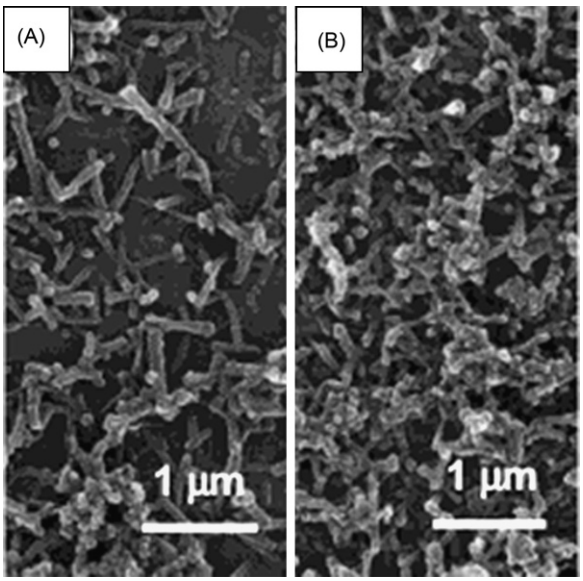

Fig. 9. SEM images of the as-synthesized PEDOT films electropolymerized at each scan rate: (a) 10, (b) 200 mV s^{-1} [194]. Copyright 2003, American Chemical Society.

lines of significance: namely, (1) 1D conducting polymer nanocomposites can be easily synthesized by applying J-aggregates of porphyrin (metal porphyrin) as templates; (2) the produced nanocomposites combine the conductivities of conducting polymers and the photoluminescence or electrocatalytic properties (or more other properties), providing a multifunctional nanomaterials; (3) 1D conducting polymers/porphyrin (metal porphyrin) nanocomposites could also be converted into 1D conducting polymer nanostructures by dissolving porphyrin (metal porphyrin) completely. It is reasonable to believe that this concept will be a landmark reference for the fabrication of 1D multifunctional nanomaterials.

2.8. 1D conducting polymer nanocomposites with multi-components

As discussed in the preceding sections, many materials have been combined with conducting polymers to form 1D nanocomposites. However, those nanocomposites only include one other component in addition to the conducting polymers. To achieve multifunctional materials, two or more than two nanocomponents are sometimes combined with conducting polymers to form 1D nanocomposites. For example, incorporating noble metal and magnetic nanoparticles into conducting polymer matrix may produce a nanocomposite with conductive, magnetic and catalytic properties. Among many kinds of 1D multicomponent nanocomposites, CNTs/conducting polymers coaxial nanocables are often employed for loading other functional nanoparticles. For example, metal and Fe_3O_4 nanoparticles are common functional nanoparticles to combine with CNTs/conducting polymer coaxial nanocables for catalytic or biosensor applications. Lee et al. prepared 1D PANI/CNTs/Au nanocomposites through a one-pot synthesis in the presence of γ-irradiation [199]. In a typical preparation, a solution containing aniline, single walled CNTs (SWNTs), CTAB, $HAuCl_4$, and HCl was irradiated by γ-ray (Co-60 source) to a total dose of 3 kGy at room temperature, resulting in the formation of 1D PANI/CNT/Au nanocomposites. TEM images showed that Au nanoparticles with a diameter of about 5 nm were decorated on the surface or entrapped in the layer of CNT/PANI nanocomposites, however, the morphology of the 1D CNT/PANI/Au nanocoposites was not very uniform. Ramaprabhu and co-workers demonstrated the fabrication of 1D CNT/PPy/Co nanocomposites via a multi-step method [200]. First, MWNTs were functionalized with carboxyl, carbonyl and hydroxyl groups by ultrasonication them in aqua regia solution for 2 h. Then coaxial MWNT/PPy nanocomposites were synthesized by chemical oxidative polymerization of pyrrole on the surface of functionalized MWNTs. At last, Co nanoparticles were deposited on the surface of coaxial MWNT/PPy nanocomposites through the reduction of cobalt nitrate by sodium borohydride in alkali solution at 80 °C. Microscopic studies have shown that a uniform dispersion of PPy was coated on the surface of MWNTs, and Co nanoparticles were well dispersed over MWNT/PPy composites. Performance studies showed that 1D MWNT/PPy/Co nanocomposites exhibited good durability for oxygen reduction activity.

In addition to metal, Fe_3O_4 nanoparticles are usually decorated on the surface or incorporated inside 1D CNTs/conducting polymer coaxial nanocomposites to form electromagnetic functional materials. Zhang et al. demonstrated the fabrication of CNT/PANI/Fe_3O_4 composite nanotubes in two steps [201]. Nanoparticles of Fe_3O_4 were achored on the surface of MWNTs via an *in situ* approach. Then the CNT/Fe_3O_4 nanocomposites were decorated with a thin PANI layer through a self-assembly process. Microscopic results proved the core-sheath structure of MWNT/PANI/Fe_3O_4 nanocomposites and the attachment of Fe_3O_4 nanoparticles with an average diameter of around 17.6 nm. The molar ratio of the oxidant to aniline monomer and the concentration of the monomer had a significant effect on the morphologies of the resultant MWNT/PANI/Fe_3O_4 nanocomposites. Chen and co-workers prepared 1D CNT/PANI/Fe_3O_4 nanocomposites and used them as electrochemical biosensors [202]. Wu et al. prepared 1D CNT/PPy/Fe_3O_4 nanocomposites through a different synthetic strategy [203]. They synthesized mono-dispersed Fe_3O_4 nanoparticles with a diameter of about 4 nm first. Then Fe_3O_4 nanoparticles were coated onto functionalized MWNT through weak interactions between Fe_3O_4 nanoparticles and the carboxyl, carbonyl and hydroxyl groups on the surface of MWNTs. Finally, PPy coatings were synthesized through *in situ* chemical oxidative polymerization in the presence of an anionic surfactant, e.g., sodium bis(2-ethylhexyl) sulfosuccinate (AOT). The average diameter of the as-synthesized 1D CNT/PPy/Fe_3O_4 nanocomposites ranged from 90 to 110 nm.

As mentioned above, 1D composite nanomaterials composed of conducting polymers and insulating polymers can be readily prepared by co-evaporation electrospinning technique [204–206]. If one dissolves or disperses one or more nanocomponents in the electrospining solution system containing conducting and insulating polymers, multi-component 1D conducting polymer nanocomposites will be obtained after electrospinning process. For example, PANI/PEO/MWNTs composite nanofibers have been fabricated by electrospinning the solutions of their blends [204]. TEM images showed that MWNTs with a diameter in the range 10–20 nm were dispersed inside PANI/PEO composite fibers, without substantial aggregation. The good dispersion of MWNTs in the conducting polymer matrix is achieved through the direct interactions between MWNTs and conducting polymers. Using a similar procedure, photoluminescent CdS quantum dots (QDs) can also be incorporated into PANI/PEO composite nanofibers [205]. CdS QDs with a size range below 6 nm have been proved to be homogenously distributed within the composite fibers. The average diameter of the as-prepared PANI/PEO/CdS composite nanofibers was around 450 nm. Enhanced photoluminescence properties have been observed in such a 1D electrospun nanocomposite, discussed in detail in the next section. Assisted by the electrospinning technique, 1D conducting polymer nanocomposites with multi-components may also be fabricated via gas phase polymerization [207]. This process is similar to that for the fabrication of two component nanocomposites. TiO_2/ZnO composite nanofibers have been prepared by electrospinning technique followed by the calcination process. After the adsorption of

$FeCl_3$ on the surface of electrospun TiO_2/ZnO composite fibers, PPy layer can be generated on their surface through vapor-phase polymerization. This synthetic strategy can be extended to the fabrication of other kinds of 1D conducting polymer nanocomposites with multi-components.

3. Properties of 1D conducting polymers nanocomposites

Compared to conducting polymers alone, 1D conducting polymer nanocomposites exhibit not only the conduction properties of conducting polymers, but also the physical or chemical or biological properties of other nanocomponents, and even some unexpected properties because of synergistic effects of the components. In this section, we describe in detail some representative properties of 1D conducting polymer nanocomposites, including spectral, electronic, magnetic, wetting, and optical properties, as well as specific surface area.

3.1. Spectral properties

3.1.1. Fourier transmission infrared (FTIR) and Raman spectra

1D conducting polymer nanocomposites have the characteristic absorption bands of conducting polymers, which can be readily established by the FTIR and Raman spectroscopy. In some cases, there are differences in the spectral properties between 1D conducting polymer nanocomposites and the neat conducting polymers because of the incorporation of one or more other nanocomponents. In general, the spectral properties of conducting polymers are quite complicated. On one hand, the backbone structure is distinct for different kinds of conducting polymers, and on the other hand, most conducting polymers have different types of reversible oxidation/reduction and doping/dedoping states. Herein, we discuss mainly some spectral properties alterred after introducing nanocomponents into conducting polymers.

Ćirić-Marjanović et al. studied the FTIR and Raman spectra of PANI/silica composite nanotubes synthesized by a self-assembly process [136]. Obviously, both the characteristic bands of PANI and silica in the FTIR spectra were observed in PANI/silica composite nanotubes. For example, the quinonoid (Q) and benzenoid (B) ring stretchings appeared at ~1580-1570 and ~1493 cm^{-1}, indicating the formation of emeraldine salt state of PANI in the PANI/silica composite nanotubes. After deprotonation by ammonium hydroxide, these two bands shifted to ~1590 and ~1504 cm^{-1}, respectively. Two additional typical bands observed at 1397 cm^{-1} and 1300–1308 cm^{-1} in the FTIR spectra of PANI/silica composite nanotubes are attributed to the C–N stretching vibration and C–N stretching of secondary aromatic amine in the emeraldine base of PANI. Furthermore, the PANI bands at 1568 and 1302 cm^{-1} shifted to 1581 and 1308 cm^{-1} when the weight ratio of silica to aniline was increased from 0.02 to 2.0, indicating the enhanced strong interactions between PANI chains and silica. Upon doping (i.e., protonation), the FTIR spectra of the PANI/silica composite nanotubes showed two bands due to the C–NH^+ stretching and the stretching of –NH^+= (in the B–NH^+=Q segment) at ~1244 and ~1146 cm^{-1}, respectively, which confirmed the formation of emeraldine salt state of PANI. Surprisingly, the two bands at ~1244 and ~1146 cm^{-1} could still be observed after dedoping (i.e., deprotanation), suggesting NH^+–$^-$O–Si^+ and NH^+–$^-$O–Si^+ interactions between PANI and silica. In addition to the bands of PANI, the typical stretching and deformation vibrations of Si–O–Si at 1105, 810, and 474 cm^{-1} have also been observed, indicating the formation of 1D PANI/silica nanocomposites. Similar to the FTIR spectra, typical Raman bands of PANI were observed in PANI/silica composite nanotubes. In particular, the observation of band at 1343-1338 cm^{-1} ascribed to the C–$NH^{\bullet+}$ stretching indicates that the PANI/silica composite nanotubes are in the doped state.

Lefrant et al. reported the vibrational properties of SWNT/PANI and SWNT/PEDOT composite nanotubes by means of FTIR and Raman spectroscopy [208]. The results showed that the vibrational properties depended on the preparation method. For the 1D SWNT/PANI nanocomposites synthesized by electrochemical polymerization approach, the intensity of Raman band associated with the radial breathing modes of bundled tubes at 178 cm^{-1} increased gradually as the number of cycles increased from 25 to 75, while the radial breathing modes of isolated tubes at 164 cm^{-1} decreased sharply, indicating that additional roping of nanotubes with PANI took place. A decrease in the intensity of the Raman band at 178 cm^{-1} was observed as the number of cycles was increased from 100 to ca. 300. After 300 cycles, the Raman spectrum exhibited the dominated features of emeraldine salt state of PANI. In the FTIR spectra, besides the typical bands of PANI, two new adsorption bands associated with deformation vibrations of the benzenoid and quinoid ring at ~770 and 740 cm^{-1} were observed, which was attributed to the strong hindrance effects induced by the strong interactions between SWNTs and PANI chain. The authors also studied the Raman spectra of SWNT/PEDOT composite nanotubes synthesized via electropolymerization. The results were similar to those with SWNT/PANI composite nanotubes in the 50–250 cm^{-1} spectral range; an up-shift of the radial breathing modes Raman line associated with individual and bundled tubes was observed. Typical adsorption bands of both PEDOT and SWNTs appeared in the 900–1780 cm^{-1} spectra range. The intensity of the PEDOT Raman signal increased with increasing numbers of cycles. The Raman spectra proved that the side walls of SWNTs were functionalized with PEDOT.

The vibrational properties 1D MWNT/PANI nanocomposites synthesized by ultrasonically assisted *in situ* chemical oxidative polymerization have been well studied [209]. As expected, the main bands attributed to the vibrations of PANI were all observed, while the specific peak of MWNTs was relatively weak for their existence as a core in the nanocomposites. Similar to the observations with the PANI/silica composite nanotubes, some of the characteristic bands of PANI shifted to higher frequency with increasing MWNTs content. For example, the C=N band shifted from 1120 cm^{-1} of pure PANI to 1140 cm^{-1}, and the C–$NH^{\bullet+}$ stretching vibration moved from 1235 to 1250 cm^{-1} in MWNT/PANI nanocomposites. Similar shifts have also been observed for C=C stretching vibration in

benzenoid and quinoid rings. Generally, the intensity of the C=C stretching vibration in benzenoid ring is smaller than that in quinoid ring for pure PANI. However, an inversed intensity ratio of benzenoid/quinoid was observed in the spectrum of MWNT/PANI nanocomposites. Moreover, the value of $I_{quinoid}/I_{benzenoid}$ increased with increasing MWNTs content in the MWNT/PANI nanocomposites, indicating the stronger interactions between MWNTs and the quinoid than the benzene ring. Raman spectra gave another evidence for the interactions between the two components in PANI/MWNTs. Compared to the spectra of pure PANI, the C–$NH^{\bullet+}$ stretching peak shifted from 1339 to 1350 cm^{-1} in the nanocomposites with more than 50 wt% MWNTs content, indicating the strong interactions between MWNTs and PANI.

3.1.2. UV–vis spectra

The electronic structure of 1D conducting polymer nanocomposites can be characterized by means of UV–vis spectroscopy. Generally, conducting polymers have a broad UV–vis adsorption band, due to the wide distribution of conjugated chain length of conducting polymers. For example, the UV–vis spectra of pure PANI in the emeraldine salt state usually display three distinct adsorption bands. One is centered at approximately 300–360 nm, attributed to a π–π^* electron transition within benzenoid segments. The second band is usually observed at around 400–450 nm, related to the polaron–π^* transition of PANI. The third absorption band which usually appears at wavelengths higher than 700 nm, with a long tail, is assigned to the π–polaron transition [50]. After combining with other components to form nanocomposites, the π–polaron transition is usually shifted to a lower wavelength, revealing interactions between nanocomponents and the quinoid rings of PANI. Our group has studied the UV–vis spectra of PANI/Fe_3O_4 composite nanotubes synthesized via ultrasonic assisted *in situ* polymerization method [129]. The characteristic bands of PANI ascribed to π–π^*, polaron–π^* and π–polaron transition were observed at ~280–340, ~400–450 and 780–900 nm, respectively. As the content of Fe_3O_4 was increased from 0 to 20 wt%, the π–polaron transition in the UV–vis adsorption spectra shifted from 870 to 830 nm, indicating strong interactions between PANI and Fe_3O_4. Furthermore, the dispersion state was also found to affect the UV–vis adsorption spectra of PANI/Fe_3O_4 composite nanotubes. The better dispersion of Fe_3O_4 nanoparticles in PANI matrix would lower the π–π^* transition in the UV–vis adsorption spectra.

In addition to 1D PANI/Fe_3O_4 nanocomposites, the UV–vis properties of 1D MWNT/PPy/Fe_3O_4 nanocomposites have been well studied, which yielded some insights of the interfacial interactions between PPy and Fe_3O_4 coated MWNTs [203]. For doped PPy, there are two characteristic absorption peaks. One is centered at around 467 nm, which is ascribed to the transition from the valence band to the antibonding polaron state. Another appears at >800 nm, with a long tail, attributed to π–polaron transition. The strong interaction between PPy and Fe_3O_4 coated MWNTs has been proved by the blue shift of the polaron–π transition. When the content of Fe_3O_4 was increased from 0 to 2.4 wt%, the polaron–π transition band shifted significantly from 467 to 431 nm, suggesting that the quinoid ring of PPy interacted strongly with Fe_3O_4 coated MWNTs.

3.1.3. Circular dichroism (CD) spectra

Chirality is an important subject in the field of chemistry, physics, materials science and especially biology [210–213]. Chiral conducting polymers have attracted much attention in the past decade for their potential applications in the field of sensors, chiral separation and surface-modified electrodes. It is commonly believed that the helical conformation of main chains could induce chirality. In many cases, the helical conformation of conducting polymer chains is induced by a chiral dopant or a chiral template. Akagi et al. demonstrated the fabrication of helical PA fibers using chiral nematic (N^*) liquid crystals (LCs) as templates [214]. The helical conformation exhibited induced circular dichroism (ICD) in CD spectra. The PA fibers synthesized in the presence of (R)- and (S)-chiral nematic LCs exhibited positive and negative Cotton effects, respectively, in the region from 450 to 800 nm, indicating that the chains of PA fibers were helically screwed. Furthermore, the positive Cotton effect was bigger than the negative one, showing the degree of helicity in R–PA chain was more than that in the S–PA. The SEM images showed the helical fibrillar morphologies of the as-prepared PA with counterclockwise and clockwise directions, consistent with the CD spectra.

In addition to PA, optically active PANI and PPy nanocomposites were widely studied because their helical conformation can be easily induced by chiral dopants. D- or L-CSA is the most used chiral dopant for the formation of chiral PANI, PPy and their nanocomposites because it could induce the helical conformation of PANI and PPy by either post processing or *in situ* polymerization methods. Wang and co-workers prepared chiral PANI/PAA/CSA nanocomposites using PAA as a template and CSA as chiral inducing agent [215]. The CD spectra of as-synthesized PANI/PAA/CSA nanocomposites exhibited their peaks. The first peak at 290 nm can be attributed to (+)-CSA. The other two peaks at 440 and 500–800 nm resulted from the chiral PANI. In order to establish this, the CD spectrum of PANI/PAA nanocomposites was also studied after removing the chiral CSA dopant; the CD peaks from PANI remained, indicating that chirality of PANI/PAA/CSA originated from the chiral conformation of the polymer, not the existence of chiral CSA molecules. To achieve the PANI nanocomposites with high chirality, the authors developed an aniline oligomer-assisted polymerization method to prepare PANI/CSA nanofibers [216]. Aniline oligomers have lower redox potentials, which accelerates the polymerization reaction and can they be used as the initiators or seeds for the growth of chiral PANI. The results showed that the as-synthesized PANI/CSA nanofibers had stronger chirality than the PANI/CSA synthesized in the absence of the aniline oligomer. Furthermore, the high chirality remained after the CSA was removed. In order to avoid the persulfate and sulfate ions competing with chiral CSA in the chemical oxidation polymerization, which could lessen the chirality of PANI, the electrochemical polymerization was also used to prepare films of optically active PANI/CSA nanofibers

[217]. The results exhibited an anisotropic factor of 25% higher than that of synthesized via a chemical polymerization method.

Wei and co-workers clearly observed helical PANI nanofibers induced by large amounts of chiral CSA as dopants [218]. SEM images showed that the dopant D-CSA induced right-handed helical PANI nanofibers, while L-CSA produced left-handed helical PANI nanofibers. The corresponding CD spectra of the two kinds of PANI nanofibers were mirror images. The peaks at 420 and 780 nm which corresponds to the π–π^* transition of the polarons in chiral PANI were observed. Moreover, the extent of the chirality was related to the concentration of aniline and the molar ratio of CSA to aniline. A high chirality of PANI nanofibers can be obtained at the concentration of aniline = 0.05 M and the molar ratio of CSA to aniline = 80. In addition to CSA, the chirality could also be induced by other chiral molecules, such as dextran sulfate, 2-pyrrolidone-5-carboxylic acid, etc [219,220].

The chirality of CSA doped conducting polymers/CNTs composite nanofibers has been widely studied for their multi-functionality. As the first example, chiral CNT/PANI composite nanofibers were synthesized by an *in situ* polymerization approach with optically active CSA as the dopant [221]. The CD spectra of CSA doped CNT/PANI composite nanofibers exhibited optical activity with bands at 424, 458 and 748 nm, similar to that for CSA doped PANI, indicating that the CNTs did not inhibit the optical activity of conducting polymers. Unfortunately, the CSA doped CNTs/conducting polymer composite nanofibers prepared by this *in situ* polymerization method had low absolute stereochemical selectivity. To enhance the chirality of CNTs/conducting polymer composite nanofibers, aniline oligomer was added to the reaction system during the chemical polymerization [222–224]. The CD spectra of such composite nanofibers dispersed in aqueous media confirmed enhanced absolute stereochemical selectivity (Fig. 10). The presence of CNTs had significant effect on the absolute stereochemical selectivity for the composite nanofibers. The highest absolute stereochemical selectivity was obtained with a 0.5:100 weight ratio of CNTs to aniline [222]. The as-prepared chiral CNT/PANI composite nanofibers under the above optimized conditions had a high anisotropy factor of 1.098×10^{-2}, 25% higher than that for chiral PANI nanofibers in the absence of CNTs.

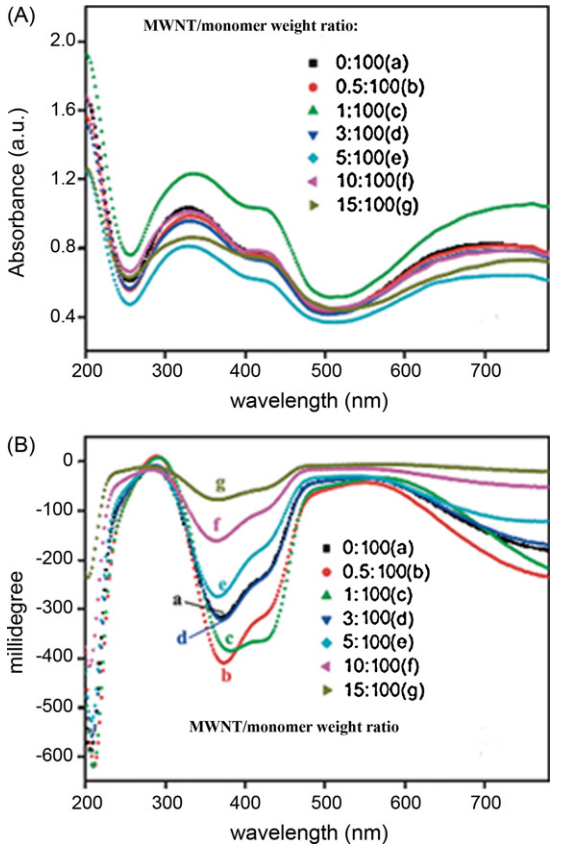

Fig. 10. (A) UV and (B) normalized CD spectra of PANI/MWNT nanocomposite with different weight ratio of MWNT/aniline in aqueous solution [222]. Copyright 2007, Wiley-VCH Verlag GmbH&Co. KGaA, Weinheim.

3.2. Electrically conductive properties

After doping, the electrical conductivity of conducting polymers can reach as high as 10^0 to 10^4 S/cm, nearly in the "metallic" conducting regime. In particular, the 1D nanostructures of conducting polymers have much higher electrical conductivities than their powders. For example, Martin prepared 1D PANI nanostructures by a hard templated method and studied their electrical conductivities [14]. The results showed that the electrical conductivity of a single nanofiber one or two orders of magnitude larger than the maerial in pellet nanotubes or nanowires. Furthermore, the conductivity of 1D PANI nanostructures increased with a decrease in diameter, exhibiting a size effect on the conductivity. Chen and co-workers studied the electrical conductivity of PANI nanotubes synthesized by a template free approach [225]. In comparison to nanotube pellet, it was found that the conductivity of a single nanotube was enhanced by two orders of magnitude.

Combining another component with conducting polymers will enhance or decrease their electrical conductivities. Generally, incorporating an insulating component into 1D conducting polymer nanomaterials will decrease the electrical conductivity because of the partial blockage of conductive path by the insulating component. A typical example is 1D conducting polymer/Fe_3O_4 composite nanofibers synthesized by a self-assembly process [226]. The results showed that the resistivity of NSA doped PANI/Fe_3O_4 composite nanowire pellets increased with decreasing temperature, which is a typical semiconducting behavior. The electrical conductivity of NSA doped PANI nanotubes in the absence of Fe_3O_4 was 0.154 S/cm, which decreased to 0.13 and 0.045 S/cm after combining with 6 and 20 wt% Fe_3O_4 nanoparticles, respectively. The decrease of the composite conductivity is attributed to the increased charge carrier scattering between NSA doped PANI and Fe_3O_4 nanoparticles. Furthermore, the conductivity of PANI/Fe_3O_4 decreased with decreasing temperature, following quasi-1D the variable range hopping conduction model. As the Fe_3O_4 nanoparticles embeded in the PANI matrix interrupted the doping process, interactions

between Fe_3O_4 and PANI increased the localization of charge carriers, and thus increased the resistivity of the sample, similar to the behavior of the system of polyaniline and Na^+-montmorillonite clay nanocomposite [227]. A similar decrease in electrical conductivity was also observed in various kinds of 1D conducting polymer nanocomposite systems [133,151].

On the hand, incorporating another nanocomponent with high electrical conductivity into conducting polymers may enhance the conductivity of nanocomposites. Generally, CNTs have much higher electrical conductivity than most of conducting polymers, such as PANI and PPy. The CNTs could serve as a "conducting bridge" between conducting domains after their introduction to the conducting polymers, thus enhance the electrical conductivities of conducting polymers [228–230]. Chen and co-workers have studied the electrical conductivities CNT/PANI composite nanocables in detail [231]. The conductivity of pure PANI was 1.1×10^{-2} S/cm, increasing to 1.27 S/cm with 24.8 wt% CNTs loading. Meanwhile, the temperature dependence of conductivity became weaker with increasing CNT loading. It was believed that the strong interactions between CNTs and PANI chains played an important role in the enhancement of the electronic properties of PANI because they increased the delocalization length of CNT/PANI composite nanocables. The conductivity of well aligned CNT/PANI nanocomposites synthesized by *in situ* polymerization has also been fully studied [232]. It was found that the room temperature conductivity was enhanced by one order of magnitude compared with that of PANI. Furthermore, the conductivity of well aligned CNT/PANI nanocomposites decreased with decreasing temperature, indicating a typical semiconductor behavior. Similar results have also been obtained for the CNT/PPy composite nanocables [233]. The conductivity increased from 7.3×10^{-3} to 0.23 S/cm as the CNT loading increased from 0 to 23.1%, representing an increase by two orders of magnitude. The results from temperature dependence of the conductivity indicated a percolation threshold in CNT/PPy composite nanocables between 15 and 20 wt%.

In addition to CNTs, incorporation of metal nanoparticles into conducting polymers can also enhance the electrical conductivity of conducting polymers [126]. Similar to the functions of CNTs, metal nanoparticles could also act as a "conducting bridge" between conducting polymer domains to enhance the electric properties of conducting polymers. For example, there was an increase by 50 times in electrical conductivity for PANI/Au composite nanofibers. The typical value of the electrical conductivity for the PANI nanofibers oxidized by APS was 0.02 S/cm, whereas that of PANI/Au composite nanofibers synthesized by γ rays irradiation method reaches about 1 S/cm. The electrical conductivity of a single Au/PANI nanocables synthesized via a self-assembly process has also been investigated [122,234]. The results showed that the conductivity of as-synthesized Au/PANI nanocables, about 77.2 S/cm, was much higher than the 31.4 S/cm of a single CSA doped PANI nanotubes (Fig. 11). These results fully demonstrated that the electrical conductivity of conducting polymers can be further improved by embedding metal nanoparticles.

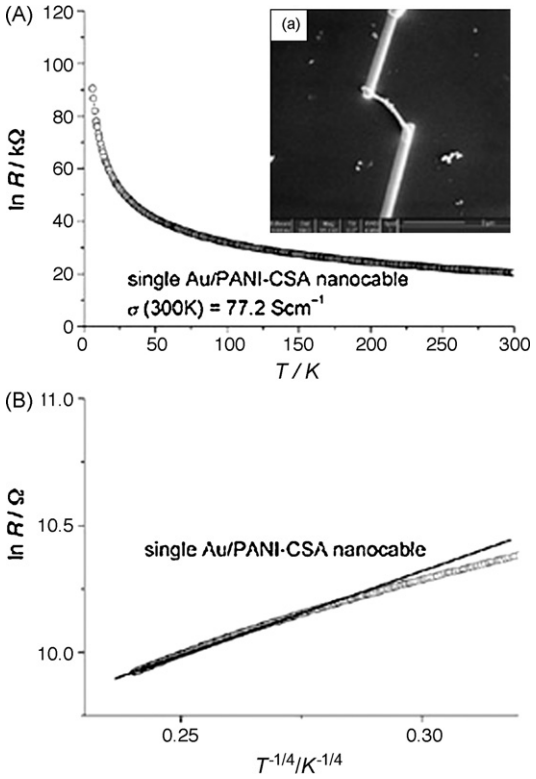

Fig. 11. (A) Temperature dependence of the resistance of the typical single Au/PANI nanocable. (B) Plot of $\ln R(T)$ versus $T^{-1/4}$ (R was measured in Ohms). Inset: SEM image of the fabrication of a single Au/PANI nanocable and one pair of Pt microleads [122]. Copyright 2006, Wiley-VCH Verlag GmbH&Co. KGaA, Weinheim.

3.3. Magnetic properties

The magnetic properties of conducting polymers have been extensively studied because they provide important information on charge carrying species and unpaired spins [235–238]. However, the usually very low magnetic susceptibility limits their practical applications. Composite nanomaterials containing conducting polymers and magnetic nanoparticles such as iron oxides have good electromagnetic functions, which can be applicable in electro-chromic devices, electromagnetic interference shielding, and nonlinear optical systems. Our group has studied the magnetic properties of PANI/Fe_3O_4 composite nanotubes synthesized by an ultrasonic irradiation technique [129]. These composite nanotubes showed a superparamagnetic behavior with zero coercive force (H_c), and a saturated magnetization (M_s) of 8 and 12 emu/g at room temperature for samples containing 10 and 20 wt% Fe_3O_4 nanoparticles, respectively. The superparamagnetism of as-synthesized PANI/Fe_3O_4 composite nanotubes was attributed to the grain size of Fe_3O_4 nanoparticles decreasing to a critical size (an order of 10 nm). Long et al. studied the magnetic properties of PANI/Fe_3O_4 composite nanorods prepared via a self-assembly technique [226]. The results showed that the coercive force was 55–65 Oe at room temperature, which may be due to large size or aggregation of a few Fe_3O_4 nanoparticles. The satu-

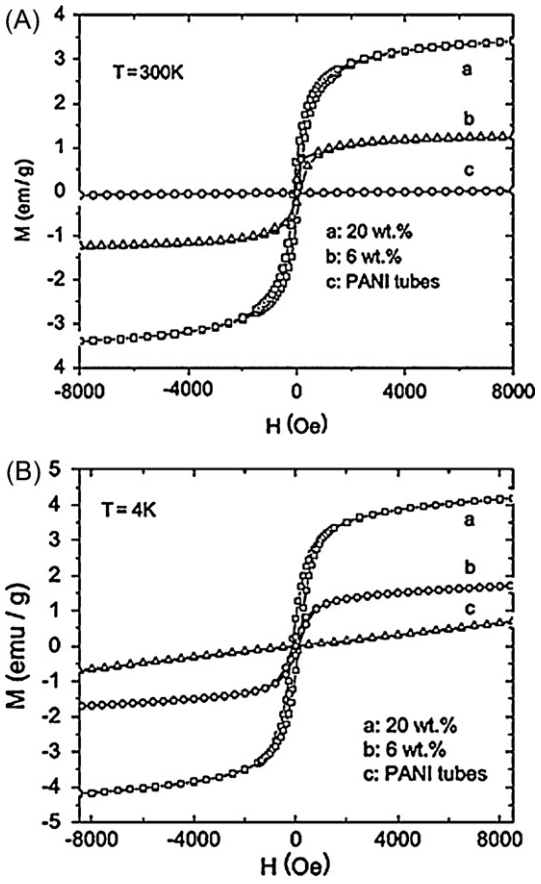

Fig. 12. Magnetization as a function of the applied field plots at (A) 300 K and (B) 4 K for PANI/Fe_3O_4 nanostructures [226]. Copyright 2005, Elsevier B.V.

rated magnetization of PANI/Fe_3O_4 composite nanorods containing 20 wt% Fe_3O_4 nanoparticles was 3.45 emu/g at 300 K, lower than that of our sample [129]. The low saturated magnetization may be due to a weak interaction between PANI and Fe_3O_4 nanoparticles. Compared to the self-assembly method, the samples synthesized through ultrasonic irradiation technique facilitate the dispersion of Fe_3O_4 nanoparticles. Furthermore, the addition of aniline dimmer-COOH enhanced the interactions between PANI and Fe_3O_4 nanoparticles, which increased the saturated magnetization. Long et al. also studied the magnetic properties of PANI/Fe_3O_4 composite nanorods at lower temperatures [226]. At 4 K, both the H_c and M_s increased. For example, the H_c and M_s reached 110 Oe and 4.21 emu/g, respectively, for PANI/Fe_3O_4 composite nanorods containing 20 wt% Fe_3O_4 nanoparticles (Fig. 12). The increase of the H_c and M_s was related to the frozen of the magnetic moments. The magnetic susceptibility of the composite nanorods was also measured. Compared to pure Fe_3O_4 nanoparticles, the peak temperature of the AC magnetic susceptibility of the composite nanorods shifted to a higher temperature because more thermal energy was needed to overcome the interactions between PANI and Fe_3O_4 nanoparticles.

In addition to 1D PANI/Fe_3O_4 nanocomposites, the magnetic properties of PANI/Fe_2O_3 composite nanoneedles have been well studied [127]. Different from PANI/Fe_3O_4 nanotubes and nanorods, PANI/Fe_2O_3 composite nanoneedles exhibited a ferromagnetic behavior. For PANI/Fe_2O_3 composite nanoneedles containing 33.3 wt% Fe_2O_3, the H_c and M_s were 416 Oe and 16 emu/g, respectively. Compared with pure Fe_2O_3 nanorods, the H_c increased because of the interactions between polaron PANI and Fe_2O_3 needles. The magnetic properties of 1D conducting polymers/Fe, Co, Ni nanocomposites have also been extensively studied [109–111]. The coercivity and remanence of the composites generally showed a characteristic of high anisotropy. As an example, for PANI/Co nanocomposite, when an applied field is parallel to PANI/Co composite nanowires, remanence reaches a maximum; while a maximum H_c was obtained with an applied field perpendicular to the PANI/Co composite nanowires.

3.4. Optical properties

As an emerging class of materials, nanostructured semiconductors have been extensively explored over the past decades for their unique tunable optical properties, which are potentially applicable in nanophotonic devices. In particular, 1D nanostructured semiconductors exhibit photonic confinement in two dimensions, suitable for the fabrication of photodetectors, photochemical sensors, and photonic wire lasers [239–242]. On the other hand, the introduction of a second phase of conjugated polymers could further modify physical and chemical properties of semiconductors. Lin and co-workers studied the optical properties of CdS/PANI composite nanocables synthesized by electrochemical technique [146]. The photoluminescence spectrum of CdS/PANI composite nanocables had similar features to CdS nanowires, however, signal intensities were significantly enhanced (Fig. 13). Such a photoluminescence enhancement was due to the photo-generated carriers transfering from PANI layer into CdS nanowires. The conduction band edge of PANI was higher than that of CdS, while the valence band edge of PANI was lower than that of CdS. The photo-generated electrons of PANI transfer to the conduction band of CdS, and the photo-generated holes of PANI transfer to the valence band of CdS. Compared to pure CdS nanowires, the total concentration of carriers of CdS increased greatly in CdS/PANI composite nanocables, enhancing the photoluminescence properties of composites. The increased optical properties of semiconductors by conducting polymers have also been observed in 1D electrospun PEO/PANI/CdS three-component systems [205]. Similarly, the photoluminescence intensity of the semiconductor has been increased remarkably by introducing the component of conducting polymers. The mechanism of the photoluminescence enhancement was similar to that of CdS/PANI composite nanocables, attributed to separation of the photo-generated electrons and holes. Furthermore, a blue shift in the photoluminescence spectra was also observed, attributed to the increase in the emissive energy. In addition to sulfide semiconductors, it was reported that composites of carbon nanomateri-

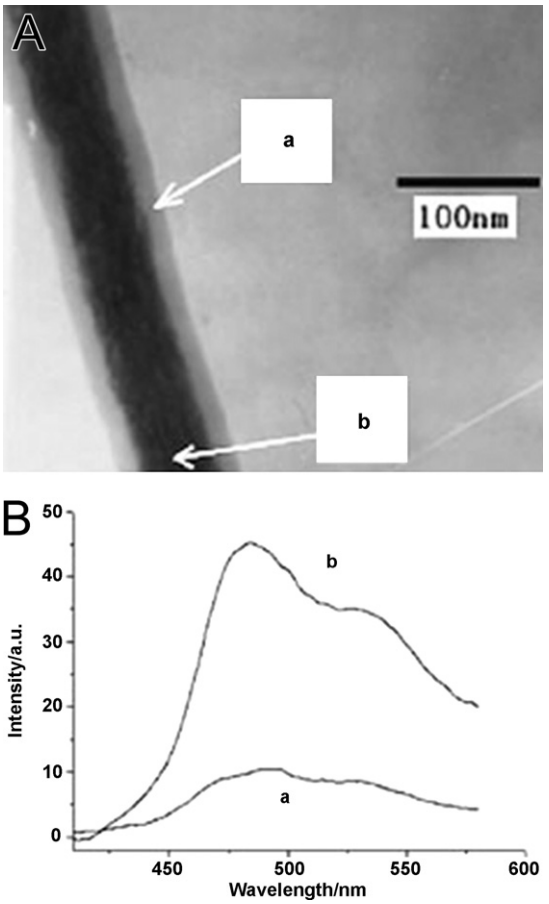

Fig. 13. (A) TEM image of CdS/PANI coaxial nanocable: (a) PANI sheath, (b) CdS core. (B) Photoluminescence spectra of CdS nanowires and CdS/PANI coaxial nanocable in distilled water. (The samples was immersed in 0.5 M NaOH solution and then washed with water several times, excitation wavelength = 300 nm) [146]. Copyright 2005, Elsevier B.V.

als with conjugated polymers had promise for application in photovoltaic devices [243]. However, the PL efficiency reduced drastically after introducing CNT into a PPV matrix. The reduction of the PL efficiency can be ascribed to the transfer of excitons and partial hole from PPV chains to MWNTs, together with scattering and absorption by the MWNTs.

The photoluminescence properties of 1D PMMA/P3HT composite fibers with core-sheath structure have also been investigated, exhibiting an interesting time-dependent characteristic [164]. The emission maxima of the as-synthesized PMMA/P3HT composite nanofibers located at 667 nm after one day, while it shifted to 567 and 507 nm upon exposure to air under light for 1 and 2 weeks, respectively. The blue shift of the luminescence spectra was attributed to the reduced conjugated length of P3HT as a result of chain scission. As shown by electron paramagnetic resonance spectra, on exposure to air under light, P3HT photo-degrades, and then forms a P3HT•O_2 charge-transfer complex. More interesting, the composite nanofibers showed much better sensitivity than that of the spin-coated P3HT film, which could be due to the porous structures and large surface area of the membrane of composite fibers.

3.5. Wettability

Wettability is one of most important properties to a solid surface, relevant in myriad applications including self-cleaning surfaces, microfluidics, controlled drug delivery, and bio-separation [244–246]. Wetting properties rely on the chemical composition and topographic structure of the solid surface. In the past several years, the wettability of conducting polymers has been widely studied. Generally, conducting polymers are hydrophilic, even in film formed of nanofibers. For example, the contact angle (CA) of PANI with sub-micro/nanostructured dendrites immobilized on poly(propylene) film grafting with PAA was close to 0°, exhibiting a superhydrophilic properties [247]. The PPy nanowires film doped by organic diacids or triacid synthesized in the presence of cationic surfactant (hexadecyltrimethylammonium bromide) also showed a superhydrophilic property with a CA about 0° [248]. As mentioned above, the wetting properties can be governed by both chemical composition and geometrical microstructure. A film of conducting polymers with superhydrophobic (CA > 150°) properties can be fabricated by doping hydrophobic acids, such as perfluorooctane sulfonic acid (PFOSA) and the construction of micro- and nanostructures. For example, the CA of water sphere formed on rambutan-like PANI hollow spheres doped with PFOSA could reach as high as 164.5°, revealing the superhydrophobic nature [249]. Similarly, the water CA on the surface of the dandelion-like microstructures was estimated to be ca. 152.3°, also exhibiting superhydrophobic characteristics [250]. A reversibly switchable superhydrophobic and superhydrophilic surface can also be observed by controlling the chemical composition of conducting polymers (doping with PFOSA and dedoping) [251,252].

Incorporating a second inorganic component into conducting polymers will enhance their CA [128]. The CA of NSA doped PANI nanotubes was estimated to be ca. 53.5°, showing hydrophilic properties. After introducing TiO_2 nanoparticles in PANI nanotubes, the composites exhibited an increased CA, about 98.5° at the concentration of TiO_2 = 0.08 M. Although the 1D nanocomposites of PANI/TiO_2 did not show a superhydrophobic charateristics, it was expected that such a research direction might provide a simple strategy for controlling the wettability of conducting polymers.

Combining a second polymer phase into conducting polymers to form membranes of composite nanofibers using electrospinning technique is another facile approach to fabricate a superhydrophobic surface. Jiang and coworkers have prepared azobenzenesulfonic acid doped PANI/PS composite film, which showed superhydrophobic properties with a CA larger than 150° [154]. The results exhibted that the wettability was correlated to the content of PS. When the content of PS increased from 4.53 to 7.10%, the CA for water decreased slightly from $166.5 \pm 2.4°$ to $154 \pm 2.1°$, due to the change of the roughness, and consistent with the PS content. Furthermore,

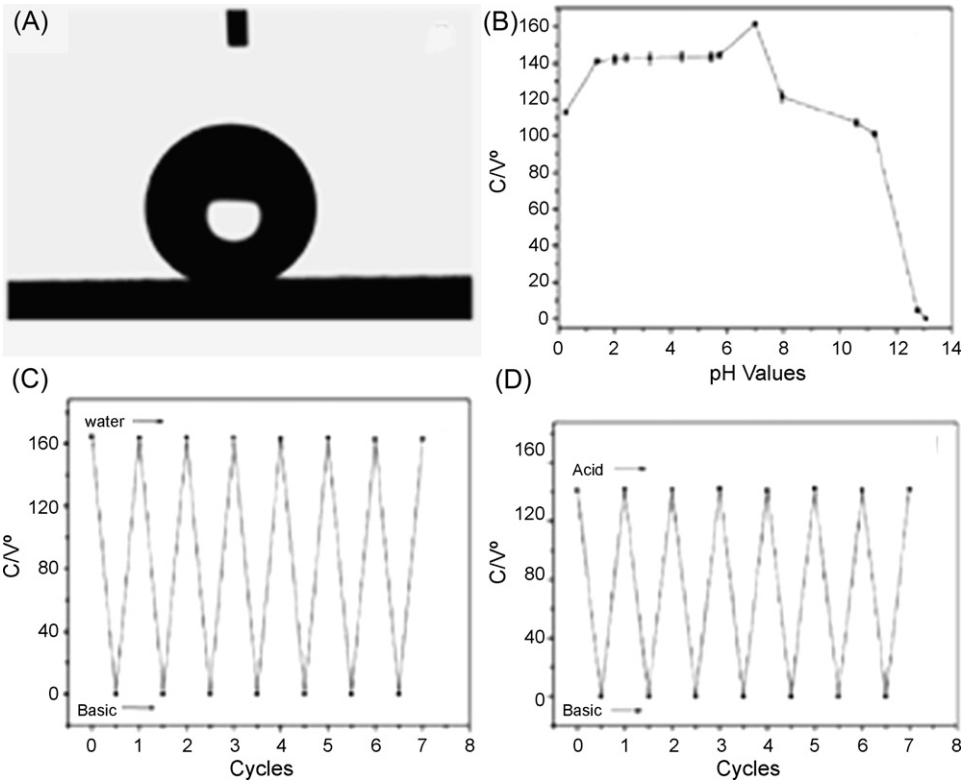

Fig. 14. (A) Water droplet on the surface of PAN/PANI coaxial nanofibers, showing a superhydrophobic characteristic; (B) the relationship between the CAs and pH values on the PFOS doped PANI/PAN coaxial nanofibers. (C) Reversible superhydrophobicity/superhydrophilicity for a water droplet and a basic droplet with pH 13.07 on the surface of PFOS doped PAN/PANI coaxial nanofibers. (D) Reversible superhydrophobicity/superhydrophilicity for an acidic (pH 1.02) and a basic droplet (pH 13.07) on the surface of PFOS doped PAN/PANI coaxial nanofibers [253]. Copyright 2007, Wiley-VCH Verlag GmbH&Co. KGaA, Weinheim.

the conductivities of the composite nanofibers were also strongly related to the content of PS. The PANI/PS composite nanofibers have a conductivity in the range of $\sim 10^{-4}$ to 10^{-5} S/cm. Below 5 wt%, the conductivities of the composite nanofibers decreased upon increasing PS content. Above 5 wt%, the conductivity showed no significant change. The wettability of films of polyacrylonitrile PAN/PANI coaxial nanofibers has also been demonstrated to have a chemical dual-responsive characteristic [253] (Fig. 14). The composite exhibited a superhydrophobic characteristic with a water CA up to 164.5° and had a conductivity of about 4.3×10^{-2} S/cm. The wettability of the composite fibers could also be triggered by adjusting pH value or redox properties. The CA would decrease from 164.5° in a doped form to about 0° for a droplet with pH 13.07, and the reversible cycles between superhydrophobicity and superhydrophilicity can be repeated many times in a short time. In addition, the PAN/PANI coaxial nanofibers also exhibited a reversible wettability with CA from $156.4 \pm 1.4°$ for a water droplet to $116.9 \pm 3.0°$ for an oxidizing droplet. Such a dual-responsive surface has potential applications in biologic separation systems and cell culture.

3.6. Specific surface area

The specific surface area is an important property of nanomaterials, which greatly affects, for example, the adsorptive and catalytic behavior of ceramics and metallic powders. The control and measurement of specific surface area for nanomaterials are of great importance, not only for academic study in the laboratory, but also for industrial production in the factory. The specific surface area is closely tied to particle size. The smaller the particle size is, the larger the specific surface area becomes. For conducting polymer nanofibers, the doping state and the fiber diameters determined the specific surface area. For example, the Brunauer–Emmett–Teller (BET) surface area of PANI nanofibers synthesized via an interfacial polymerization and doped with camphorsulfonic acid was 41.2 m^2/g, increasing to 49.3 m^2/g after dedoping with base, attributed to the increase of the free volume of the PANI nanofibers after the removal of dopants [254]. The surface area of PANI nanofibers increases slightly the decreasing diameter. The measured BET surface area of dedoped PANI increased from 37.2 to 54.6 m^2/g when the fiber diameter was changed from 120 to 30 nm. The specific surface area and pore size of mesoporous conducting polymer nanofibers synthesized by chiral lipid ribbon templating and seeding route have also been extensively demonstrated [255]. The BET surface area and pore diameters of PPy nanofibers strongly depended on the chain length of the template molecules. When the n in C_n-L-Glu increased from 12 to 18, the BET surface area of as-synthesized PPy nanofibers increased from 38.7 to

59.4 m^2/g. Meanwhile, the pore diameters increased from 5.4 to 14.4 nm. The BET surface area was also related to the presence of the template molecules. The BET surface area increased a little after the templates were extracted from PPy nanofibers.

Incorporating highly mesoporous inorganic nanocomponent into conducting polymers enhances the BET surface area of conducting polymers significantly. Ćirić-Marjanović fabricated PANI/zeolite (HZSM-5) composite nanofibers via a self-assembly process and studied their BET surface area [256]. The BET surface area of the PANI/HZSM-5 composite nanofibers could reach 125 and 193 m^2/g when the composite contains 77.9 and 86.32 wt% HZSM-5. Compared to pure zeolite (HZSM-5), the decrease of specific surface area with the decrease of HZSM-5 content in PANI/zeolite composite nanofibers was attributed to the partial covering of the entrances of mesopores by PANI. The specific surface area of PANI/titanate coaxial nanocables has also been studied [141]. The results showed the BET surface area and pore volume of 306 m^2/g and 0.87 cm^3/g for pure titanate nanotubes, while 103 m^2/g and 0.2 cm^3/g for titanate/PANI coaxial nanocables. Similarly, the decrease in surface area and pore volume was due to the blockage of titanate pores by PANI. Mihranyan et al. presented the fabrication of *Cladophor*a cellulose/PPy composite fibers via a chemical oxidation polymerization [257]. The results showed that the specific surface area reached 57 m^2/g and the total pore volume was 0.18 cm^3/g, attributed to the maintenance of the large surface area and pore volume characteristic of *Cladophora* cellulose in the composite fibers.

4. Applications of 1D conducting polymers nanocomposites

As described in previous sections, various kinds of 1D conducting polymer nanocomposites have been fabricated using a number of facile and effective strategies. Because of the synergistic effect of multi-components, 1D conducting polymer nanocomposites exhibited multifunctional and unique properties. Therefore, such 1D conducting polymer nanocomposites are expected to find applications in many fields, such as nanoelectronic devices, chemical or biological sensors, catalysis or electrocatalysis, energy, microwave absorption and EMI shielding, ER fluids and biomedicine.

4.1. Electronic nanodevices

Most conducting polymers are suited for the construction of electronic devices because of their high electrical conductivity, mechanical flexibility and low cost. 1D nanostructured conducting polymers are expected to be excellent candidates for nanoelectronic devices in the future because they are molecular wires themselves. Incorporating metals, semiconductors and carbon nanomaterials and even insulating polymers into conducting polymers to form 1D nanocomposites may affect the conductivity of conducting polymers or induce efficient electron transfer, which is potentially applicable in light-emitting diodes, transistors, memory and photovoltaic devices [258–264].

Using electrospinning technique, conducting polymers have been successfully fabricated into 1D nanostructures with other processible polymers. A Schottky diode can be fabricated from such composite electrospun nanofibers on n-doped silicon substrate [258,259]. Current–voltage characteristic of the Schottky diode exhibited strong dependence on the diameter of composite nanofibers. Clear rectification was observed for diodes fabricated from thick fibers. When the diameter of the composite fibers was reduced, the rectification ratio and the diode turn-on voltage decreased. The surface states on the semiconductor had a weaker influence on diodes fabricated from thin fibers. On the other hand, the doping level of the composite fibers also affected the diode rectification ratio. When the doping level was lowered, the device rectification ratio reduced, but other diode parameters were unchanged. In addition to a Schottky diode, a field effect transistor (FET) could also be constructed using electrospun PANI/PEO composite nanofibers [260]. The results showed that saturation currents were obtained in the electrospun devices at low source-drain voltages. The hole mobility in the depletion regime was 1.4×10^{-4} cm^2/Vs. The device parameters were expected to be enhanced by reducing or eliminating the PEO content.

Both diode and FET devices could also be fabricated by 1D conducting polymers with metal nanocomponents. Mirkin and co-workers constructed a nanodevice from single Au–Ppy–Cd–Au four segment nanorods via a template method, which exhibited “diode” behavior at room temperature [262]. In the forward bias, holes moved from the PPy block to the Cd block. In reverse bias, the current was zero from −0.61 to 0 V. The turn-on voltage of these diode nanorods was around 0.15 V and the rectifying ratio was 200 at ±0.6 V. FETs can be produced by patterning a gate on one side of the segment nanorods composed of conducting polymers and metal (Co–Ppy–Co), [263]. The field-effect mobility of the bipolaron and the estimated threshold voltage of such FETs were 0.56 $cm^2/V\,s$ and 1.2 V, respectively. The gain of the wire FETs can be much increased by successive doping.

With the development of semiconductor technology, nonvolatile memory devices with high speed and density became more and more important for information processing. Yang and co-workers demonstrated the fabrication of bistable memory device using PANI/Au composite nanofibers [102,264]. For a potential lower than +3 V, the current was low, indicating that the composite nanofibers had a high impedance. As the potential reached +3 V, the current increased abruptly, corresponding to a sharp decrease of resistance. When the potential decreased from +3 V back to 0 V, the device remained at the low resistance state (ON state). To change back to OFF state (high resistance state), the reverse bias of −5 V had to be applied. The memory device composed of PANI/Au composite exhibited the characteristics of a long retention time and fast response to applied voltage pulses (Fig. 15). The bistable electric behavior was due to the electric-field-induced charge transfer between PANI nanofibers and Au nanoparticles. In principle, such a memory device with high performance would have an important impact on the information technology in the future.

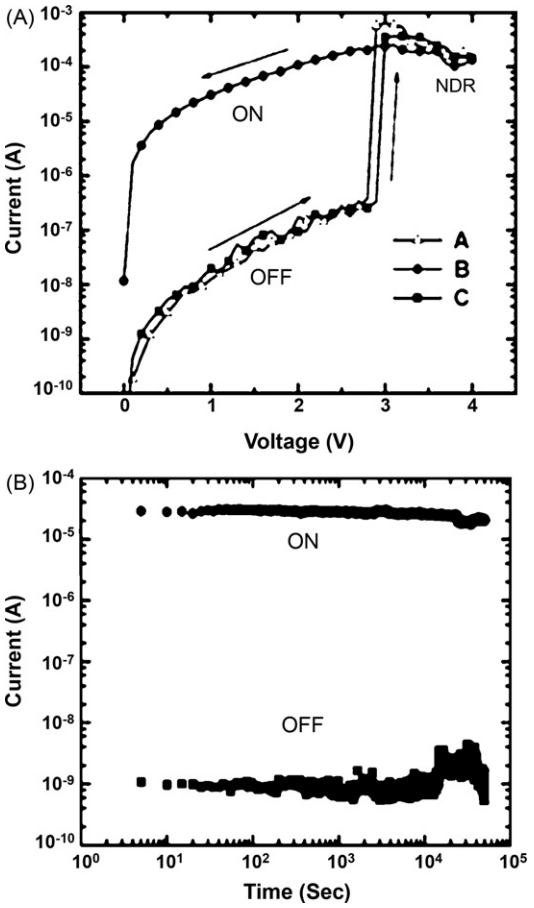

Fig. 15. (A) Current–voltage characteristics of PANI/Au composite nanofibers device. The potential is scanned from (a) 0 to +4 V, (b) +4 to 0 V, and (c) 0 to +4 V. (B) Retention time test of the On-state (top) and OFF-state (bottom) currents when biased at 1 V with a width of 0.167 s, recorded every 5 s [102]. Copyright 2005, American Chemical Society.

4.2. Sensors

Conducting polymers are good candidates for chemical and biological sensors because the interactions with various analytes may influence the redox and doping states of conducting polymers, leading to a change of resistance, current, or electrochemical potential [265–268]. Although neat conducting polymers are good materials for chemical and biological sensing, their low sensitivity and poor selectivity are limitations and must be improved. The fabrication of nanostructured conducting polymers is an effective strategy to enhance their sensing properties for their large surface area per unit mass than conventional films or powders. Adding a second nanocomponent, such as carbon nanotubes, metal and metal oxide particles, metal salts, insulating polymers, and biological materials, into conducting polymer matrix is another way to address the above issues because the second component may increase the chain mobility of conducting polymers or change the affinity of the composite, or even act as a catalyst.

4.2.1. Gas sensors

Gas sensors have a broad range of ever-increasing applications in everyday life, such as industrial production, food processing, environmental monitoring, health care, etc. [269–271]. 1D nanostructured conducting polymers are good candidates for gas sensors because of their large specific surface areas. Upon interaction with the gas analyte, the electrical conductivity of 1D nanostructured conducting polymers could change drastically. The PANI nanofibers synthesized via interfacial polymerization have shown that they have much higher sensitivity for the detection of NH_3 than conventional PANI film. On the other hand, the addition of a second component into 1D nanostructured conducting polymers could enhance or extend their applications as gas sensors. For example, in the detection of NH_3, MWNT/PPy composite nanofibers exhibited a higher sensitivity of 10–28% over a wide range of concentration from 400 to 10,000 ppm [272]. In addition, the MWNT/PPy composite nanofibers also exhibited a reversible response towards 50–12,500 ppm NH_3 at room temperature. The mechanism of the enhanced sensitivity may be attributed to the increased surface area of PPy, providing more active sites for adsorption of NH_3 vapor. The similar properties were also observed in carbon nanofiber/PPy nanocomposites [98]. The sensing properties of the PPy coated TiO_2/ZnO composite nanofibers in NH_3 detection were also studied in detail [207]. Eletrospinning followed by vapor-phase polymerization afforded a membrane of TiO_2/ZnO/PPy composite nanofibers that had a porous structure with an ultrathin PPy layer (about 7 nm), allowing free access of NH_3 to PPy and minimizing gas diffusion resistance, leading to high sensitivity, with a detection limit of 60 ppb and fast response/recovery in NH_3 detection. Sensors based on PANI/DNA composite nanowires fabricated on Si surfaces have also been demonstrated for the detection NH_3 and HCl [174]. The results showed that the response time of the as-synthesized PANI/DNA composite nanowires to NH_3 and HCl was within 1 s, which was 100 times faster than PANI nanofibers alone.

Besides NH_3, the addition of metal oxide nanoparticles into 1D nanostructured conducting polymers can extend their applications in detecting other gases. For example, PANI/In_2O_3 composite nanofibers synthesized via chemical polymerization were used as sensor in detection of H_2, CO and NO_2 at room temperature [273]. In fact, the sensor based on pure In_2O_3 had large response towards H_2, CO and NO_2, but the operation temperature was relatively high (100–350 °C). The sensor responses were around 11.0, 2.0 and 2.5 kHz to 1% of H_2, 500 ppm CO and 2.12 ppm NO_2, respectively. The 90% response and recovery times were 30 and 40 s for H_2, 24 and 36 s for CO, and 30 and 65 s for NO_2, respectively. Furthermore, a sensor based on PANI/In_2O_3 composite nanofibers exhibited a repeatable response towards H_2 and CO. Similarly, PANI/WO_3 composite nanofibers were also employed in sensors for detection of H_2 gas, however, the sensitivity was worse than PANI/In_2O_3 composite nanofibers based sensors [274].

Metal salts can also be incorporated into 1D a nanostructured conducting polymer matrix as gas sensors. For example, pristine PANI nanofibers have limited sensitivity for H_2S gas, but PANI/$CuCl_2$ composite nanofibers exhib-

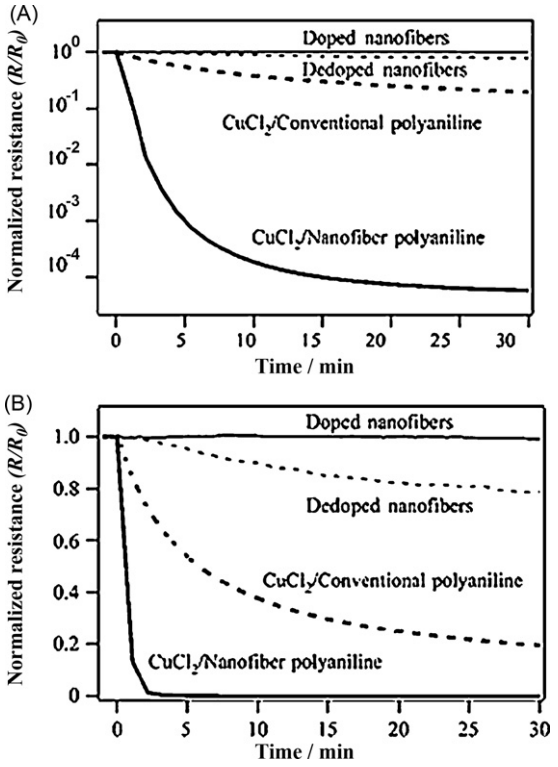

Fig. 16. (A) Resistance changes of different kinds of PANI nanostructures upon exposure to H_2S. The H_2S concentration was 10 ppm with 45% relative humidity. (B) The data from (A) with an expanded linear scale [275]. Copyright 2005, Wiley-VCH Verlag GmbH&Co. KGaA, Weinheim.

ited a high response for H_2S gas [275]. Compared to PANI nanofibers, the sensitivity of the composite nanofibers to H_2S gas was enhanced by four orders of magnitude (Fig. 16). The mechanism of the improved sensitivity was due to the formation of strong acid (i.e., HCl) through the reaction between H_2S gas and $CuCl_2$, which increased the doping level of conducting polymers. The 1D conducting polymer nanocomposites were also used as gas sensors to detect volatile organic compounds. As examples, PMMA/PANI coaxial composite nanofibers constructed as gas sensors towards triethylamine (TEA) vapor exhibited sensitivity as high as 77–500 ppm TEA [276]. Nanocomposites of MWNT/P3HT developed for the detection of chloromethanes gase showed a response time around 60–120 s [277]. The nanocomposite sensors also showed a selective sensing for methane.

4.2.2. Biosensors

In recent years, conducting polymers have been used to construct a variety of biosensors because of their unique electronic, chemical and mechanical properties [278]. In particular, 1D nanostructured conducting polymers provide an excellent platform for bio-recognition. As biosensors, the detection of H_2O_2 is important because it is often a product in enzymatic reactions. PANI/PS composite nanofibers, prepared by electrospinning technique, were employed to detect H_2O_2 by means of cyclic voltammetry [153]. Composite nanofibers exhibited superior sensing properties for H_2O_2 corresponding composite thin films. The enhanced sensitivity of the composite nanofibers was attributed to their large surface area and good electrical properties. The excellent sensing performance of PANI/PS composite nanofibers in H_2O_2 detection makes it attractive for the fabrication of oxidase-based glucose biosensors because H_2O_2 is generated in the reaction between glucose and oxygen in the presence of glucose oxidase (GOX). As more GOX was immobilized on the composite nanofibers with large specific surface area, the sensitivity of the sensor based on the composite nanofibers was much higher than that for the film sensor. The results showed that the sensitivity enhanced by nearly 20 times.

GOX could also be incorporated into aligned CNT/PPy composite nanofibers with Fe nanoparticles on the tip of CNTs [279]. Inclusion of Fe nanoparticles was the key factor to reduce the potential of the redox reaction of H_2O_2. A near linear increase in the current up to 20 mM glucose was observed for the aligned composite nanofibers. In comparison to GOX immobilized PPy matrix on gold electrode, the aligned CNT/PPy composite fibers with immobilized GOX exhibited a higher response by at least an order of magnitude. Three component composite nanofibers containing PANI, Fe_3O_4 and CNTs were prepared and doped with enzyme for the fabrication of glucose biosensors [202]. The PANI/Fe_3O_4/CNTs composite nanofibers based glucose sensor showed high sensitivity and linearity. The presence of CNTs in the composite not only increased the conductivity and specific surface area of the composite, but also lowered the over-potential for H_2O_2 oxidation. The composite nanofibers based biosensor showed a fast response time within 5–6 s and a good reproducibility.

Use of conducting polymer/metal composite nanofibers for H_2O_2 and glucose detection has been examined [108]. The response time of the composite nanofibers in detection of H_2O_2 was very fast, within 3 s. The sensor exhibited linearity in H_2O_2 detection in the concentration range of 0.1 μM–1.4 mM. A detection limit of 50 nM based on a signal-to-noise ratio of 3 was achieved for the PANI/Pt/Pd composite nanofibers sensor (Fig. 17). For detecting glucose, GOX was immobilized on the PANI/Pt/Pd composite nanofibers. The sensor had a linear response in glucose detection in the concentration range of 1 μM–4.32 mM. The detection limit was 0.4 μM. The stability of the biosensor based on PANI/metal composite nanofibers was good. The response current remained at 81% after the composite nanofiber electrode was stored for 1 month.

Triglyceride monitoring in blood is a medically important task because its high concentration is related to the increased risk of atherosclerotic events. 1D conducting polymer nanocomposites with encapsulation of lipase have been utilized as biosensors to detect triglyceride [183]. In the study, the lipase was covalently immobilized on PANI nanotubes via glutaraldehyde reactions, which prevented lipase leaching in solution. The PANI/lipase composite nanofiber sensor was sensitive to triglyceride over a concentration range of 25–300 mg/dL with good linearity. In addition, the PANI/lipase composite nanofibers based biosensor exhibited high sensitivity (2.59×10^{-3} kΩ^{-1} mg^{-1} dL), fast response time (20 s) and regression coefficient (0.99). Furthermore, the covalent

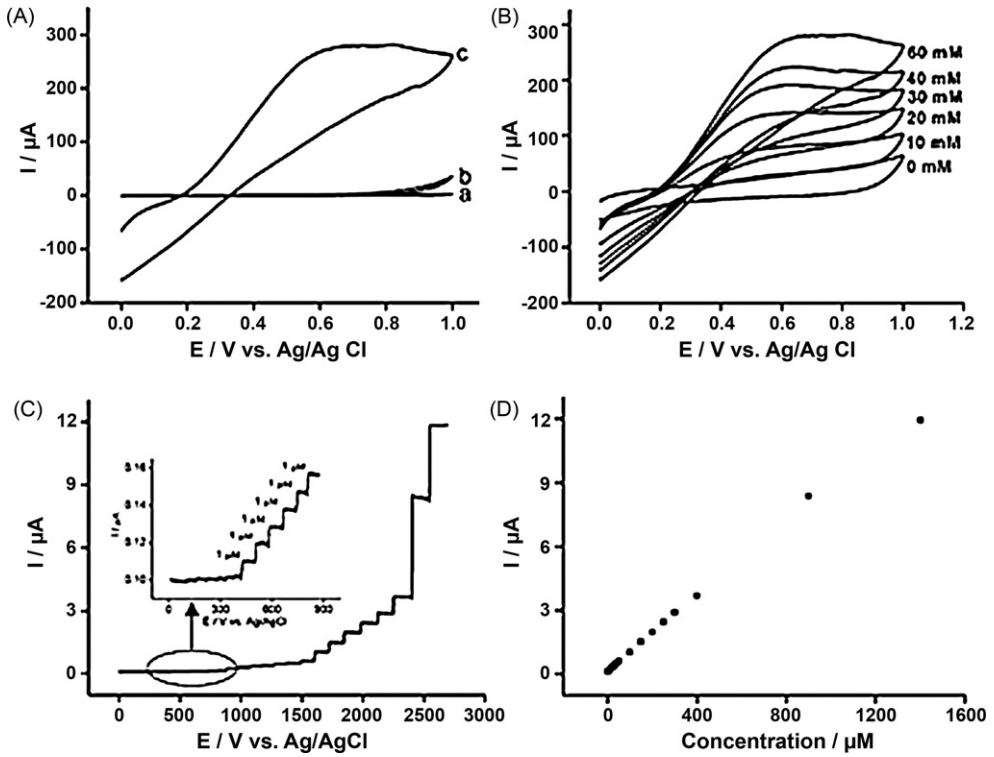

Fig. 17. (A) CV curves of the oxidation of H_2O_2 at bare GCE (a and b) and PANI/Pt/Pd composite nanofibers modified GCEs (c) in a 0.1 M PBS (pH 7.4) in the absence (a) and presence (b and c) of 60 mM H_2O_2. Scan rate: 100 mV s^{-1}. (B) CV curves of the oxidation of H_2O_2 at the PANI/Pt/Pd composite nanofibers modified GCE in 0.1 M PBS in the presence of H_2O_2 with defferent concentrations. Scan rate: 100 mV s^{-1}. (C) Amperometric current responses of PANI/Pt/Pd composite nanofibers modified GCE for successive addition H_2O_2. Applied potential: 0.6 V. (D) The plot of electrocatalytic current of H_2O_2 as a function of its concentrations [108]. Copyright 2009, Wiley-VCH Verlag GmbH&Co. KGaA, Weinheim.

immobilization improved the stability of the sensor with a shelf life up to 10 weeks.

Immobilization of DNA onto conducting polymers has been extensively studied for detection of various DNA target sequences and microorganisms [176]. In a synthetic procedure for BdNG immobilization onto PANI nanofibers for the detection of dNG complementary target, avidin-biotin was used as a cross-linking agent to improve the stability of the electrode. The detection limit of the sensor based on PANI/DNA composite nanofibers was 0.5×10^{-5} M with 60 s of hybridization time. The PANI/DNA composite nanofiber sensor could distinguish presence of *N. gonorrhoeae* from *N. meningitides* and other gram-negative bacteria, e.g., *E. coli*. DNA could also be immobilized onto PPy nanorods via physisorption, which was used to study the interaction of spermidine with DNA [177]. The dynamic range, correlation coefficient and detection limit of the biosensor based on PPy/DNA composite nanorods were 0.05–1.0 μM, 0.9983 and 0.02 μM, respectively, exhibiting an excellent characteristic for biosensing.

Incorporation of uricase into conducting polymers nanotubes for measuring the urea concentration has been achieved [182]. Urease was immobilized by a physical entrapment method. The sensor displayed a linear concentration range of urea between 1.22 μM and 3.85 mM. The sensitivity and detection limits of the composite nanotube sensor were 53.74 mV/decade and 1.0 μM, respectively, both superior to the others reported. A rapid response time (60–100 s) was also obtained for the composite nanofibers. In addition, compared to the reports in literature, the PPy/urease composite nanofibers on carbon paper electrode exhibited superior long-term stability and reusability.

4.3. Catalysis

Metal nanoparticles can be readily prepared with uniform size and shape and can be used as catalysts for various types of chemical and electrochemical reactions with high activity and selectivity. However, metal nanoparticles are easily aggregated during the preparation, reducing their activity. To achieve high catalytic activity, metal nanoparticles are generally dispersed on support materials. As relatively inexpensive nanomaterials, 1D nanostructured conducting polymers are good media for the confinement of metal nanoparticles as catalysts because the conductive support facilitates the shuttling of electronic charges to the catalyst centers.

4.3.1. Chemical and photocatalysis

The conducting polymers have the ability to reduce metal salt into zero valent metal, offering a versatile approach for the fabrication of conducting polymer/metal composites. For example, PANI/Pd composite nanofibers can be prepared by simply mixing palladium nitrate with

PANI nanofibers. The catalytic properties of the composite nanofibers have been examined for use in Suzuki coupling reactions [103]. The nanofibers exhibited good catalytic activity for the reaction between aryl chlorides and phenylboronic acid and for phenol formation from aryl halides and potassium hydroxide in water and air. Another superior characteristic of the PANI/Pd composite nanofibers as catalyst was the low Pd nanoparticle loading. Only 10^{-5} mol% Pd loaded on PANI nanofibers was effective in catalyzing the reaction between 4-acetylphenyl chloride and phenylboronic acid. In addition, the composite nanofibers were recyclable, a yield of 89% in the same reaction performed after 10 cycles.

1D nanocomposites of PANI/Pd nanotubes were also synthesized via a templating method for chemical catalysis [118]. In order to avoid the leaching of Pd nanoparticles from conducting polymer matrix, they were prepared on the inner walls of PANI nanotubes. The typical procedure involved three main steps: (1) fabrication of sulfonated PS nanofibers and reducing palladium chloride to form Pd nanoparticles on their surface; (2) preparation PANI layer on the surface of PS/Pd composite nanofibers; and (3) removing sulfonated PS nanofibers by washing with THF. The composite nanofibers were used as catalyst for the reduction of *p*-nitroaniline by hydrazine hydroxide in ethanol. A yield of 85.14% was achieved that was superior to that with Pd/C catalyst.

It is well known that TiO_2 is an effective photocatalyst with strong oxidizing power and non-toxicity. The TiO_2 catalysis for the decomposing toxic inorganic or organic compounds is attributed to the formation of superoxidant ($^{\bullet}OH$ and $O_2^{\bullet -}$) generated from water decomposing in the presence of TiO_2 under radiation [280]. However, one of the disadvantages of TiO_2 catalyst is the rapid recombination of photo-induced electrons and holes, which reduces the photocatalytic efficiency of TiO_2. Another disadvantage is that little visible light can be absorbed because the forbidden band gap of TiO_2 is 3.2 eV. Thus organic dyes with visible light absorbing chromophores are usually used as sensitizers to enhance the catalysis efficiency of TiO_2. As a dye with a forbidden band gap of 2.8 eV, PANI can be used to photosensitize TiO_2 semiconductors. The photocatalytic properties of TiO_2/PANI bilayer microtubes synthesized via a template method have been studied [281]. The results demonstrated that TiO_2/PANI bilayer microtubes had an increased catalytic property to decompose methyl orange under visible light. The enhanced catalysis was ascribed to the red shift of the absorption region of TiO_2 because of photosensitization by PANI.

4.3.2. Electrocatalysis

As mentioned in Section 4.2.2, 1D conducting polymer nanocompsites are good candidates as biosensors. In fact, most of the reactions for biosensing involve electrocatalysis. For example, Zhu and co-workers fabricated PANI/Au composite nanotubes and studied their electrocatalysis towards NADH [282]. With glass carbon electrode (GCE) as the substrate electrode, they could also be regarded as biosensors. However, in this section, we will focus our attention to the process of electrocatalysis properties of 1D conducting polymer nanocompsites. It was reported that the electrochemical oxidation of NADH on carbon and platinum electrodes occured at high over potentials of 1.1 and 1.3 V, respectively, attributed to the transfer of two electrons and one proton and the cleavage of a C–H bond. Using PANI/Au composite nanotubes as an electrode, the potential for electrochemical oxidation was significantly decreased to around 0.6 V. Compared with pure PANI-modified electrode, PANI/Au composite nanotube modified electrode displayed enhanced electrocatalytic activity towards the oxidation of NADH.

The field of electrocatalysis in oxygen reduction has also benefited from 1D conducting polymer/metal porphyrin nanocomposites. For example, PPy/cobalt porphyrin composite nanorods displayed good electrocatalytic properties for oxygen reduction in neutral electrolyte [197]. The electrocatalysis of the nanocomposite was mainly generated from cobalt porphyrin, conducting through a four-electron transfer process, proved by the rotating ring-disc (RRDE) method. Similar results were obtained with PANI/cobalt porphyrin composite nanorods.

Our group investigated the electrocatalysis of PEDOT/β-$Fe^{3+}O(OH,Cl)$ nanospindles for the oxidation of KI and reduction of KIO_3 [283]. In comparison to bare GCE, an enhanced anodic and cathodic responses were observed for the composite nanospindles, due to the increased surface area and reaction sites. The results on scanning rate also showed that the oxidation process of KI was diffusion control, while the reduction process of KIO_3 was surface control.

Au/PEDOT/β-$Fe^{3+}O(OH,Cl)$ composite nanospindles prepared by a one-step approach, were used as electrocatalysts for the oxidation of D-AA [284]. Compared to bare GCE, a cathodic shift was observed and the current response was also much higher for the composite nanospindles, indicating the excellent electrocatalytic oxidation of D-AA. The enhanced catalysis of the composite nanospindles can be attributed to the accumulation of ascorbate anions at the interface of the electrode as a doping form. The scanning rate result showed that the oxidation process of D-AA proceeded by diffusion control.

4.4. Energy applications

Energy has become more and more an important global concern because fossil fuels are going to be exhausted eventually. Therefore, studies of the exploitation of other forms of energy processes including energy conversion, storage and generation have increased in recent decades. Many efforts have been devoted to the fabrication of nanostrutured conducting polymer nanocomposites as electrode materials in energy conversion devices such as solar cells and fuel cells, and energy storage devices such as lithium ion batteries and supercapacitors. It is anticipated that the synergistic effect of each component in the nanocomposites could significantly enhance the performance of the energy devices.

4.4.1. Solar cells

Solar cells are energy conversion devices that convert sun light to electric energy. Efforts to reduce the cost and increase the energy conversion efficiency of

solar cells have become top tasks of research. In comparison to sintered nanoparticles, metal oxide nanofibers are excellent candidates for the fabrication of solar cells because they provide better charge conduction owing to their reduced grain boundaries and high electron mobility along the nanofibers. On the other hand, conducting polymer/inorganic hybrid solar cells are of particular interest because they combine the unique properties of metal oxides with the good light absorbing and hole transporting properties of conducting polymers, which may contribute to the improvement of the photovoltaic efficiencies [285–291]. Conductive polymer composites are particularly attractive because of their low cost and good mechanical properties.

Photovoltaic devices fabricated with vertically aligned ZnO nanofibers/P3HT composites have an open circuit voltage (V_{oc}) of 440 mV, a circuit current density (J_{sc}) of 2.2 mA/cm^2, a fill factor (EF) of 0.56, and a conversion efficiency (η) of 0.53% [285]. The performance of the device can be further enhanced by incorporating a blend of P3HT and (6,6)-phenyl C61 butyric acid methyl ester (C60-PCBM) into ZnO nanofibers. A photovoltaic device based on ZnO/P3HT/PCBM composite nanofibers exhibited a V_{oc} of 475 mV, J_{sc} of 10.0 mA/cm^2, EF of 0.43, and η of 2.03%. Furthermore, the external quantum efficiency of the device increased from 17% for ZnO/P3HT composite nanofibers to 57% for ZnO/P3HT/PCBM composite nanofibers.

Coating TiO_2 thin film on the surface of ZnO nanofibers can improve the performance of ZnO/P3HT solar cells. Yang and co-workers demonstrated that solar cells with a vertical ZnO nanorod array/P3HT composite exhibited an efficiency of only 0.04% [286]. However, the efficiency could reach 0.34% by coating with a thin TiO_2 layer after storing in air for one month. TiO_2 nanotube arrays are considered as the good candidates for the construction of solar cells because they provide good pathways for electron migration. The device was prepared by infiltrating a blend of regioregular P3HT and a methanofullerene (phenyl C71-butyic acid methyl ester) (C70-PCBM) into TiO_2 nanotubes arrays [287]. Charge separation can be provided by the interfaces not only between P3HT and C70-PCBM, but also between P3HT and TiO_2 nanotubes. Therefore, the solar cell device for the frontside illumination geometry exhibited a V_{oc} of 641 mV, J_{sc} of 12.4 mA/cm^2, EF of 0.51, and η of 4.1% under AM 1.5 one sun illumination, which was much better than those based on non-transparent nanotube arrays with backside illumination (Fig. 18).

CNT/PEDOT-PSS composite nanotubes were also used as DSCs, which exhibit good photovoltaic performance with a V_{oc} of 660 mV, J_{sc} of 15.5 mA/cm^2, EF of 0.63, and η of 6.5% tested with AM 1.5 solar simulator, significantly better than that of CNT/Poly(styrenesulfonate acid) (PSSA) composite nanotubes [288]. For CNT/PEDOT-PSS composite nanotubes, the charge transfer was not affected because CNTs were wrapped by conductive PEDOT, while it would be lowered in CNT/PSSA composite nanotubes because CNTs were wrapped by the insulating PSSA.

4.4.2. Fuel cells

Fuel cells, which convert the chemical energy of a fuel directly into electricity by electrochemical reactions,

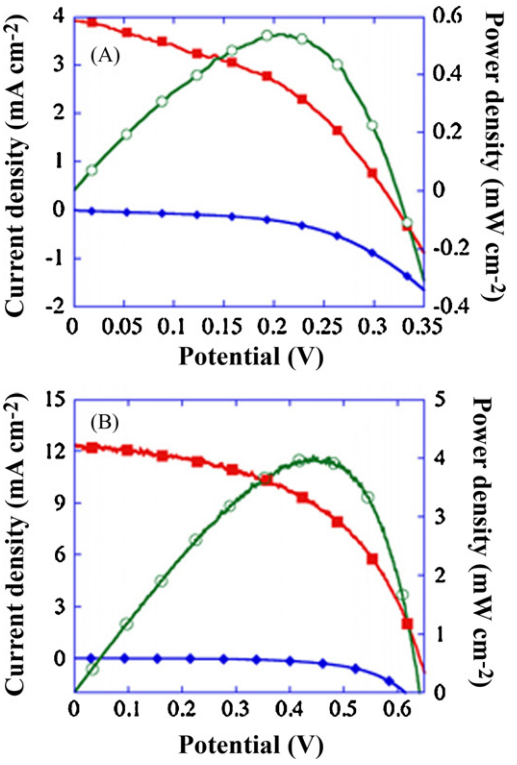

Fig. 18. Current and power density versus voltage for (A) backside illuminated heterojunction solar cells and (B) frontside illuminated solar cells. -■- stands for photocurrent density, -♦- stands for the dark current density, and -○- stands for the power density [287]. Copyright 2007, Elsevier B.V.

have attracted increasing attention in recent decades for applications in electric vehicles [292,293]. With the advantages of high energy conversion efficiency, fuel portability and environment friendliness, direct methanol fuel cells (DMFCs) have become a research focus in the field of energy applications [294]. The effects of an electrocatalyst on the performance of DMFCs have been extensively studied. Recent studies revealed that CNTs and carbon nanofibers are good candidates as supports for Pt nanoparticle loading because of their superior electrical conductivity and large surface areas. Conducting polymers with 1D nanostructures have been investigated as a new class of electrocatalyst supports. In comparison to conventionally synthesized conducting polymers, the new electrocatalyst displayed enhanced methanol oxidation activity. Nanotubules of PPy can be synthesized via a template method [295]. Pt nanoparticles were electrodeposited on the surface of PPy nanotubes through the Galyanostatic Square Wave (GSW) method. After removing the template by dissolution, PPy/Pt composite nanotubes placed on the Nafion coated carbon cloth showed superior catalytic activity for the electrooxidation of methanol. In addition, the stability of the PPy/Pt composite nanotubes was good, only about 14.3% decrease in catalytic activity was observed, compared to a decrease of about 67.5% for samples synthesized without a template. Pt/poly(*o*-phenylenediamine) (PoPD) composite nanotubes were also prepared by a templating and electrodeposition method [296]. The methanol

oxidation activity of the as-synthesized Pt/PoPD composite nanofibers was about 13 times more active than that of conventional Pt/PoPD nanocomposites loaded with the same amount of Pt nanoparticles.

In addition to electrodeposition, Pt nanoparticles can be formed on the surface of PPy nanofibers using the chemical microwave-polyol method [107]. Compared to commercial carbon black powder of Vulcan XC-72 (XC-72) and carbon nitride (CN_x) nanofibers supports, Pt nanoparticles on the surface of PPy nanofibers had the smallest diameters. Also, the PPy/Pt composite nanofibers exhibited much better electrocatalytic activity for the oxidation of methanol than Pt/CN_x and Pt/XC-72 nanocomposites. The maximum stable peak current density for PPy/Pt composite nanofibers were about two and three times higher than those of CN_x/Pt and Pt/XC-72 nanocomposites. Moreover, the CO-poisoning tolerance of the Pt/PPy composite catalysts was superior to those of CN_x/Pt and Pt/XC-72 nanocomposites. Pt/PANI composite nanofibers were also used as electrocatalyst for DMFCs [106]. The results showed that the diameters of PANI nanofibers and Pt nanoparticles for Pt/PANI composite were 60 and 1.5–3 nm, respectively. In comparison to conventional Pt/C catalyst, Pt/PANI composite nanofiber catalysts exhibited higher electrocatalytic activity and tolerance for methanol oxidation reaction, which might be related to the 1D nanostructures of PANI (Fig. 19).

All of the 1D conducting polymer/metal composites for the oxidation of methanol described in the preceding were used as anode electrocatalysts in DMFCs. In fact, most of the cathode electrocatalysts for the reduction of oxygen were also Pt-based nanomaterials. However, the high cost of Pt-based electrocatalysts is one of the barriers for their commercially viability. The use of other, inexpensive metal nanoparticles as electrocatalysts has been investigated. For example, Ppy–Co–MWNTs composite nanotubes were prepared and used as the cathode electrocatalysts for the reduction of oxygen in a polymer electrolyte fuel cell (PEMFC), DMFCs and direct ethanol fuel cells (DEFCs) [200]. In comparison to other non Pt based electrocatalysts, improved power densities were observed for the PEMFC, DMFCs and DEFCs with Ppy–Co–MWNTs composite nanotubes as a cathode electrocatalyst and Pt–Ru/MWNTs and Pt–Sn/MWNTs as an anode electrocatalysts. In addition, the durability of Ppy–Co–MWNTs composite nanotubes for the reduction of oxygen was excellent, and no noticeable decrease in current density was observed over long PEMFC operating time.

4.4.3. Lithium ion batteries

Rechargeable batteries are energy storage devices are widely used in daily life, such as in cell phones, laptop computers and electric vehicles [297]. Conventional rechargeable nickel-cadmium or nickel-metal hydride batteries are limited by their capacity and durability. By contrast, lithium ion batteries, which are lighter and have much greater capacity, are considered to be one of the most promising and practical rechargeable batteries [298–301]. The materials used in the cathode, anode and electrolyte are three determining the energy density and electrochemical performance of Li-ion batteries [302]. Graphite

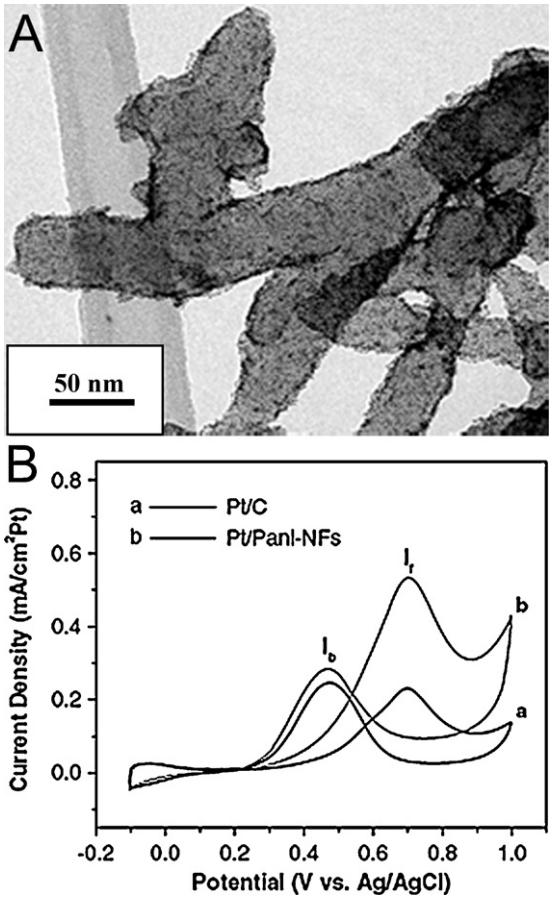

Fig. 19. (A) TEM image of Pt/PANI composite nanofibers, showing the diameter of the Pt nanoparticles on PANI nanofibers around 1.5–3 nm. (B) CVs of Pt/C and Pt/PANI composite nanofibers in 1 M CH_3OH + 0.5 M H_2SO_4, at a scan rate of 50 mV s^{-1} [106]. Copyright 2006, IOP Publishing Ltd.

is the most utilized anode material, while $LiCoO_2$, $LiMn_2O_4$ and $LiFePO_4$ are common commercial cathode materials in Li-ion batteries. Recently, 1D nanostructured materials proved to be good candidates as Li-ion battery electrodes because of their large surface to volume ratio to contact with electrolyte, high specific capacity and good cycle performance. For example, storage capacity the anode charge based on Si nanowires increased by 10 times over that of a carbon anode [303].

1D nanostructured composite of vanadium oxide/PANI synthesized through the reaction between V_2O_5/PANI nanocomposite and hexadecylamine in a hydrothermal medium has been used as cathode materials in Li-ion batteries [304]. The results showed that the electrochemical properties of the vanadium oxide/PANI composite nanofibers were better than those with vanadium oxide nanotubes. The charge capacity based on vanadium oxide/PANI composite nanofibers was about 150 A h Kg^{-1} during 10 initial cycles, while only 100 A h Kg^{-1} of charge capacity was obtained with V_2O_5 nanotubes. In addition, the cyclability based on vanadium oxide/PANI composite nanofibers was also superior to that of V_2O_5 nanotubes. This example suggests directions to try with other 1D

nanostructured systems utilizing existing electrode materials and conducting polymers for Li-ion batteries. It is anticipated that Li-ion battery with high specific capacity and good cycle performance will be obtained by using 1D conducting polymer nanocomposites as electrodes.

4.4.4. Supercapacitors

Supercapacitors, also called electrochemical capacitors, are recognized as one of the most promising energy storage devices for a wide range of civilian and military applications in electric vehicles, uninterruptible power supplies and so on [305,306]. In contrast to conventional capacitors, supercapacitors possess much higher energy density. Compared to lithium ion batteries, supercapacitors also exhibit higher specific power. To date, there are mainly three kinds of electrode materials for supercapacitors, i.e., carbon, metal oxides and conducting polymers [307–315]. Among these materials, carbon has a relatively low specific capacitance, usually under 200 F/g, metal oxides are either expensive (such as ruthenium oxide) or poor conductors (such as MnO_2, NiO, etc.), conducting polymers have a high specific capacitance, but their cyclic stability is poor. Therefore, fabrication of conducting polymer nanocomposites is critical in the construction of supercapacitors with both high capacitance and excellent cyclic stability.

Supercapacitors based on the CNTs/conducting polymer nanocomposites can be prepared via chemical or electrochemical polymerization. A high specific capacitance per gram of 192 F/g was observed for 1D nanostructured CNT/PPy composites, [316]. The specific capacitance per area of CNT/PPy nanocomposites was as high as 1.0 F cm^{-2}, much larger than those previously reported for supercapacitors based on the similar electrode materials. The per gram capacitance of PPy based nanocomposites was further enhanced by construction of an activated carbon nanofibers (ACNF)/CNT/PPy three component system [317]. In comparison to ACNF, the nanocomposites had larger specific surface area and higher electrical conductivity. The capacitance of ACNF/CNT/PPy was 333 F/g, much better than those of ACNF and ACNF/PPy electrodes. The 1D nanostructured CNT/PANI and CNT/PPy composites containing 20 wt% CNTs synthesized by *in situ* chemical polymerization method have also been employed for supercapacitors [318]. The specific capacitances of CNT/PPy and CNT/PANI nanocomposites were 190 and 360 F/g, respectively, with a fairly good cycling life for the supercapacitor. Gupta and Miura studied the performance of a supercapacitor based on single walled CNTs, SWNT/PANI nanocomposites [319]. Their results showed that the specific capacitances were strongly dependent on the PANI content. When 73 wt% PANI was deposited on the surface of SWNTs, the highest specific capacitance of 463 F/g was obtained. Furthermore, the stability of the supercapacitor based on SWNT/PANI nanocomposites was excellent, as evidenced by the fact that the capacitance only decreased 5% after 500 cycles and just 1% after the next 1000 cycles. Besides PANI and PPy, CNT/PEDOT composites with 1D core-sheath nanostructures prepared by *in situ* polymerization under hydrothermal condition have also been used for the fabrication of supercapacitors [320]. The highest capacitance of 198.2 F/g at the current density of 0.5 A/g

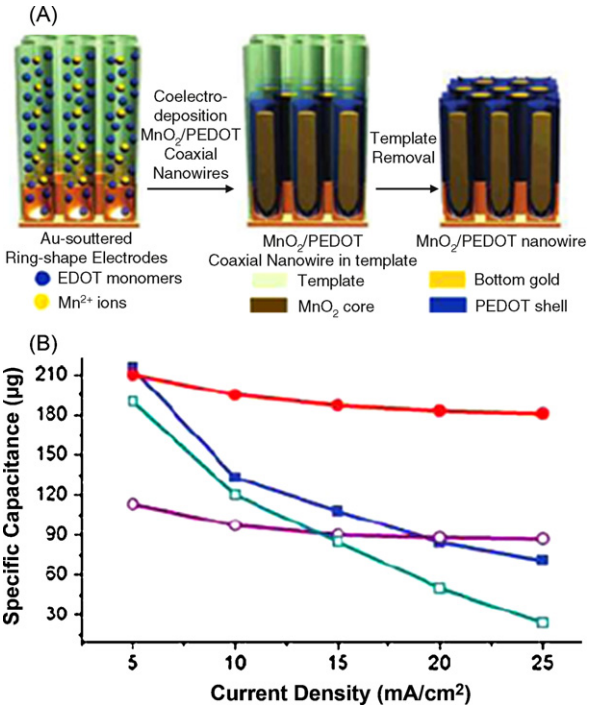

Fig. 20. (A) Schematic illustration for the fabrication of MnO_2/PEDOT coaxial nanowires. (B) Specific capacitance of MnO_2 nanowires (closed square), PEDOT nanowires (open dots), MnO_2 thin film (open square) and MnO_2/PEDOT coaxial nanowires (closed dots) at difference charge/discharge current densities [321]. Copyright 2008, American Chemical Society.

was achieved when the content of PEDOT reached 50%. After 2000 cycles, the capacitance of the supercapacitor decreased by 26.9%. Both the capacitance and stability of the supercapacitor based on the CNT/PEDOT nanocomposites with core-sheath nanostructures were superior to those of pristine PEDOT and CNT/PEDOT composites without core-sheath strucutures.

In addition to CNTs, nanocomposites comprising MnO_2 and conducting polymers have also been intensively investigated as building components in supercapacitors. MnO_2/PEDOT coaxial nanowires were prepared by a co-electrodeposition approach using an AAO template [321]. In comparison to MnO_2 nanowires, PEDOT nanowires and even MnO_2 films, the MnO_2/PEDOT coaxial nanowires exhibited higher specific capacitance (from 210 to 185 F/g) when the current density was increased from 5 to 25 mA/cm^2 (Fig. 20). The high and well maintained capacitance can be attributed to the inclusion of MnO_2 and the short paths of ion diffusion in the nanowires.

4.5. Microwave absorption and EMI shielding

Electromagnetic frequency interference (EMI), also called radio frequency interferene, is a serious issue caused by the rapid proliferation of electronics, wireless systems and the development in navigation, space technology, etc. [322]. EMI not only affects the performance of the electric device, but may also be harmful to life forms, including humans. Therefore, some kind of shielding mate-

rials must be employed to prevent the electromagnetic noise or pollution. Various types of materials have been used in EMI shielding, including metals, carbon materials and conducting polymers. Recently, the EMI shielding and microwave absorption properties of conducting polymers have attracted increased attention owing to their good electrical conductivity and processability [323].

Conducting polymers can be combined with other nanocomponents to enhance EMI shielding performance. For example, the microwave absorption propertiesCNT/conducting polymer nanocomposites with core-sheath nanostructure prepared by an *in situ* polymerization approach were studied [324]. The conductivity of the CNT/PANI nanocomposites was higher than not only pure PANI but also CNTs, an example of the synergistic effect of the two components. CNT/PANI nanocomposites can be applied for the shielding purposes in the Ku-band (12.4–18.0 GHz) for their total shielding effectiveness was in the range of −27.5–39.2 dB. The microwave absorption property of 1D PANI/HA/TiO_2 nanocomposites has also been studied [325]. The results showed that the conductivity of the composite significantly decreased after addition of TiO_2 and that the PANI/HA/TiO_2 nanocomposites synthesized at 0 °C could achieve a maximum RL of 31 dB (>99.9% power absorption) at 10 GHz. To increase the conductivity and microwave absorption performance of the above system, SWNTs were also incorporated [326]. When the content of SWNT was 20%, the PANI/HA/TiO_2/CNTs nanocomposite exhibited RL < −15 dB with broad bandwidth (4 GHz). While RL < −20 dB with narrow bandwidth (1 GHz) was observed when the content of SWNT reached 60%. Although only a few reports on the application of 1D nanostructured conducting polymers for microwave absorption and EMI shielding are available, it is believed that 1D nanocomposites could be important candidates in this field.

4.6. Electrorheological fluids

Over the past decades, smart materials have attracted much attention for their adjustable properties under an external stimulus. Smart fluids in the form of electrorheological (ER) fluids have been widely studied for their broad applications in clutch systems, hydraulic valves, brakes, dampers for vehicle vibration control, general motors, etc [327]. Generally, ER suspensions are composed of particles with a high dielectric constant and low conductivity dispersed in a non-conducting fluid medium. Under an electric field, the rheological properties of ER can reversibly change in a short time. Among many ER materials, conducting polymers have been extensively used as polarizable particles because of their superior physical properties, such as good environmental stability and high polarizability [328]. However, the yield stress and modulus of ER fluids based on conducting polymer materials were not higher than those of magneto-rheological (MR) fluids. In order to enhance the performance of conducting polymer-based ER fluids, one or more components were usually combined with conducting polymers to form nanocomposites. For example, conducting polymers/clay nanocomposites based ER fluids have been extensively studied in the past few years [329–332]. It was reported that a distinct enhancement in yield stress can be achieved when an aminosilane-treated organoclay was introduced into the conducting PANI as an ER fluid [333]. In addition to clay, silica-based mesoporous molecular sieves, ceramics and carbon nanotubes have been added to conducting polymers to form nanocomposites as ER fluids [334–339].

In addition to optimizing the composition of the conducting polymer nanocomposites, fabricating novel structure of conducting polymers is another effective approach to enhance the performance of ER fluids. It was reported that a nano-fibrous PANI ER fluid exhibited improved suspended stability, gave a larger ER effect under electric fields and higher shear stresses in comparison to the conventional granular PANI ER fluid [340]. Based on these points, it seemed that the fabrication of a 1D conducting polymer nanocomposite ER fluid was a meaningful objective. Recently, 1D PANI/titanate composite nanotubes prepared through an *in situ* chemical polymerization approach were used as a dispersed phase in ER fluids [341]. 1D PANI/titanate composite suspensions had a higher ER effect in comparison to that of sphere-like PANI/TiO_2 composite nanoparticles. It was concluded that the higher ER activity was attributed to the larger dielectric loss and faster rate of interfacial polarization for 1D PANI/titanate nanocomposites. Choi and co-workers synthesized 1D PANI/silica nanocomposites through an interfacial polymerization followed by a modified Stöber method and used it as a dispersed phase of ER fluid [342]. In comparison to silica-based mesoporous PANI system, ER fluids based on 1D PANI/silica nanocomposites exhibited better dependence of shear stress on the electric field strength. It is expected that the ER performance would further enhance by increasing the compatibility between conducting polymers and inorganic component.

4.7. Biomedical applications

Since the 1980s, biomedical applications based on conducting polymers have emerged and attracted much attention [343,344]. Among various kinds of conducting polymers, PANI and PPy are attractive candidates in biomedical applications for their biocompatibility, ease of synthesis, low cost and rich redox chemistry. In particular, the reversible doping/dedoping properties of PANI or PPy showed the ability to entrap and release biologically active molecules, which can be applied for controlled drug delivery. On the other hand, since most biological cells are sensitive to electrical impulses, conducting polymers can be applicable in the field of tissue engineering to modulate cellular activities through electrical stimulation. In the following, we illustrate some examples of applications of 1D conducting polymer nanocomposites for controlled drug delivery and tissue engineering.

4.7.1. Drug delivery

To enhance drug targeting specificity and decrease systemic drug toxicity, many drug delivery systems have been derived, including polymeric microspheres, polymer micelles, polymeric nanofibers, micro (nano) gels, etc [345,346]. 1D conducting polymer nanocomposites for

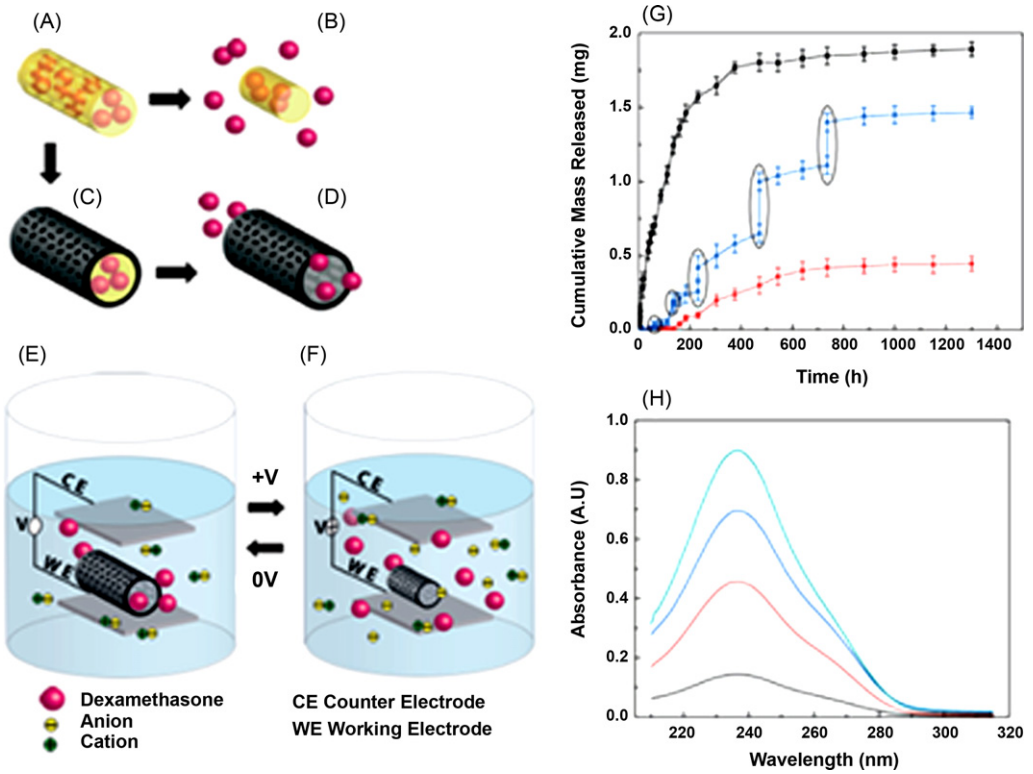

Fig. 21. Schematic illustration of the controlled drug release: (A) drug-loaded electrospun PLGA nanofibers. (B) Drug release for the hydrolytic degradation of PLGA fibers. (C, D) PEDOT/PLGA core-sheath fibers slows down the drug release. (E, F) Drug releases from PEDOT nanotubes under external electrical stimulation. (G) Cumulative mass release of drug from PLGA fibers (squares), PEDOT/PLGA core-sheath fibers without (circles) and with (triangles) electrical stimulation of 1 V applied voltage. (H) The UV spectra of dexamethasone-loaded PEDOT nanotubes after 16, 87, 160 and 730 h (from down to top) [168]. Copyright 2006, Wiley-VCH Verlag GmbH&Co. KGaA, Weinheim.

drug delivery have many advantages, such as easy loading, little influence on the drug activity and well controlled release rate. It is well known that conducting polymers showed a reversible electrochemical response, they will contract upon reduction and expand after oxidation. The induced volume change will favor the controlled release of various kinds of drugs. For example, conductive PPy film was used for the covalent immobilization of PVA-heparin hydrogel, which displayed electrically controlled release properties of heparin [347]. Under an electric current of 3.5 mA, the release rate of heparin from the substrate was two times higher than that without the current.

In comparison to the film, 1D nanostructures of conducting polymers are better suitable to the applications in drug delivery for their large surface area. Martin and co-workers demonstrated that PLGA/PEDOT or PLGA/PPy composite nanofibers synthesized via electrospinning approach and followed by electrochemical deposition could function as controlled drug delivery systems [168]. The electrospinning technique affords a facile and versatile method to fabricate polymer nanofibers. During the process of electrospinning, the drug of dexamethasone can be easily incorporated into the polymer nanofibers. After electrochemical deposition, the as-synthesized core-sheath PLGA/conducting polymers had lower impedance and much higher charge-transfer capacity compared to that of electrospun PLGA nanofibers. The results showed that 75% of the dexamethasone was released after seven days for drug-loaded electrospun PLGA nanofibers. In contrast, for drug-loaded PLGA/PEDOT composite nanofibers, less than 25% of the dexamethasone was released after 54 days. This indicated that the PEDOT layer on the surface of PLGA fibers delayed the release of dexamethasone from PLGA nanofibers. Most importantly, the dexamethasone can be control-released from PLGA/PEDOT composite nanofibers by using an electrical simulation (Fig. 21). Under a voltage bias, the drug release rate increased significantly, attributed to the contraction of PEDOT shell for a fast expulsion of dexamethasone. The controlled drug release based on conducting polymer nanocomposites provides a useful means to fabricate electronically active devices with living tissues.

4.7.2. Tissue engineering

As already mentioned, 1D conducting polymers have good electrical properties, electroactivity and large surface area, and are good candidates for use in the field of tissue engineering. In particular, it is expected that electrical stimulation could modulate cell attachment, proliferation, migration, and differentiation. For example, a PPy film has been found to enhance the neurite extension of pheochromacytoma 12 (PC12) cells with immediate electrical stimulation [348]. Combined with another 1D nanostructured malleable material, the drawbacks of crys-

talline and limited porosity of conducting polymers can be overcomed. Again, electrospinning offers a simple and versatile method for the fabrication of polymer nanofibers. Electrospinning a blended polymer solution containing conducting polymers and another kind of biocompatible polymer could produce conductive composite nanofibers with high-surface area, high porosity, good biocompatibility and sometime biodegradability that can be used for tissue engineering. The natural protein gelatin is often used as scaffold for tissue engineering. Lelkes and co-workers fabricated PANI/gelatin composite nanofibers by electrospinning their mixed solution in 1,1,1,3,3,3-hexafluoro-2-propanol [187]. SEM images showed that the size of the composite fibers decreased with increasing concentration of PANI in the solution. The typical diameter of the composite fibers was 61 ± 13 nm for 60:40 PANI/gelatin composites. It was also found that the tensile strength of the composite nanofibers increased with increasing content of PANI. The attachment and proliferation of H9c2 cardiac rat myoblast cells on PANI/gelatin composite fibers were similar to those on tissue culture-treated plastic (TCP). However, the celluar response to PANI/gelatin composite nanofibers under electrical stimulation has yet to be reported.

In addition to PANI/gelatin, CSA doped PANI can also be blended with poly(L-lactide-*co*-ε-caprolactone) (PLCL) to form PANI/PLCL composite nanofibers via electrospinning technique [349]. The diameters of the as-synthesized PANI/PLCL composite nanofibers ranged from 100 to 700 nm. In comparison to the membrane of pure PLCL nanofibers, the membrane of PANI/PLCL composite nanofibers exhibited higher adhesion for three different types of cells: human dermal fibroblasts, NIH-3T3 fibroblasts, and C2C12 myoblasts. For an example of human primary fibroblasts cultured on PANI/PLCL composite nanofibers containing 30% PANI, the relative activity was almost three times greater than that on pure PLCL nanofibers. In particular, the cell growth under the electrical simulation was also investigated. The results showed that the growth of NIH-3T3 fibroblasts was enhanced under an electrical current. Kim et al. demonstrated the fabrication of PANI/collagen composite films through solvent evaporation of the mixed solution of PANI and collagen, followed by cross-linking with glutaraldehyde vapor [350]. Adult porcine skeletal muscle cells attached and grew well on the as-synthesized PANI/collagen composite films, indicating their good supports for cell growth.

Composite nanofibers with a core-sheath structure are also good candidates for tissue engineering applications. By chemical or electrochemical depositon of conducting polymers on the surface of electrospun polymer nanofibers, 1D conducting polymer composites with core-sheath structure can be fabricated. Xia and co-workers prepared PCL/PPy and PLA/PPy core-sheath nanofibers using using electrospun PCL and PLA nanofibers as templates and studied their applications in neural tissue engineering [351]. Fig. 22 gives a fluorescence micrograph of a DRG neurite field on both random and aligned PCL/PPy core-sheath nanofibers. The results showed that the neuritis grow radially on the scafford of random PCL/PPy core-sheath nanofibers, while they grew in the orientation of the aligned nanofibers. In comparison to random PCL/PPy core-sheath nanofibers, it was found that the rate of neurite extension can be enhanced by the aligned nanofibers. In order to verify the effect of the presence of conductive PPy, the neurite outgrowth on both random and aligned

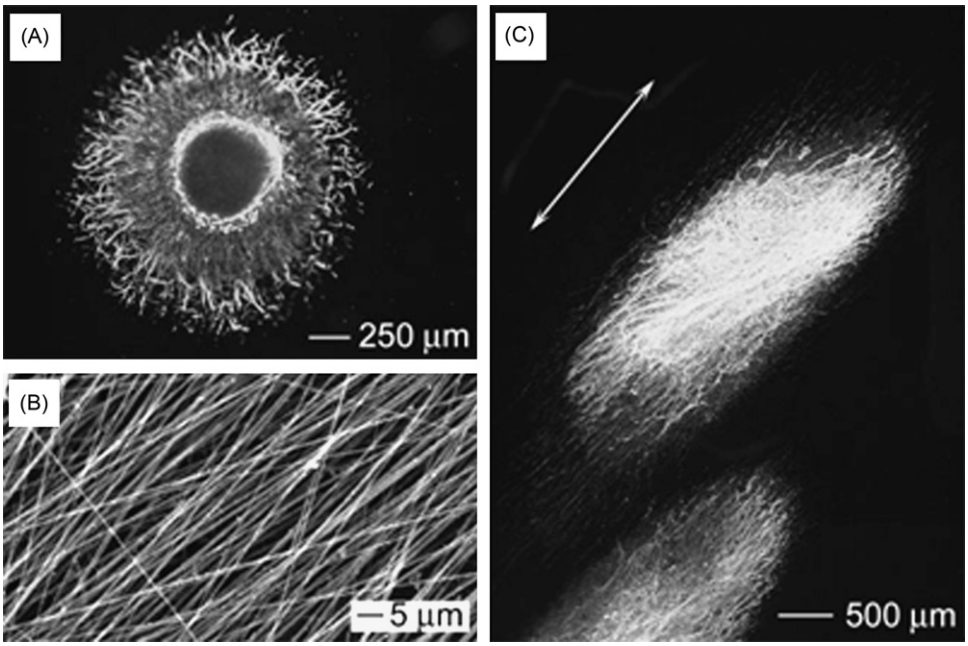

Fig. 22. (A) Fluorescence micrograph of DRG neurite growth on random PCL/PPy core-sheath nanofibers. (B) SEM images of aligned PCL/PPy core-sheath nanofibers. (C) Fluorescence micrograph of DRG neurite growth on aligned PCL/PPy core-sheath nanofibers [351]. Copyright 2009, Wiley-VCH Verlag GmbH&Co. KGaA, Weinheim.

PCL/PPy core-sheath nanofibers under electrical stimulation has been demonstrated. Compared to the length of neuritis in the absence of electrical stimulation, the maximum length of neuritis for random and aligned samples increased by 83% and 47%, respectively, indicating its potential applications for neural tissue engineering. Random and aligned PLGA/PPy core-sheath nanofibers have also been fabricated using the electrospinning technique and *in situ* chemical polymerization for neural tissue engineering [352]. For rat PC12 cells and hippocampal neurons, the growth and differentiation are similar with that of pure PLGA nanofibers. Electrical stimulation for the neutite outgrowth has been demonstrated. It was found that lower potential (10 mV/cm) was more beneficial for the neutite growth than higher potential (100 mV/cm). Under the stimulation with a potential of 10 mV/cm, more neurite-bearing PC12 cells and longer neuritis were obtained relative to unstimulated controls. In addition, aligned PLGA/PPy core-sheath nanofibers also exhibited the formation of more neurite-bearing cells and longer neurites compared to the random PLGA/PPy core-sheath nanofibers under the electrical stimulation.

5. Conclusions and outlook

1D conducting polymer nanocomposites exhibit high conductivity, large surface area and many other properties originating from the second component in the composite. Both size and composition control are important to prepare conducting polymer nanocomposites with desirable properties. As described in this review, many innovative synthetic approaches have been developed in the recent years, including *in situ* chemical polymerization, electrochemical polymerization, emulsion polymerization, γ-irradiation-induced chemical polymerization, surfactant assistant chemical polymerization, vapor-phase polymerization, self-assembly, template method, post-treatment, hydrothermal reaction, co-electrospinning, one-step redox reaction, and so on, for the fabrication of 1D conducting polymer nanocomposites with carbon nanotubes, metals, metal oxides, chalcogenides, polymers, biological materials, porphyrins and metal phthalocyanines. Functional 1D conducting polymer nanocomposites synthesized by these methods exhibit many intriguing properties, which have been extensively explored in the applications of electronic nanodevices, chemical and biological sensors, catalysis and electrocatalysis, energy devices, microwave absorption and EMI shielding, ER fluids and biomedicine.

While research on 1D conducting polymer nanocomposites has progressed quickly, many tasks remain. For conducting polymers, the main challenge is still to increase their electrical conductivity. Size, shape and composition control may provide a potential approach to synthesize nanostructured materials with high electrical conductivity. Therefore, future developments should focus on improving synthetic methods and deriving novel assembly processes for better control of the size, composition, structure, and interface of 1D conducting polymer nanocomposites. In terms of the applications of 1D conducting polymer nanocomposites, many important questions also remain. For example, in the field of sensor appications, improvement of the sensitivity and decreasing the operation temperature are very important. It is anticipated that the combination of another suitable component with conducting polymers and the formation of 1D nanostructures may effectively achieve these objectives. For microwave-absorbing applications, it has been shown that both dielectric and magnetic losses can be observed for 1D tubular nanostructures, while conventional conducting polymers only belong to dielectric loss materials [39]. In particular, in the area of energy applications, supercapacitors based on conducting polymers attracted more and more attention for their large specific capacitance. However, their stability is not very good. It is expected that adding another nanocomponent as the sacfford of conducting polymers may enhance the stability of the supercapacitor device.

The preceding demonstrates that 1D conducting polymer nanocomposites are very promising materials for various kinds of applications. However, studies are still desired on new methods for the fabrication of such materials, finding intriguing and enhanced properties, and expanding their applications. It is anticipated that more and more exciting discoveries will be made in this field in the years to come.

Acknowledgements

This work was supported by the research grants from the National 973 Project (No. 2007CB936203 and S2009061009), National 863 Project (2007 AA03z324) and the National Natural Science Foundation of China (NSFC Nos. 50973038 and 50873045). Y. Wei thanks the support by the Chinese Ministry of Education via the Chang-Jiang Scholar Program and by the Cheng Kung University in Taiwan via a Visiting Chair Professor appointment. We wish to dedicate this article to late Professor Alan G. MacDiarmid (1927–2007) for his professional guidance and personal friendship. We also dedicate this article to the memory of our co-author and colleague, Professor Wanjin Zhang, who sadly passed away in March, 2010.

References

[1] Timp G. Nanotechnology. New York: Springer–Verlag; 1999.
[2] Hu J, Odom TW, Lieber CM. Chemistry and physics in one dimension: synthesis and properties of nanowires and nanotubes. Acc Chem Res 1999;32:435–45.
[3] Wang ZL. Characterizing the structure and properties of individual wire-like nanoentities. Adv Mater 2000;12:1295–8.
[4] Xia Y, Yang P, Sun Y, Wu Y, Mayers B, Gates B, Yin Y, Kim F, Yan H. One-dimensional nanostructures: synthesis, characterization, and applications. Adv Mater 2003;15:353–89.
[5] Trentler TJ, Hickman KM, Goel SC, Viano AM, Gibbons PC, Buhro WE. Solution-liquid-solid growth of crystalline III-V semiconductors: an analogy to vapor-liquid-solid growth. Science 1995;270:1791–4.
[6] Heath JR, Legoues FK. A liquid solution synthesis of single crystal germanium quantum wires. Chem Phys Lett 1993;208:263–8.
[7] Holmes JD, Johnston KP, Doty RC, Korgel BA. Control of thickness and orientation of solution-grown silicon nanowires. Science 2000;287:1471–3.
[8] Sun Y, Gates B, Mayers B, Xia Y. Crystalline silver nanowires by soft solution processing. Nanolett 2002;2:165–8.
[9] Morales AM, Lieber CM. A laser ablation method for the synthesis of crystalline semiconductor nanowires. Science 1998;279:208–10.

[10] Zhang YF, Tang YH, Wang N, Yu DP, Lee CS, Bello I, Lee ST. Silicon nanowires prepared by laser ablation at high temperaturemm. Appl Phys Lett 1998;72:1835–7.
[11] Wang ZL, Dai ZR, Gao RP, Bai ZG, Gole JL. Side-by-side silicon carbide-silica biaxial nanowires: synthesis, structure, and mechanical properties. Appl Phys Lett 2000;77:3349–51.
[12] Wu Y, Yang P. Germanium nanowire growth via simple vapor transport. Chem Mater 2000;12:605–7.
[13] Tang CC, Fan SS, Dang HY, Li P, Liu YM. Simple and high-yield method for synthesizing single-crystal GaN nanowires. Appl Phys Lett 2000;77:1961–3.
[14] Martin CR. Nanomaterials – A membrane-based synthetic approach. Science 1994;266:1961–6.
[15] Martin CR. Template synthesis of electronically conductive polymer nanostructures. Acc Chem Res 1995;28:61–8.
[16] Huang ZM, Zhang YZ, Kotaki M, Ramakrishna S. A review on polymer nanofibers by electrospinning and their applications in nanocomposites. Composites Sci Technol 2003;63:2223–53.
[17] Li D, Xia Y. Electrospinning of nanofibers: reinventing the wheel? Adv Mater 2004;16:1151–70.
[18] Greiner A, Wendorff JH. Electrospinning: a fascinating method for the preparation of ultrathin fibres. Angew Chem Int Ed 2007;46:5670–703.
[19] Lu X, Wang C, Wei Y. One-dimensional composite nanomaterials: synthesis by electrospinning and their applications. Small 2009;5:2349–70.
[20] Lu X, Zhao Y, Wang C. Fabrication of PbS nanoparticles in polymer-fiber matrices by electrospinning. Adv Mater 2005;17:2485–8.
[21] Wang X, Peng Q, Li Y. Interface-mediated growth of monodispersed nanostructures. Acc Chem Res 2007;40:635–43.
[22] Li Y, Wang J, Deng Z, Wu Y, Sun X, Yu D, Yang P. Bismuth nanotubes: a rational low-temperature synthetic route. J Am Chem Soc 2001;123:9904–5.
[23] Wang X, Li Y. Selected-control hydrothermal synthesis of alpha- and beta-MnO_2 single crystal nanowires. J Am Chem Soc 2002;124:2880–1.
[24] Pacholski C, Kornowski A, Weller H. Self-assembly of ZnO: from nanodots, to nanorods. Angew Chem Int Ed 2002;41:1188–91.
[25] Schenning A, Meijer EW. Supramolecular electronics; nanowires from self-assembled π-conjugated systems. Chem Commun 2005:3245–58.
[26] Hoeben F, Jonkheijm P, Meijer EW, Schenning A. About supramolecular assemblies of pi-conjugated systems. Chem Rev 2005;105:1491–546.
[27] Pron A, Rannou P. Processible conjugated polymers: from organic semiconductors to organic metals and superconductors. Prog Polym Sci 2002;27:135–90.
[28] Shirakawa H. The discovery of polyacetylene film: the dawning of an era of conducting polymers. Angew Chem Int Ed 2001;40:2575–80.
[29] MacDiarmid AG. Synthetic metals": a novel role for organic polymers. Angew Chem Int Ed 2001;40:2581–90.
[30] Heeger AJ. Semiconducting and metallic polymers: the fourth generation of polymeric materials. Angew Chem Int Ed 2001;40:2591–611.
[31] Strenger-Smith JD. Intrinsically electrically conducting polymers. Synthesis, characterization and their applications. Prog Polym Sci 1998;23:57–79.
[32] Kang ET, Neoh KG, Tan KL. Polyaniline: a polymer with many interesting redox states. Prog Polym Sci 1998;23:277–324.
[33] Gospodinova N, Terlemezyan L. Conducting polymers prepared by oxidative polymerization: polyaniline. Prog Polym Sci 1998;23:1443–84.
[34] Palaniappan S, John A. Polyaniline materials by emulsion polymerization pathway. Prog Polym Sci 2008;33:732–58.
[35] Bhadra S, Khastgir D, Singha NK, Lee JH. Progress in preparation, processing and applications of polyaniline. Prog Polym Sci 2009;34:783–810.
[36] Pud A, Ogurtsov N, Korzhenko A, Shapoval G. Some aspects of preparation methods and properties of polyaniline blends and composites with organic polymers. Prog Polym Sci 2003;28:1701–53.
[37] Huang J, Kaner RB. The intrinsic nanofibrillar morphology of polyaniline. Chem Commun 2006:367–76.
[38] Zhang D, Wang Y. Synthesis and applications of one-dimensional nano-structured polyaniline: an overview. Mater Sci Eng B 2006;134:9–19.
[39] Wan M. A template-free method towards conducting polymer nanostructures. Adv Mater 2008;20:2926–32.
[40] Wan M. Some issues related to polyaniline micro-/nanostructures. Macromol Rapid Commun 2009;30:963–75.
[41] Li D, Huang J, Kaner RB. Polyaniline nanofibers: a unique polymer nanostructure for versatile applications. Acc Chem Res 2009;42:135–45.
[42] Tran HD, Li D, Kaner RB. One-dimensional conducting polymer nanostructures: bulk synthesis and applications. Adv Mater 2009;21:1487–99.
[43] Li C, Bai H, Shi GQ. Conducting polymer nanomaterials: electrosynthesis and applications. Chem Soc Rev 2009;38:2397–409.
[44] Long Y, Zhang L, Ma Y, Chen Z, Wang N, Zhang Z, Wan M. Electrical conductivity of an individual polyaniline nanotube synthesized by a self-assembly method. Macromol Rapid Commun 2003;24:938–42.
[45] Huang J, Virji S, Weiller BH, Kaner RB. Polyaniline nanofibers: facile synthesis and chemical sensors. J Am Chem Soc 2003;125:314–5.
[46] Zhang X, Goux WJ, Manohar SK. Synthesis of polyaniline nanofibers by "nanofiber seeding". J Am Chem Soc 2004;126:4502–3.
[47] Huang J, Kaner RB. Nanofiber formation in the chemical polymerization of aniline: a mechanistic study. Angew Chem Int Ed 2004;43:5817–21.
[48] Pillalamarri SK, Blum FD, Tokuhiro AT, Story JG, Bertino MF. Radiolytic synthesis of polyaniline nanofibers: a new templateless pathway. Chem Mater 2005;17:227–9.
[49] Jing X, Wang Y, Wu D, She L, Guo Y. Polyaniline nanofibers prepared with ultrasonic irradiation. J Polym Sci Part A Polym Chem 2006;44:1014–9.
[50] Lu X, Mao H, Chao D, Zhang W, Wei Y. Fabrication of polyaniline nanostructures under ultrasonic irradiation: from nanotubes to nanofibers. Macromol Chem Phys 2006;207:2142–52.
[51] Hatchett DW, Josowicz M. Composites of intrinsically conducting polymers as sensing nanomaterials. Chem Rev 2008;108:746–69.
[52] Zhang X, Zhang J, Wang R, Zhu T, Liu Z. Surfactant-directed polypyrrole/CNT nanocables: synthesis, characterization, and enhanced electrical properties. ChemPhysChem 2004;5:998–1002.
[53] Zhang Z, Wan M. Nanostructures of polyaniline composites containing nano-magnet. Synth Met 2003;132:205–12.
[54] Iijima S. Helical microtubules of graphitic carbon. Nature 1991;354:56–8.
[55] Andrews R, Jacques D, Qian DL, Rantell T. Multiwall carbon nanotubes: synthesis and application. Acc Chem Res 2002;35:1008–17.
[56] Ajayan PM. Nanotubes from carbon. Chem Rev 1999;99:1787–99.
[57] Dai H. Carbon nanotubes: synthesis, integration, and properties. Acc Chem Res 2002;35:1035–44.
[58] Fischer JE. Chemical doping of single-wall carbon nanotubes. Acc Chem Res 2002;35:1079–86.
[59] Sun Y, Fu K, Lin Y, Huang W. Functionalized carbon nanotubes: properties and applications. Acc Chem Res 2002;35:1096–104.
[60] Niyogi S, Hamon MA, Hu H, Zhao B, Bhowmik P, Sen R, Itkis ME, Haddon RC. Chemistry of single-walled carbon nanotubes. Acc Chem Res 2002;35:1105–13.
[61] Lu X, Chen Z. Curved π-conjugation, aromaticity, and the related chemistry of small fullerenes (<C60) and single-walled carbon nanotubes. Chem Rev 2005;105:3643–96.
[62] Tasis D, Tagmatarchis N, Bianco A, Prato M. Chemistry of carbon nanotubes. Chem Rev 2006;106:1105–36.
[63] Chen J, Hamon MA, Hu H, Chen Y, Rao AM, Eklund PC, Haddon RC. Solution properties of single-walled carbon nanotubes. Science 1998;282:95–8.
[64] Qin S, Qin D, Ford WT, Resasco DE, Herrera JE. Polymer brushes on single-walled carbon nanotubes by atom transfer radical polymerization of n-butyl methacrylate. J Am Chem Soc 2004;126:170–6.
[65] Kong H, Gao C, Yan DY. Controlled functionalization of multiwalled carbon nanotubes by in situ atom transfer radical polymerization. J Am Chem Soc 2004;126:412–3.
[66] Kong H, Gao C, Yan DY. Functionalization of multiwalled carbon nanotubes by atom transfer radical polymerization and defunctionalization of the products. Macromolecules 2004;37:4022–30.
[67] Cui J, Wang W, You Y, Liu C, Wang P. Functionalization of multiwalled carbon nanotubes by reversible addition fragmentation chain-transfer polymerization. Polymer 2004;45:8717–21.
[68] Gómez FJ, Chen RJ, Wang D, Waymouth RM, Dai H. Ring opening metathesis polymerization on non-covalently functionalized single-walled carbon nanotubes. Chem Commun 2003:190–1.
[69] Kumar SA, Chen SM. Electroanalysis of NADH using conducting and redox active polymer/carbon nanotubes modified electrodes – a review. Sensors 2008;8:739–66.

[70] Downs C, Nugent J, Ajayan PM, Duquette DJ, Santhanam KSV. Efficient polymerization of aniline at carbon nanotube electrodes. Adv Mater 1999;11:1028–31.
[71] Chen GZ, Shaffer MSP, Coleby D, Dixon G, Zhou W, Fray DJ, Windle AH. Carbon nanotube and polypyrrole composites: coating and doping. Adv Mater 2000;12:522–6.
[72] Gao M, Huang S, Dai L, Wallace G, Gao R, Wang Z. Aligned coaxial nanowires of carbon nanotubes sheathed with conducting polymers. Angew Chem Int Ed 2000;39:3664–7.
[73] Wang J, Dai J, Yarlagadda T. Carbon nanotubes-conducting-polymer composite nanowires. Langmuir 2005;21:9–12.
[74] Huang J, Li X, Xu J, Li H. Well-dispersed single-walled carbon nanotube/polyaniline composite films. Carbon 2003;41:2731–6.
[75] Han G, Yuan J, Shi G, Wei F. Electrodeposition of polypyrrole/multiwalled carbon nanotube composite films. Thin Solid Films 2005;474:64–9.
[76] Hughes M, Chen GZ, Shaffer MSP, Fray DJ, Windle AH. Controlling the nanostructure of electrochemically grown nanoporous composites of carbon nanotubes and conducting polymers. Composites Sci Technol 2004;64:2325–31.
[77] Bhandari S, Deepa M, Srivastava AK, Lal C, Kant R. Poly(3,4-ethylenedioxythiophene) (PEDOT)-coated MWCNTs tethered to conducting substrates: facile electrochemistry and enhanced coloring efficiency. Macromol Rapid Commun 2008;29:1959–64.
[78] Cochet M, Maser WK, Benito AM, Callejas MA, Martínez MT, Benoit JM, Schreiber J, Chauvet O. Synthesis of a new polyaniline/nanotube composite: "in-situ" polymerisation and charge transfer through site-selective interaction. Chem Commun 2001:1450–1.
[79] Wu TM, Lin YW, Liao CS. Preparation and characterization of polyaniline/multi-walled carbon nanotube composites. Carbon 2005;43:734–40.
[80] Fan J, Wan M, Zhu D, Chang B, Pan Z, Xie S. Synthesis and properties of carbon nanotube-polypyrrole composites. Synth Met 1999;102:1266–7.
[81] Zengin H, Zhou W, Jin J, Czerw R, Smith DW, Echegoyen L, Carroll DL, Foulger SH, Ballato J. Carbon nanotube doped polyaniline. Adv Mater 2002;14:1480–3.
[82] Sainz R, Benito AM, Martínez MT, Galindo JF, Sotres J, Baró AM, Corraze B, Chauvet O, Maser WK. Soluble self-allinged carbon nanotube/polyaniline composites. Adv Mater 2005;17:278–81.
[83] Karim MR, Lee CJ, Park YT, Lee MS. SWNTs coated by conducting polyaniline: synthesis and modified properties. Synth Met 2005;151:131–5.
[84] Tang B, Xu H. Preparation, alignment, and optical properties of soluble poly(phenylacetylene)-wrapped carbon nanotubes. Macromolecules 1999;32:2569–76.
[85] Philip B, Xie J, Abraham JK, Varada VK. Polyaniline/carbon nanotube composites: starting with phenylamino functionalized carbon nanotubes. Polym Bull 2005;53:127–38.
[86] Xu J, Yao P, Li X, He F. Synthesis and characterization of water-soluble and conducting sulfonated polyaniline/paraphenylenediamine-functionalized multi-walled carbon nanotubes nano-composite. Mater Sci Eng B 2008;151:210–9.
[87] Zhao B, Hu H, Haddon RC. Synthesis and properties of a water-soluble single-walled carbon nanotube-poly(*m*-aminobenzene) sulfonic acid graft copolymer. Adv Funct Mater 2004;14:71–6.
[88] Philip B, Xie J, Chandrasekhar A, Abraham J, Varadan VK. A novel nanocomposite from multiwalled carbon nanotubes functionalized with a conducting polymer. Smart Mater Struct 2004;13:295–8.
[89] Zhang X, Zhang J, Wang R, Liu Z. Cationic surfactant directed polyaniline/CNT nanocables: synthesis, characterization, and enhanced electrical properties. Carbon 2004;42:1455–61.
[90] Zhang X, Zhang J, Liu Z. Tubular composite of doped polyaniline with multi-walled carbon nanotubes. Appl Phys A 2005;80:1813–7.
[91] Zhang X, Lü Z, Wen M, Liang H, Zhang J, Liu Z. Single-walled carbon nanotube-based coaxial nanowires: synthesis, characterization, and electrical properties. J Phys Chem B 2005;109:1101–7.
[92] Park JE, Saikawa M, Atobe M, Fuchigami T. Highly-regulated nanocoatings of polymer films on carbon nanofibers using ultrasonic irradiation. Chem Commun 2006:2708–10.
[93] Karim MR, Yeum JH, Lee MS, Lim KT. Synthesis of conducting polythiophene composites with multi-walled carbon nanotube by the γ-radiolysis polymerization method. Mater Chem Phys 2008;112:779–82.
[94] Wei Z, Wan M, Lin T, Dai L. Polyaniline nanotubes doped with sulfonated carbon nanotubes made via a self-assembly process. Adv Mater 2003;15:136–9.
[95] Yu Y, Ouyang C, Gao Y, Si Z, Chen W, Wang Z, Xue G. Synthesis and characterization of carbon nanotube/polypyrrole core-shell nanocomposites via in situ inverse microemulsion. J Polym Sci Part A Polym Chem 2005;43:6105–15.
[96] Yu Y, Che B, Si Z, Li L, Chen W, Xue G. Carbon nanotube/polyaniline core-shell nanowires prepared by in situ inverse microemulsion. Synth Met 2005;150:271–7.
[97] Guo H, Zhu H, Lin H, Zhang J. Polypyrrole – multi-walled carbon nanotube nanocomposites synthesized in oil–water microemulsion. Colloid Polym Sci 2008;286:587–91.
[98] Jang J, Bae J. Carbon nanofiber/polypyrrole nanocable as toxic gas sensor. Sens Actuators B 2007;122:7–13.
[99] Steinmetz J, Kwon S, Lee HJ, Abou-Hamad E, Almairac R, Goze-Bac C, Kim H, Park YW. Polymerization of conducting polymers inside carbon nanotubes. Chem Phys Lett 2006;431:139–44.
[100] Xia Y, Xiong Y, Lim B, Skrabalak SE. Shape-controlled synthesis of metal nanocrystals: simple chemistry meets complex physics? Angew Chem Int Ed 2008;48:60–103.
[101] Huang J, Virji S, Weiller BH, Kaner RB. Nanostructured polyaniline sensors. Chem A Eur J 2004;10:1314–9.
[102] Tseng RJ, Huang J, Ouyang J, Kaner RB, Yang Y. Polyaniline nanofiber/gold nanoparticle nonvolatile memory. NanoLett 2005;5:1077–80.
[103] Gallon BJ, Kojima RW, Kaner RB, Diaconescu PL. Palladium nanoparticles supported on polyaniline nanofibers as a semiheterogeneous catalyst in water. Angew Chem Int Ed 2007;46:7251–4.
[104] Zhang X, Manohar SK. Narrow pore-diameter polypyrrole nanotubes. J Am Chem Soc 2005;127:14156–7.
[105] Xu J, Hu J, Quan B, Wei Z. Decorating polypyrrole nanotubes with Au nanoparticles by an in situ reduction process. Macromol Rapid Commun 2009;30:936–40.
[106] Chen Z, Xu L, Li W, Waje M, Yan Y. Polyaniline nanofibre supported platinum nanoelectrocatalysts for direct methanol fuel cells. Nanotechnology 2006;17:5254–9.
[107] Ma Y, Jiang S, Jian G, Tao H, Yu L, Wang X, Wang X, Zhu J, Hu Z, Chen Y. CN_x nanofibers converted from polypyrrole nanowires as platinum support for methanol oxidation. Energy Environ Sci 2009;2:224–9.
[108] Guo S, Dong S, Wang E. Polyaniline/Pt hybrid nanofibers: high-efficiency nanoelectrocatalysts for electrochemical devices. Small 2009;5:1869–76.
[109] Cao H, Xu Z, Sang H, Sheng D, Tie C. Template synthesis and magnetic behavior of an array of cobalt nanowires encapsulated in polyaniline nanotubules. Adv Mater 2001;13:121–3.
[110] Cao H, Xu Z, Sheng D, Hong J, Sang H, Du Y. An array of iron nanowires encapsulated in polyaniline nanotubules and its magnetic behavior. J Mater Chem 2001;11:958–60.
[111] Cao H, Tie C, Xu Z, Hong J, Sang H. Array of nickel nanowires enveloped in polyaniline nanotubules and its magnetic behavior. Appl Phys Lett 2001;78:1592–4.
[112] Zhang J, Shi G, Liu C, Qu L, Fu M, Chen F. Electrochemical fabrication of polythiophene film coated metallic nanowire arrays. J Mater Sci 2003;38:2423–7.
[113] Drury A, Chaure S, Kröll M, Nicolosi V, Chaure N, Blau WJ. Fabrication and characterization of silver/polyaniline composite nanowires in porous anodic alumina. Chem Mater 2007;19:4252–8.
[114] Park S, Lim JH, Chung SW, Mirkin CA. Self-assembly of mesoscopic metal-polymer amphiphiles. Science 2004;303:348–51.
[115] Lahav M, Weiss EA, Xu Q, Whitesides GM. Core-shell and segmented polymer-metal composite nanostructures. NanoLett 2006;6:2166–71.
[116] Hernandez RM, Richter L, Semancik S, Stranick S, Mallouk TE. Template fabrication of protein-functionalized gold-polypyrrole-gold segmented nanowires. Chem Mater 2004;16:3431–8.
[117] Reynes O, Demoustier-Champagne S. Template electrochemical growth of polypyrrole and gold-polypyrrole-gold nanowire arrays. J Electrochem Soc 2005;152:D130–5.
[118] Kong L, Lu X, Jin E, Jiang S, Wang C, Zhang W. Templated synthesis of polyaniline nanotubes with Pd nanoparticles attached onto their inner walls and its catalytic activity on the reduction of p-nitroanilinum. Composites Sci Technol 2009;69:561–6.
[119] Feng X, Sun Z, Hou W, Zhu J. Synthesis of functional polypyrrole/prussian blue and polypyrrole/Ag composite microtubes by using a reactive template. Nanotechnology 2007;18:195603/1–7.
[120] Chen A, Wang H, Li X. One-step process to fabricate Ag–polypyrrole coaxial nanocables. Chem Commun 2005:1863–4.

[121] Munoz-Rojas D, Oro-Solé J, Ayyad O, Gomez-Romero P. Facile one-pot synthesis of self-assembled silver@polypyrrole core/shell nanosnakes. Small 2008;4:1301–6.
[122] Huang K, Zhang Y, Long Y, Yuan J, Han D, Wang Z, Niu L, Chen Z. Preparation of highly conductive, self-assembled gold/polyaniline nanocables and polyaniline nanotubes. Chem Eur J 2006;12:5314–9.
[123] Lu G, Li C, Shen J, Chen Z, Shi G. Preparation of highly conductive gold-poly(3,4-ethylenedioxythiophene) nanocables and their conversion to poly(3,4-ethylenedioxythiophene) nanotubes. J Phys Chem C 2007;111:5926–31.
[124] Mallick K, Witcomb MJ, Dinsmore A, Scurrell MS. Fabrication of a metal nanoparticles and polymer nanofibers composite material by an in situ chemical synthetic route. Langmuir 2005;21: 7964–7.
[125] Chen A, Xie H, Wang H, Li H, Li X. Fabrication of Ag/polypyrrole coaxial nanocables through common ions adsorption effect. Synth Met 2006;156:346–50.
[126] Pillalamarri SK, Blum FD, Tokuhiro AT, Bertino MF. One-pot synthesis of polyaniline-metal nanocomposites. Chem Mater 2005;17:5941–4.
[127] Zhang Z, Wan M, Wei Y. Electromagnetic functionalized polyaniline nanostructures. Nanotechnology 2005;16:2827–32.
[128] Zhang L, Wan M. Polyaniline/TiO_2 composite nanotubes. J Phys Chem B 2003;107:6748–53.
[129] Lu X, Mao H, Chao D, Zhang W, Wei Y. Ultrasonic synthesis of polyaniline nanotubes containing Fe_3O_4 nanoparticles. J Solid State Chem 2006;179:2609–15.
[130] Wang X, Liu N, Yan X, Zhang W, Wei Y. Alkali-guided synthesis of polyaniline hollow microspheres. Chem Lett 2005;34:42–3.
[131] Ding H, Wan M, Wei Y. Controlling the diameter of polyaniline nanofibers by adjusting the oxidant redox potential. Adv Mater 2007;19:465–9.
[132] Ding H, Shen J, Wan M, Chen Z. Formation mechanism of polyaniline nanotubes by a simplified template-free method. Macromol Chem Phys 2008;209:864–71.
[133] Zhang Z, Deng J, Shen J, Wan M, Chen Z, Zhang Z, Wan M, Wei Y. Chemical one step method to prepare polyaniline nanofibers with electromagnetic function. Macromol Rapid Commun 2007;28:585–90.
[134] Han J, Song G, Guo R. Synthesis of rectangular tubes of polyaniline/NiO composites. J Polym Sci Part A Polym Chem 2006;44:4229–34.
[135] Song G, Han J, Guo R. Synthesis of polyaniline/NiO nanobelts by a self-assembly process. Synth Met 2007;157:170–5.
[136] Ćirić-Marjanović G, Dragičević L, Milojević M, Mojović M, Mentus S, Dojčinović B, Marjanović B, Stejskal J. Synthesis and characterization of self-Assembled polyaniline nanotubes/silica nanocomposites. J Phys Chem B 2009;113:7116–27.
[137] Mao H, Lu X, Chao D, Cui L, Li Y, Zhang W. Preparation and characterization of PEDOT/β-Fe^{3+}O(OH,Cl) nanospindles with controllable sizes in aqueous solution. J Phys Chem C 2008;112:20469–80.
[138] Li G, Zhang C, Peng H, Chen K. One-dimensional V_2O_5@polyaniline core/shell nanobelts synthesized by an in situ polymerization method. Macromol Rapid Commun 2009;30:1841–5.
[139] Lu X, Zhao Q, Liu X, Wang D, Zhang W, Wang C, Wei Y. Preparation and characterization of polypyrrole/TiO_2 coaxial nanocables. Macromol Rapid Commun 2006;27:430–4.
[140] Lu X, Mao H, Zhang W. Surfactant directed synthesis of polypyrrole/TiO_2 coaxial nanocables with a controllable sheath size. Nanotechnology 2007;18:025604/1–5.
[141] Cheng Q, Pavlinek V, He Y, Li C, Lengalova A, Saha P. Facile fabrication and characterization of novel polyaniline/titanate composite nanotubes directed by block copolymer. Eur Polym J 2007;43:3780–6.
[142] Xu J, Li X, Liu J, Wang X, Peng Q, Li Y. Solution route to inorganic nanobelt-conducting organic polymer core-shell nanocomposites. J Polym Sci Part A Polym Chem 2005;43:2892–900.
[143] Huynh WU, Dittmer JJ, Alivisatos AP. Hybrid nanorod-polymer solar cells. Science 2002;295:2425–7.
[144] Huynh WU, Dittmer JJ, Libby WC, Whiting GL, Alivisatos AP. Controlling the morphology of nanocrystal-polymer composites for solar cells. Adv Funct Mater 2003;13:73–9.
[145] Lu X, Yu Y, Chen L, Mao H, Zhang W, Wei Y. Preparation and characterization of polyaniline microwires containing CdS nanoparticles. Chem Commun 2004:1522–3.
[146] Xi Y, Zhou J, Guo H, Cai C, Lin Z. Enhanced photoluminescence in core-sheath CdS-PANI coaxial nanocables: a charge transfer mechanism. Chem Phys Lett 2005;412:60–4.
[147] Zhang W, Wen X, Yang S. Synthesis and characterization of uniform arrays of copper sulfide nanorods coated with nanolayers of polypyrrole. Langmuir 2003;19:4420–6.
[148] Ota J, Srivastava SK. Polypyrrole coating of tartaric acid-assisted synthesized Bi_2S_3 nanorods. J Phys Chem C 2007;111:12260–4.
[149] Guo Y, Tang Q, Liu H, Zhang Y, Li Y, Hu W, Wang S, Zhu D. Light-controlled organic/inorganic p-n junction nanowires. J Am Chem Soc 2008;130:9198–9.
[150] Zhao Q, Huang Z, Wang C, Zhao QD, Sun H, Wang J. Preparation of PVP/MEH-PPV composite polymer fibers by electrospinning and study of their photoelectronic character. Mater Lett 2007;61:2159–63.
[151] Norris ID, Shaker MM, Ko FK, MacDiarmid AG. Electrostatic fabrication of ultrafine conducting fibers: polyanilinerpolyethylene oxide blends. Synth Met 2000;114:109–14.
[152] Bianco A, Bertarelli C, Frisk S, Rabolt JF, Gallazzi MC, Zerbi G. Electrospun polyalkylthiophene/polyethyleneoxide fibers: optical characterization. Synth Met 2007;157:276–81.
[153] Aussawasathien D, Dong JH, Dai L. Electrospun polymer nanofibers sensors. Synth Met 2005;154:37–40.
[154] Zhu Y, Zhang J, Zheng Y, Huang Z, Feng L, Jiang L. Stable, superhydrophobic, and conductive polyaniline/polystyrene films for corrosive environments. Adv Funct Mater 2006;16:568–74.
[155] Hong KH, Kang TJ. Polyaniline-nylon 6 composite nanowires prepared by emulsion polymerization and electrospinning process. J Appl Polym Sci 2006;99:1277–86.
[156] Picciani PHS, Medeiros ES, Pan Z, Orts WJ, Mattoso LHC, Soares BG. Development of conducting polyaniline/poly(lactic acid) nanofibers by electrospinning. J Appl Polym Sci 2009;112:744–53.
[157] Nair S, Natarajan S, Kim SH. Fabrication of electrically conducting polypyrrole-poly(ethylene oxide) composite nanofibers. Macromol Rapid Commun 2005;26:1599–603.
[158] Granato F, Bianco A, Bertarelli C, Zerbi G. Composite polyamide 6/polypyrrole conductive nanofibers. Macromol Rapid Commun 2009;30:453–8.
[159] Bai H, Zhao L, Lu C, Li C, Shi G. Composite nanofibers of conducting polymers and hydrophobic insulating polymers: preparation and sensing applications. Polymer 2009;50:3292–301.
[160] Nair S, Hsiao E, Kim SH. Melt-welding and improved electrical conductivity of nonwoven porous nanofiber mats of poly(3,4-ethylenedioxythiophene) grown on electrospun polystyrene fiber template. Chem Mater 2009;21:115–21.
[161] Wei M, Lee J, Kang B, Mead J. Preparation of core-sheath nanofibers from conducting polymer blends. Macromol Rapid Commun 2005;26:1127–32.
[162] Wei M, Kang B, Sung C, Mead J. Core-sheath structure in electrospun nanofibers from polymer blends. Macromol Mater Eng 2006;291:1307–14.
[163] Fong H, Chun I, Reneker DH. Beaded nanofibers formed during electrospinning. Polymer 1999;40:4585–92.
[164] Kuo CC, Wang CT, Chen WC. Poly(3-hexylthiophene)/poly(methyl methacrylate) core-shell electrospun fibers for sensory applications. Macromol Symp 2009;279:41–7.
[165] Dong H, Nyame V, MacDiarmid AG, Jones Jr WE. Polyaniline/poly(methyl methacrylate) coaxial fibers: the fabrication and effects of the solution properties on the morphology of electrospun core fibers. J Polym Sci Part B Polym Phys 2004;42:3934–42.
[166] Dong H, Jones Jr WE. Preparation of submicron polypyrrole/poly(methyl methacrylate) coaxial fibers and conversion to polypyrrole tubes and carbon tube. Langmuir 2006;22:11384–7.
[167] Hong KH, Oh KW, Kang TJ. Preparation of conducting nylon-6 electrospun fiber webs by the in situ polymerization of polyaniline. J Appl Polym Sci 2005;96:983–91.
[168] Abidian MR, Kim DH, Martin DC. Conducting-polymer nanotubes for controlled drug release. Adv Mater 2006;18:405–9.
[169] Jang J, Lim B, Lee J, Hyeon T. Fabrication of a novel polypyrrole/poly(methyl methacrylate) coaxial nanocable using mesoporous silica as a nanoreactor. Chem Commun 2001:83–4.
[170] Hopkins AR, Sawall DD, Villahermosa RM, Lipeles RA. Interfacial synthesis of electrically conducting polyaniline nanofiber composites. Thin Solid Films 2004;469–470:304–8.
[171] Masdarolomoor F, Innis PC, Ashraf S, Kaner RB, Wallace GG. Nanocomposites of polyaniline/poly(2-methoxyaniline-5-sulfonic acid). Macromol Rapid Commun 2006;27:1995–2000.
[172] Malhortra BD, Chaubey A, Singh SP. Prospects of conducting polymers in biosensors. Anal Chim Acta 2006;578:59–74.
[173] Ramanavičius A, Ramanavičienė, Malinauskas A. Electrochemical sensors based on conducting polymer—polypyrrole. Electrochem Acta 2006;51:6025–37.

[174] Ma Y, Zhang J, Zhang G, He H. Polyaniline nanowires on Si surfaces fabricated with DNA templates. J Am Chem Soc 2004;126:7097–101.
[175] Nickels P, Dittmer WU, Beyer S, Kottthaus JP. Polyaniline nanowire synthesis templated by DNA. Nanotechnology 2004;15:1524–9.
[176] Singh R, Prasad R, Sumana G, Arora K, Sood S, Gupta RK, Malhotra BD. STD sensor based on nucleic acid functionalized nanostructured polyaniline. Biosens Bioelectronics 2009;24:2232–8.
[177] Ghanbari K, Bathaie SZ, Mousavi MF. Electrochemically fabricated polypyrrole nanofiber-modified electrode as a new electrochemical DNA biosensor. Biosens Bioelectronics 2008;23:1825–31.
[178] Ko S, Jang J. Label-free target DNA recognition using oligonucleotide-functionalized polypyrrole nanotubes. Ultramicroscopy 2008;108:1328–33.
[179] Yang T, Wei G, Niu L, Li Z. Fabrication of linear aniline-DNA complex nanowires and DNA-templated polyaniline nanowires. Chem J Chin Univ 2006;27:1126–30.
[180] Dawn A, Nandi AK. Slow doping rate in DNA-poly(*o*-methoxyaniline) hybrid:uncoiling of poly(*o*-methoxyaniline) chain on DNA template. Macromolecules 2005;38:10067–73.
[181] Fan Y, Chen X, Trigg AD, Tung C, Kong J, Gao Z. Detection of microRNAs using target-guided formation of conducting polymer nanowires in nanogaps. J Am Chem Soc 2007;129:5437–43.
[182] Syu MJ, Chang YS. Ionic effect investigation of a potentiometric sensor for urea and surface morphology observation of entrapped urease/polypyrrole matrix. Biosens Bioelectronics 2009;24:2671–7.
[183] Dhand C, Solanki PR, Sood KN, Datta M, Malhotra BD. Polyaniline nanotubes for impedimetric triglyceride detection. Electrochem Commun 2009;11:1482–6.
[184] Numata M, Hasegawa T, Fujisawa T, Sakurai K, Shinkai S. β-1,3-glucan (schizophyllan) can act as a one-dimensional host for creation of novel poly(aniline) nanofiber structures. Org Lett 2004;6:4447–50.
[185] Shi W, Ge D, Wang J, Jiang Z, Ren L, Zhang Q. Heparin-controlled growth of polypyrrole nanowires. Macromol Rapid Commun 2006;27:926–30.
[186] Yu Y, Si Z, Chen S, Bian C, Chen W, Xue G. Facile synthesis of polyaniline-sodium alginate nanofibers. Langmuir 2006;22:3899–905.
[187] Li M, Guo Y, Wei Y, MacDiarmid AG, Lelkes PI. Electrospinning polyaniline-contained gelatin nanofibers for tissue engineering applications. Biomaterials 2006;27:2705–15.
[188] Saravanan S, Anantharaman MR, Venkatachalam S. Structural and electrical studies on tetrameric cobalt phthalocyanine and polyaniline composites. Mater Sci Eng B 2006;135:113–9.
[189] Zucolotto V, Ferreira M, Cordeiro MR, Constantino CJL, Moreira WC, Oliveira Jr ON. Nanoscale processing of polyaniline and phthalocyanines for sensing applications. Sens Actuators B 2006;113:809–15.
[190] Miras MC, Badano A, Bruno MM, Barbero C. Nitric oxide electrochemical sensors based on hybrid films of conducting polymers and metal phtalocyanines. Port Electrochim Acta 2003;21:235–43.
[191] Koti ASR, Taneja J, Periasamy N. Control of coherence length and aggregate size in the J-aggregate of porphyrin. Chem Phys Lett 2003;375:171–6.
[192] Schwab AD, Smith DE, Rich CS, Young ER, Smith WF, De Paula JC. Porphyrin nanorods. J Phys Chem B 2003;107:11339–45.
[193] Rotomskis R, Augulis R, Snitka V, Valiokas R, Liedberg B. Hierarchical structure of TPPS4 J-aggregates on substrate revealed by atomic force microscopy. J Phys Chem B 2004;108:2833–8.
[194] Hatano T, Takeuchi M, Ikeda A, Shinkai S. Nano-rod structure of poly(ethylenedioxythiophene) and poly(pyrrole) as created by electrochemical polymerization using anionic porphyrin aggregates as template. Org Lett 2003;5:1395–8.
[195] Hatano T, Takeuchi M, Ikeda A, Shinkai S. New morphology controlled poly(aniline) synthesis using anionic porphyrin aggregate as a template. Chem Lett 2003;32:314–5.
[196] Hatano T, Bae AH, Takeuchi M, Ikeda A, Shinkai S. New morphology-controlled poly(aniline) synthesis using anionic porphyrin aggregate as a template and proton-driven structural changes in the porphyrin aggregate. Bull Chem Soc Jpn 2004;77:1951–7.
[197] Zhou Q, Li C, Li J, Cui X, Gervasio D. Template-synthesized cobalt Porphyrin/polypyrrole nanocomposite and its electrocatalysis for oxygen reduction in neutral medium. J Phys Chem C 2007;111:11216–22.
[198] Zhou Q, Li C, Li J, Lu J. Electrocatalysis of template-electrosynthesized cobalt-porphyrin/polyaniline nanocomposite for oxygen reduction. J Phys Chem C 2008;112:18578–83.
[199] Lee KP, Gopalan AY, Santhosh P, Lee SH, Nho YC. Gamma radiation induced distribution of gold nanoparticles into carbon nanotube-polyaniline composite. Composites Sci Technol 2007;67:811–6.
[200] Reddy ALM, Rajalakshmi N, Ramaprabhu S. Cobalt-polypyrrole-multiwalled carbon nanotube catalysts for hydrogen and alcohol fuel cells. Carbon 2008;46:2–11.
[201] Kong L, Lu X, Zhang W. Facile synthesis of multifunctional multiwalled carbon nanotubes/Fe_3O_4 nanoparticles/polyaniline composite nanotubes. J Solid State Chem 2008;181:628–36.
[202] Liu Z, Wang J, Xie D, Chen G. Polyaniline-coated Fe_3O_4 nanoparticle–carbon-nanotube composite and its application in electrochemical biosensing. Small 2008;4:462–6.
[203] Wu TM, Yen SJ, Chen EC, Chiang RK. Synthesis, characterization, and properties of monodispersed magnetite coated multi-walled carbon nanotube/polypyrrole nanocomposites synthesized by in-situ chemical oxidative polymerization. J Polym Sci Part B Polym Phys 2008;46:727–33.
[204] Shin MK, Kim YJ, Kim SI, Kim SK, Lee H, Spinks GM, Kim SJ. Enhanced conductivity of aligned PANi/PEO/MWNT nanofibers by electrospinning. Sens Actuators B 2008;134:122–6.
[205] Yu G, Li X, Cai X, Cui W, Zhou S, Weng J. The photoluminescence enhancement of electrospun poly(ethylene oxide) fibers with CdS and polyaniline inoculations. Acta Mater 2008;56:5775–82.
[206] Kang MS, Shin MK, Ismail YA, Shinb SR, Kim SI, Kim H, Lee H, Kim SJ. The fabrication of polyaniline/single walled carbon nanotube fibers containing a highly-oriented filler. Nanotechnology 2009;20:085701/1–5.
[207] Wang Y, Jia W, Strout T, Schempf A, Zhang H, Li B, Cui J, Lei Y. Ammonia gas sensor using polypyrrole-coated TiO_2/ZnO nanofibers. Electroanalysis 2009;21:1432–8.
[208] Lefrant S, Baibarac M, Baltog I, Mevellec JY, Godon C, Chauvet O. Functionalization of single-walled carbon nanotubes with conducting polymers evidenced by Raman and FTIR spectroscopy. Diam Relat Mater 2005;14:867–72.
[209] Li L, Qin Z, Liang X, Fan Q, Lu Y, Wu W, Zhu M. Facile fabrication of uniform core-shell structured carbon nanotube-polyaniline nanocomposites. J Phys Chem C 2009;113:5502–7.
[210] Green MM, Peterson NC, Sato T, Teramoto A, Cook R, Lifson S. A helical polymer with a cooperative response to chiral information. Science 1995;268:1860–6.
[211] Okamoto Y, Yashima E. Polysaccharide derivatives for chromatographic separation of enantiomers. Angew Chem Int Ed 1998;37:1020–43.
[212] Huang J, Egan VM, Guo H, Yoon JY, Briseno AL, Rauda IE, Carrell RL, Knobber CM, Zhou F, Kaner RB. Enantioselective discrimination of D- and L-phenylalanine by chiral polyaniline thin films. Adv Mater 2003;15:1158–61.
[213] Fireman-Shoresh S, Popov I, Avnir D, Marx S. Enantioselective, chirally templated sol-gel thin films. J Am Chem Soc 2005;127:2650–5.
[214] Akagi K, Piao G, Kaneko S, Higuchi I, Shirakawa H, Kyotani M. Helical polyacetylene synthesized under chiral nematic liquid crystals. Synth Met 1999;102:1406–9.
[215] Li W, McCarthy PA, Liu D, Huang J, Yang SC, Wang HL. Toward understanding and optimizing the template-guided synthesis of chiral polyaniline nanocomposites. Macromolecules 2002;35:9975–82.
[216] Li W, Wang HL. Oligomer-assisted synthesis of chiral polyaniline nanofibers. J Am Chem Soc 2004;126:2278–9.
[217] Li W, Wang HL. Electrochemical synthesis of optically active polyaniline films. Adv Funct Mater 2005;15:1793–8.
[218] Yan Y, Yu Z, Huang Y, Yuan W, Wei Z. Helical polyaniline nanofibers induced by chiral dopants by a polymerization process. Adv Mater 2007;19:3353–7.
[219] Yuan G, Kuramoto N. Water-processable chiral polyaniline derivatives doped and intertwined with dextran sulfate: synthesis and chiroptical properties. Macromolecules 2002;35:9773–9.
[220] Yang Y, Wan M. Chiral nanotubes of polyaniline synthesized by a template-free method. J Mater Chem 2002;12:897–901.
[221] In Het Panhuis M, Sainz R, Innis PC, Kane-Maguire LAP, Benito AM, Martnez MT, Moulton SE, Wallace GG, Maser WK. Optically active polymer carbon nanotube composite. J Phys Chem B 2005;109:22725–9.
[222] Zhang X, Song W, Harris PJF, Mitchell GR, Bui TTT, Drake AF. Chiral polymer–carbon-nanotube composite nanofibers. Adv Mater 2007;19:1079–83.
[223] Zhang X. Comparison of chiral polyaniline carbon nanotube nanocomposites synthesized by aniline dimer-assisted chemistry and electrochemistry methods. Synth Met 2008;158:336–44.

[224] Zhang X, Song W, Harris PJF, Mitchell GR. Electrodeposition of chiral polymer-carbon nanotube composite films. ChemPhysChem 2007;8:1766–9.
[225] Long Y, Chen Z, Wang N, Zhang Z, Wan M. Resistivity study of polyaniline doped with protonic acids. Physica B 2003;325:208–13.
[226] Long Y, Chen Z, Duvail JL, Zhang Z, Wan M. Electrical and magnetic properties of polyaniline/Fe_3O_4 nanostructures. Physical B 2005;370:121–30.
[227] Kim BH, Jung JH, Hong SH, Joo J, Epstein AJ, Mizoguchi K, Kim JW, Choi HJ. Nanocomposite of polyaniline and Na^+-montmorillonite clay. Macromolecules 2002;35:1419–23.
[228] Lu X, Zheng J, Chao D, Chen J, Zhang W, Wei Y. Poly (N-methylaniline)/multi-walled carbon nanotube composites—synthesis, characterization, and electrical Properties. J Appl Polym Sci 2006;100:2356–61.
[229] Lu X, Chao D, Zheng J, Chen J, Zhang W, Wei Y. Preparation and characterization of polydiphenylamine/multi-walled carbon nanotube composites. Polym Int 2006;55:945–50.
[230] Su C, Wang G, Huang F. Preparation and characterization of composites of polyaniline nanorods and multiwalled carbon nanotubes coated with polyaniline. J Appl Polym Sci 2007;106: 4241–7.
[231] Long Y, Chen Z, Zhang X, Zhang J, Liu Z. Synthesis and electrical properties of carbon nanotube polyaniline composites. Appl Phys Lett 2004;85:1796–8.
[232] Feng W, Bai X, Lian Y, Liang J, Wang X, Yoshino K. Well-aligned polyaniline/carbon-nanotube composite films grown by in-situ aniline polymerization. Carbon 2003;41:1551–7.
[233] Long Y, Chen Z, Zhang X, Zhang J, Liu Z. Electrical properties of multi-walled carbon nanotube/polypyrrole nanocables: percolation-dominated conductivity. J Phys D Appl Phys 2004;37: 1965–9.
[234] Long Y, Huang K, Yuan J, Han D, Niu L, Chen Z, Gu C, Jin A, Duvail JL. Electrical conductivity of a single Au/polyaniline microfiber. Appl Phys Lett 2006;88:162113/1–3.
[235] Weinberger BR, Kaufer J, Heeger AJ, Pron A, MacDiarmid AG. Magnetic susceptibility of doped polyacetylene. Phys Rev B 1979;20:223–30.
[236] Ginder JM, Richter AF, MacDiarmid AG, Epstein AJ. Insulator-to-metal transition in polyaniline. Solid State Commun 1987;63:97–101.
[237] Nalwa HS. Phase transitions in polypyrrole and polythiophene conducting polymers demonstrated by magnetic susceptibility measurements. Phys Rev B 1989;39:5964–74.
[238] Long Y, Chen Z, Shen J, Zhang Z, Zhang L, Xiao H, Wan M, Duvail JL. Magnetic properties of conducting polymer nanostructures. J Phys Chem B 2006;110:23228–33.
[239] Cui Y, Lieber CM. Functional nanoscale electronic devices assembled using silicon nanowire building blocks. Science 2001;291:851–3.
[240] Law M, Kind H, Messer B, Kim F, Yang P. Photochemical sensing of NO_2 with SnO_2 nanoribbon nanosensors at room temperature. Angew Chem Int Ed 2002;42:2405–8.
[241] Zhang JP, Chu DY, Wu SL, Ho ST, Bi WG, Tu CW, Tiberio RC. Photonic-wire laser. Phys Rev Lett 1995;75:2678–81.
[242] Huang MH, Mao S, Feick H, Yan H, Wu Y, Kind H, Weber E, Russo R, Yang P. Room-temperature ultraviolet nanowire nanolasers. Science 2001;292:1897–9.
[243] Ago H, Petritsch K, Shaffer MSP, Windle AH, Friend RH. Composites of carbon nanotubes and conjugated polymers for photovoltaic devices. Adv Mater 1999;11:1281–5.
[244] Feng L, Li S, Li Y, Li H, Zhang L, Zhai J, Song Y, Liu B, Jiang L, Zhu D. Super-hydrophobic surfaces: from natural to artificial. Adv Mater 2002;14:1857–60.
[245] Xia F, Jiang L. Bio-inspired, Smart, multiscale interfacial materials. Adv Mater 2008;20:2842–58.
[246] Zhang X, Shi F, Niu J, Jiang Y, Wang Z. Superhydrophobic surfaces: from structural control to functional application. J Mater Chem 2008;18:621–33.
[247] Zhong W, Chen X, Liu S, Wang Y, Yang W. Synthesis of highly hydrophilic polyaniline nanowires and sub-micro/nanostructured dendrites on poly(propylene) film surfaces. Macromol Rapid Commun 2006;27:563–9.
[248] Zhong W, Liu S, Chen X, Wang Y, Yang W. High-yield synthesis of superhydrophilic polypyrrole nanowire networks. Macromolecules 2006;39:3224–30.
[249] Zhu Y, Hu D, Wan M, Jiang L, Wei Y. Conducting and superhydrophobic rambutan-like hollow spheres of polyaniline. Adv Mater 2007;19:2092–6.
[250] Zhu Y, Li J, Wan M, Jiang L. Superhydrophobic 3D microstructures assembled from 1D nanofibers of polyaniline. Macromol Rapid Commun 2008;29:239–43.
[251] Xu L, Chen Z, Chen W, Mulchandani A, Yan Y. Electrochemical synthesis of perfluorinated ion doped conducting polyaniline films consisting of helical fibers and their reversible switching between superhydrophobicity and superhydrophilicity. Macromol Rapid Commun 2008;29:832–8.
[252] Xu L, Chen W, Mulchandani A, Yan Y. Reversible conversion of conducting polymer films from superhydrophobic to superhydrophilic. Angew Chem Int Ed 2005;44:6009–12.
[253] Zhu Y, Feng L, Xia F, Zhai J, Wan M, Jiang L. Chemical dual-responsive wettability of superhydrophobic PANI-PAN coaxial nanofibers. Macromol Rapid Commun 2007;28:1135–41.
[254] Huang J, Kaner RB. A general chemical route to polyaniline nanofibers. J Am Chem Soc 2004;126:851–5.
[255] Fan C, Qiu H, Ruan J, Terasaki O, Yan Y, Wei Z, Che S. Formation of chiral mesopores in conducting polymers by chiral-lipid-ribbon templating and "seeding" route. Adv Funct Mater 2008;18:2699–707.
[256] Ćirić-Marjanović C, Dondur V, Milojević M, Mojović M, Mentus S, Radulović A, Vuković Z, Stejskal J. Synthesis and characterization of conducting self-assembled polyaniline nanotubes/zeolite nanocomposite. Langmuir 2009;25:3122–31.
[257] Mihranyan A, Nyholm L, Bennett AEG, Stromme M. A novel high specific surface area conducting paper material composed of polypyrrole and *Cladophora* cellulose. J Phys Chem B 2008;112:12249–55.
[258] Pérez R, Pinto NJ, Johnson Jr AT. Influence of temperature on charge transport and device parameters in an electrospun hybrid organic/inorganic semiconductor Schottky diode. Synth Met 2007;157:231–4.
[259] Rivera R, Pinto NJ. Schottky diodes based on electrospun polyaniline nanofibers: effects of varying fibe diameter and doping level on device performance. Physica E 2009;41:423–6.
[260] Pinto NJ, Johnson Jr AT, MacDiarmid AG, Mueller CH, Theofylaktos N, Robinson DC, Miranda FA. Electrospun polyaniline/polyethylene oxide nanofiber field-effect transistor. Appl Phys Lett 2003;83:4244–6.
[261] Lefenfeld M, Blanchet G, Rogers JA. High-performance contacts in plastic transistors and logic gates that use printed electrodes of DNNSA-PANI doped with single walled carbon nanotubes. Adv Mater 2003;15:1188–91.
[262] Park S, Chung SW, Mirkin CA. Hybrid organic-inorganic, rod-shaped nanoresistors and diodes. J Am Chem Soc 2004;126:11772–3.
[263] Chung HJ, Jung HH, Cho YS, Lee S, Ha JH, Choi JH, Kuk Y. Cobalt–polypyrrole–cobalt nanowire field-effect transistors. Appl Phys Lett 2005;86:213113/1–3.
[264] Tseng RJ, Baker CO, Shedd B, Huang J, Kaner RB, Ouyang J, Yang Y. Charge transfer effect in the polyaniline-gold nanoparticle memory system. Appl Phys Lett 2007;90:053101/1–3.
[265] Rajesh, Ahuja T, Kumar D. Recent progress in the development of nano-structured conducting polymers/nanocomposites for sensor applications. Sens Actuators B 2009;136:275–86.
[266] Adhikari B, Majumdar S. Polymers in sensor applications. Prog Polym Sci 2004;29:699–766.
[267] Lange U, Roznyatovskaya NV, Mirsky VM. Conducting polymers in chemical sensors and arrays. Anal Chim Acta 2008;614: 1–26.
[268] Gupta N, Sharma S, Mir IA, Kumar D. Advances in sensors based on conducting polymers. J Sci Ind Res 2006;65:549–57.
[269] Hopkins AR, Lewis NS. Detection and classification characteristics of arrays of carbon black/organic polymer composite chemiresistive vapor detectors for the nerve agent simulants dimethylmethylphosphonate and diisopropylmethylphosponate. Anal Chem 2001;73:884–92.
[270] Doleman BJ, Lewis NS. Comparison of odor detection thresholds and odor discriminablities of a conducting polymer composite electronic nose versus mammalian olfaction. Sens Actuators B 2001;72:41–50.
[271] Jin G, Norrish J, Too C, Wallace G. Polypyrrole filament sensors for gases and vapors. Curr Appl Phys 2004;4:366–9.
[272] Chen Y, Li Y, Wang H, Yang M. Gas sensitivity of a composite of multi-walled carbon nanotubes and polypyrrole prepared by vapor phase polymerization. Carbon 2007;45:357–63.
[273] Sadek AZ, Wlodarski W, Shin K, Kaner RB, Kalantar-zadeh K. A layered surface acoustic wave gas sensor based on a polyaniline/In_2O_3 nanofibre composite. Nanotechnology 2006;17: 4488–92.

[274] Sadek AZ, Wlodarski W, Shin K, Kaner RB, Kalantar-zadeh K. A polyaniline/WO_3 nanofiber composite-based ZnO/64-YX $LiNbO_3$ SAW hydrogen gas sensor. Synth Met 2008;158:29–32.
[275] Virji S, Fowler JD, Baker CO, Huang J, Kaner RB, Weiller BH. Polyaniline nanofiber composites with metal salts: chemical sensors for hydrogen sulfide. Small 2005;1:624–7.
[276] Ji S, Li Y, Yang M. Gas sensing properties of a composite composed of electrospun poly(methyl methacrylate) nanofibers and in situ polymerized polyaniline. Sens Actuators B 2008;133: 644–9.
[277] Santhanam KSV, Sangoi R, Fuller L. A chemical sensor for chloromethanes using a nanocomposite of multiwalled carbon nanotubes with poly(3-methylthiophene). Sens Actuators B 2005;106:766–71.
[278] Dhand C, Singh SP, Arya SK, Datta B, Malhotra BD. Cholesterol biosensor based on electrophoretically deposited conducting polymer film derived from nano-structured polyaniline colloidal suspension. Anal Chim Acta 2007;602:244–51.
[279] Gao M, Dai L, Wallace GG. Biosensors based on aligned carbon nanotubes coated with inherently conducting polymers. Electroanalysis 2003;15:1089–94.
[280] Fujishima A, Honda K. Electrochemicalphotolysis of water at a semiconductor electrode. Nature 1972;238:37–8.
[281] Xiong S, Wang Q, Xia H. Template synthesis of polyaniline/TiO_2 bilayer microtubes. Synth Met 2004;146:37–42.
[282] Huang H, Feng X, Zhu J. Synthesis, characterization and application in electrocatalysis of polyaniline/Au composite nanotubes. Nanotechnology 2008;19:145607/1–7.
[283] Mao H, Lu X, Wang C, Zhang W. Investigation on PEDOT/β-Fe^{3+}O(OH,Cl) nanospindles as a new steady electrode material for detecting iodic compounds. Electrochem Commun 2009;11: 603–7.
[284] Mao H, Lu X, Liu X, Tang J, Wang C, Zhang W. One-step synthesis of Au/PEDOT/β-Fe^{3+}O(OH,Cl) nanospindles in aqueous solution. J Phys Chem C 2009;113:9465–72.
[285] Olson DC, Piris J, Collins RT, Shaheen SE, Ginley DS. Hybrid photovoltaic devices of polymer and ZnO nanofiber composites. Thin Solid Films 2006;496:26–9.
[286] Greene LE, Law M, Yuhas BD, Yang P. ZnO-TiO_2 core-shell nanorod/P3HT solar cells. J Phys Chem C 2007;111:18451–6.
[287] Shankar K, Mor GK, Paulose M, Varghese OK, Grimes CA. Effect of device geometry on the performance of TiO_2 nanotube array-organic semiconductor double heterojunction solar cells. J Non-Crystal Solids 2008;354:2767–71.
[288] Fan B, Mei X, Sun K, Ouyang J. Conducting polymer/carbon nanotube composite as counter electrode of dye-sensitized solar cells. Appl Phys Lett 2008;93:143103/1–3.
[289] Tepavcevic S, Darling SB, Dimitrijevic NM, Rajh T, Sibener SJ. Improved hybrid solar cells via in situ UV polymerization. Small 2009;5:1776–83.
[290] Houarner-Rassin C, Blart E, Buvat P, Odobel F. Solid-state dye-sensitized TiO_2 solar cells based on a sensitizer covalently wired to a hole conducting polymer. Photochem Photobiol Sci 2008;7:789–93.
[291] Khatri I, Adhikari S, Aryal HR, Soga T, Jimbo T, Umeno M. Improving photovoltaic properties by incorporating both single walled carbon nanotubes and functionalized multiwalled carbon nanotubes. Appl Phys Lett 2009;94:093509/1–3.
[292] Costamagna P, Srinivasan S. Quantum jumps in the PEMFC science and technology from the 1960s to the year 2000: Part II. Engineering, technology development and application aspects. J Power Sources 2001;102:253–69.
[293] Carrette L, Friedrich KA, Stimming U. Fuel cells-fundamentals and applications. Fuel Cells 2001;1:5–39.
[294] Thomas SC, Ren XM, Gottesfeld S, Zelenay P. Direct methanol fuel cells: progress in cell performance and cathode research. Electrochim Acta 2002;47:3741–8.
[295] Rajesh B, Thampi KR, Bonard JM, Mathieu HJ, Xanthopoulos N, Viswanathan B. Conducting polymeric nanotubules as high performance methanol oxidation catalyst support. Chem Commun 2003:2022–3.
[296] Maiyalagan T. Electrochemical synthesis, characterization and electro-oxidation of methanol on platinum nanoparticles supported poly(*o*-phenylenediamine) nanotubes. J Power Sources 2008;179:443–50.
[297] Winter M, Brodd RJ. What are batteries, fuel cells, and supercapacitors? Chem Rev 2004;104:4245–69.
[298] Whittingham MS. Lithium batteries and cathode materials. Chem Rev 2004;104:4271–301.
[299] Armand M, Tarascon JM. Building better batteries. Nature 2008;451:652–7.
[300] Kang K, Meng YS, Bréger J, Grey CP, Geder G. Electrodes with high power and high capacity for rechargeable lithium batteries. Science 2006;311:977–80.
[301] Chen J, Cheng F. Combination of lightweight elements and nanostructured materials for batteries. Acc Chem Res 2009;42: 713–23.
[302] Tarascon JM, Armand M. Issues and challenges facing rechargeable lithium batteries. Nature 2001;414:359–67.
[303] Chan CK, Peng H, Liu G, McIlwrath K, Zhang XF, Huggins RA, Cui Y. High performance lithium battery anodes using silicon nanowires. Nat Nanotech 2008;3:31–5.
[304] Malta M, Louarn G, Errien N, Torresi RM. Nanofibers composite vanadium oxide/polyaniline: synthesis and characterization of an electroactive anisotropic structure. Electrochem Commun 2003;5:1011–5.
[305] Sarangapani S, Tilak BV, Chen CP. Materials for electrochemical capacitors. J Electrochem Soc 1996;143:3791–9.
[306] Faggioli E, Rena P, Danel V, Andrieu X, Mallant R, Kahlen H. Supercapacitors for the energy management of electric vehicles. J Power Sources 1999;84:261–9.
[307] Shiraishi S, Kurihara H, Okabe K, Hulicova D, Oya A. Electric double layer capacitance of highly pure single-walled carbon nanotubes (HiPco (TM) Buckytubes (TM)) in propylene carbonate electrolytes. Electrochem Commun 2002;4:593–8.
[308] Liu CG, Fang HT, Li F, Liu M, Cheng HM. Single-walled carbon nanotubes modified by electrochemical treatment for application in electrochemical capacitors. J Power Sources 2006;160:758–61.
[309] Zheng JP, Huang J, Jow TR. The limitations of energy density for electrochemical capacitors. J Electrochem Soc 1997;144:2026–31.
[310] Zheng JP, Cygon PJ, Jow TR. Hydrous ruthenium oxide as an electrode material for electrochemical capacitors. J Electrochem Soc 1995;142:2699–703.
[311] Nam KW, Yoon WS, Kim KB. X-ray absorption spectroscopy studies of nickel oxide thin film electrodes for supercapacitors. Electrochim Acta 2002;47:3201–9.
[312] Hu CC, Wang CC. Nanostructures and capacitive characteristics of hydrous manganese oxide prepared by electrochemical deposition. J Electrochem Soc 2003;150:A1079–84.
[313] Chang JK, Tsai WT. Material characterization and electrochemical performance of hydrous manganese oxide electrodes for use in electrochemical pseudocapacitors. J Electrochem Soc 2003;150:A1333–8.
[314] Sung JH, Kim SJ, Lee KH. Fabrication of microcapacitors using conducting polymer microelectrodes. J Power Sources 2003;124:343–50.
[315] Mi HY, Zhang XG, Ye XG, Yang SD. Preparation and enhanced capacitance of core-shell polypyrrole/polyaniline composite electrode for supercapacitors. J Power Sources 2008;176:403–9.
[316] Hughes M, Chen GZ, Shaffer MSP, Fray DJ, Windle AH. Electrochemical capacitance of a nanoporous composite of carbon nanotubes and polypyrrole. Chem Mater 2002;14:1610–3.
[317] Ju YW, Choi GR, Jung HR, Lee WJ. Electrochemical properties of electrospun PAN/MWCNT carbon nanofibers electrodes coated with polypyrrole. Electrochim Acta 2008;53:5796–803.
[318] Khomenko V, Frackowiak E, Béguin F. Determination of the specific capacitance of conducting polymer/nanotubes composite electrodes using different cell configurations. Electrochim Acta 2005;50:2499–506.
[319] Gupta V, Miura N. Polyaniline/single-wall carbon nanotube (PANI/SWCNT) composites for high performance supercapacitors. Electrochim Acta 2006;52:1721–6.
[320] Chen L, Yuan CZ, Dou H, Gao B, Chen S, Zhang X. Synthesis and electrochemical capacitance of core-shell poly(3,4-ethylenedioxythiophene)/poly(sodium 4-styrenesulfonate)-modified multiwalled carbon nanotube nanocomposites. Electrochim Acta 2009;54:2335–41.
[321] Liu R, Lee SB. MnO_2/Poly(3,4-ethylenedioxythiophene) coaxial nanowires by one-step coelectrodeposition for electrochemical energy storage. J Am Chem Soc 2008;130:2942–3.
[322] Geetha S, Kumar KKS, Trivedi DC. Polyaniline reinforced conducting E-glass fabric using 4-chloro-3-methyl phenol as secondary dopant for the control of electromagnetic radiations. Composites Sci Technol 2005;65:973–80.
[323] Stafström S, Brédas JL, Epstein AJ, Woo HS, Tanner DB, Huang WS, MacDiarmid AG. Polaron lattice in highly conducting polyaniline: theoretical and optical studies. Phys Rev Lett 1987;59: 1464–7.

[324] Saini P, Choudhary V, Singh BP, Mathur RB, Dhawan SK. Polyaniline-MWCNT nanocomposites for microwave absorption and EMI shielding. Mater Chem Phys 2009;113:919–26.
[325] Phang SW, Tadokoro M, Watanabe J, Kuramoto N. Microwave absorption behaviors of polyaniline nanocomposites containing TiO_2 nanoparticles. Curr Appl Phys 2008;8:391–4.
[326] Phang SW, Tadokoro M, Watanabe J, Kuramoto N. Synthesis, characterization and microwave absorption property of doped polyaniline nanocomposites containing TiO_2 nanoparticles and carbon nanotubes. Synth Met 2008;158:251–8.
[327] Block H, Kelly JP. Electrorheology. J Phys D Appl Phys 1988;21:1661–7.
[328] Choi HJ, Jhon MS. Electrorheology of polymers and nanocomposites. Soft Matter 2009;5:1562–7.
[329] Kim JW, Kim SG, Choi HJ, Jhon MS. Synthesis and electrorheological properties of polyaniline-Na^+-montmorillonite suspensions. Macromol Rapid Commun 1999;20:450–2.
[330] Choi HJ, Kim JW, Joo J, Kim BH. Synthesis and electrorheology of emulsion intercalated PANI-clay nanocomposite. Synth Met 2001;121:1325–6.
[331] Kim JW, Liu F, Choi HJ, Hong SH, Joo J. Intercalated polypyrrole/Na^+-montmorillonite nanocomposite via an inverted emulsion pathway method. Polymer 2003;44:289–93.
[332] Park DP, Lim ST, Lim JY, Choi HJ, Choi SB. Electrorheological characteristics of solvent-cast polypyrrole/clay nanocomposite. J Appl Polym Sci 2009;112:1365–71.
[333] Park JH, Lim YT, Park OO. New approach to enhance the yield stress of electro-rheological fluids by polyaniline coated layered silicate nanocomposites. Macromol Rapid Commun 2001;22:616–9.
[334] Cho MS, Choi HJ, Kim KY, Ahn WS. Synthesis and characterization of polyaniline/mesoporous SBA-15. Macromol Rapid Commun 2002;23:713–6.
[335] Cho MS, Choi HJ, Ahn WS. Enhanced electrorheology of conducting polyaniline confined in MCM-41 channels. Langmuir 2004;20:202–7.
[336] Cheng Q, Pavlinek V, Lengalova A, Li C, Belza T, Saha P. Electrorheological properties of new mesoporous material with conducting polypyrrole in mesoporous silica. Microporous Mesoporous Mater 2006;94:193–9.
[337] Fang FF, Kim JH, Choi HJ, Seo Y. Organic/inorganic hybrid of polyaniline/$BaTiO_3$ composites and their electrorheological and dielectric characteristics. J Appl Polym Sci 2007;105:1853–60.
[338] Choi HJ, Park SJ, Kim ST, Jhon MS. Electrorheological application of polyaniline/multi-walled carbon nanotube composites. Diam Relat Mater 2005;14:766–9.
[339] Choi CS, Park SJ, Choi HJ. Carbon nanotube/polyaniline nanocomposites and their electrorheological characteristics under an applied electric field. Curr Appl Phys 2007;7:352–5.
[340] Yin J, Zhao X, Xia X, Xiang L, Qiao Y. Electrorheological fluids based on nano fibrous polyaniline. Polymer 2008;49:4413–9.
[341] Cheng Q, Pavlinek V, He Y, Li C, Saha P. Electrorheological characteristics of polyaniline/titanate composite nanotube suspensions. Colloid Polym Sci 2009;287:435–41.
[342] Liu Y, Fang F, Choi HJ. Silica nanoparticle decorated conducting polyaniline fibers and their electrorheology. Mater Lett 2010;64:154–6.
[343] Guimard NK, Gomez N, Schmidt CE. Conducting polymers in biomedical engineering. Prog Polym Sci 2007;32:876–921.
[344] Geetha S, Rao CRK, Vijayan M, Trivedi DC. Biosensing and drug delivery by polypyrrole. Anal Chim Acta 2006;568:119–25.
[345] Kim S, Kim JH, Jeon O, Kwon IC, Park K. Engineered polymers for advanced drug delivery. Eur J Pharm Biopharm 2009;71:420–30.
[346] Oh JK, Drumright R, Siegwart DJ, Matyjaszewski K. The development of microgels/nanogels for drug delivery applications. Prog Polym Sci 2008;33:448–77.
[347] Li Y, Neoh KG, Kang ET. Controlled release of heparin from polypyrrole-poly(vinyl alcohol) assembly by electrical stimulation. J Biomed Mater Res Part A 2005;73A:171–81.
[348] Kotwal A, Schmidt CE. Electrical stimulation alters protein adsorption and nerve cell interactions with electrically conducting biomaterials. Biomaterials 2001;22:1055–64.
[349] Jeong SI, Jun ID, Choi MJ, Nho YC, Lee YM, Shin H. Development of electroactive and elastic nanofibers that contain polyaniline and poly(L-lactide-co-ε-caprolactone) for the control of cell adhesion. Macromol Biosci 2008;8:627–37.
[350] Kim HS, Hobbs HL, Wang L, Rutten MJ, Wamser CC. Biocompatible composites of polyaniline nanofibers and collagen. Synth Met 2009;159:1313–8.
[351] Xie J, MacEwan MR, Willerth SM, Li X, Moran DW, Sakiyama-Elbert SE, Xia Y. Conductive core-sheath nanofibers and their potential application in neural tissue engineering. Adv Funct Mater 2009;19:2312–8.
[352] Lee JY, Bashur CA, Goldstein AS, Schmidt CE. Polypyrrole-coated electrospun PLGA nanofibers for neural tissue applications. Biomaterials 2009;30:4325–35.